Ebihara, Y. and Y. Miyoshi, Dynamic inner magnetosphere: Tutorial and recent advances, in Dynamic Magnetosphere, IAGA Special Sopron Book Series Vol. 3, doi:10.1007/978-94-007-0501-2, pp. 145-187, 2011.

Dynamic Inner Magnetosphere: A Tutorial and Recent Advances

Y. Ebihara[1] and Y. Miyoshi[2]

1. Institute for Advanced Research, Nagoya University, Aichi, Japan.

2. Solar-Terrestrial Environment Laboratory, Nagoya University, Aichi, Japan

Accepted on 8 September 2010
for "Dynamic Magnetosphere," IAGA Special Sopron Book Series

Abstract. The purpose of this paper is to present a tutorial and recent advances on the Earth's inner magnetosphere, which includes the plasmasphere, warm plasma, ring current, and radiation belts. Recent analysis and modeling efforts have revealed the detailed structure and dynamics of the inner magnetosphere. In addition, it has been clearly recognized that elementary processes can affect and be affected by each other. From this sense, the following two different approaches can be used to understand the inner magnetosphere and magnetic storms. The first is to investigate its elementary processes, which would include the transport of single particles, interaction between particles and waves, and collisions. The other approach is to integrate the elementary processes in terms of cross energy and cross region couplings. Multi-satellite observations along with ground-network observations and comprehensive simulations are one of the promising avenues to incorporate the two approaches and treat the inner magnetosphere as a non-linear, compound system.

1. Preface

The inner magnetosphere is a natural cavity in which various types of charged particles are trapped by a planet's inherent magnetic field. With regard to the Earth, the kinetic energy of these trapped particles ranges from ~eV to ~10^8 eV. These particles undergo different physical processes and are never stable, even in geomagnetically quiet times, due to variations in the solar wind and self-excited instabilities in the inner magnetosphere.

The following terms have traditionally been used to identify the Earth's energy regimes. In the order of low to high energies, they are the plasmasphere (~eV),

ring current (~1–100 keV), and radiation belts (>~100 keV) (Figure 1). In a broad sense, the plasmasphere is the region where the number density of particles is high. The ring current is the torus-like region where the energy density (or the plasma pressure) is high. Van Allen radiation belts consist of energetic particles of electrons and ions of more than a few hundred keV (Van Allen and Frank, 1959). The electron radiation belts consist of the inner and outer radiation belts. There exists a slot region between them, in which electron flux is small. The proton/ion radiation belt consists of a single belt.

These energy regimes are directly or indirectly coupled with one another. Mass and energy are exchanged with the other regions such as the outer magnetosphere and the ionosphere. Research efforts directed toward cross energy and cross region couplings are therefore needed for a comprehensive understanding and modeling of the inner magnetosphere. In this paper, we review the progress of research on the inner magnetosphere and offer perspectives on future research directions in terms of the elementary processes involved and their role in the coupled evolution of the inner magnetospheric system.

2. Plasmasphere

2.1. Structure of Plasmasphere

The region where the number density of the plasma is higher than the ambient number density is called the plasmasphere. The plasmasphere consists of cold and dense plasmas that originate in the topside ionosphere. The number density of these plasmas exceeds ~10^3 cm^{-3} at L = 2 and gradually decreases with L (e.g., Carpenter and Anderson, 1992). The typical temperature of the ions is ~1–2 eV, a value which increases with L (Farrugia et al. 1989). At a certain L, the density shows a sharp drop by an order of magnitude; this region is called the plasmapause (Carpenter, 1963). The L-value of the plasmapause depends on the magnetic local time (MLT) (Carpenter, 1966) and magnetic activity (Chappell et al. 1970, Carpenter and Anderson 1992, Carpenter and Lemaire 1997, Moldwin et al. 2002). During magnetically quiet times, the plasmapause is located at $L \approx 7$. During active times, it moves to $L \approx 2$. Baker et al. (2004) have indicated an extremely shrunk plasmasphere with a plasmapause location of L = 1.5 that occurred during the Halloween storm of October 2003.

On average, the plasmapause has a bulge on the duskside when mapped to the equatorial plane (Figure 2a; see Carpenter 1966). Nishida (1966) and Brice (1967) have pointed out that the shape of the plasmasphere is understood to be a combination of the convection electric field and the corotation electric field (Figure 2b). Grebowsky (1970) has suggested that the plasmasphere is elongated

sunward on the duskside when the convection electric field becomes strong (Figure 2c). In-situ satellite observations sometimes show a "detached" dense plasma cloud outside the plasmapause (Chappell, 1974). Chen and Grebowsky (1974) have suggested that this "detached" plasma cloud can be explained by the elongated form of the plasmasphere, which has what is called a plasma tail (Figure 2d). This "detached" feature can also be formed by a strong poleward electric field in the subauroral region (Ober et al. 1997), or by an interchange instability (Lemaire, 2001).

Schematic density profile patterns of the plasmasphere are summarized by Singh and Horwitz (1992) and displayed in Figure 3, indicating that identification of the plasmapause is not always easy. Moldwin et al. (2002) investigated the thermal plasma density acquired by the CRRES satellite near the equatorial plane. They found that the plasmapause could be identified in ~73% of all the inbound and outbound trajectories investigated, but only ~16% of them displayed a "classical" plasmapause. The difficulty in identifying the plasmapause arises from its small density gradient, and the relatively smooth and highly structured variations in density. Irregular variations in density are often observed near the plasmapause (Chappell 1972, Oya and Ono 1987, Koons 1989, Horwitz et al. 1990b, Singh and Horwitz 1992, Carpenter et al. 2000, Darrouzet et al. 2004, Green and Fung 2005). Due to the complex nature of the plasmapause, Carpenter and Lemaire (2004) encourage the use of the term Plasmasphere Boundary Layer (PBL) instead of the conventional term plasmapause.

In the late 1990's, semiglobal imaging of the plasmasphere was achieved for the first time by the Japanese NOZOMI (PLANET-B) satellite (Nakamura et al. 2000). After the launch of NASA's IMAGE satellite in 2000 (Burch et al. 2001), the Extreme Ultraviolet Image (EUV) instrument on board the satellite provided completely global images of the emission of He^+ with a time resolution of 10 min and a spatial resolution of 0.1 Re (Sandel et al. 2003). The brightness of the He^+ emission is proportional to the line-of-sight density of He^+. The images from IMAGE/EUV reveal more complicated and dynamic features of the plasmasphere (Figure 2e), such as a shoulder (Burch et al. 2001), notch/bite-out (Green and Reinisch 2002), channel (Sandel et al. 2001), and plume (Sandel et al. 2001). For the determination of the equatorial plasmapause from the IMAGE/EUV observations, at least two algorithms have been used: the Edge Algorithm (Roelof and Skinner 2000) and the Minimum *L* Algorithm (Wang et al. 2007). In the late 2000's, the Japanese KAGUYA (SELENE) satellite, from its lunar orbit, succeeded in capturing images of emissions from the plasmasphere (Yoshikawa et al. 2010; Murakami et al. 2010). Yoshikawa et al. (2010) found a large depression of the plasmaspheric plasma near the equatorial plane.

In general, identifying the plasmapause at a low altitude (in the ionosphere) is more difficult than identifying it at a high altitude (in the magnetosphere). A close coincidence between the ionospheric trough and the plasmapause has been suggested by Grebowsky et al. (1976, 2009) and Yizengaw et al. (2005). When an electron density trough cannot be identified, the H^+ density can be used to identify a mid-latitude trough (Taylor 1972, Morgan et al. 1976, Grebowsky et al. 2009

and references therein). Anderson et al. (2008) developed a 7-step method to identify the plasmapause location from the low-altitude satellite DMSP in the topside ionosphere. Their results agree well with those derived from IMAGE/EUV observations. Foster et al. (2004b) reconstructed a two-dimensional distribution of the total electron contents (TEC) using a network of GPS TEC receivers. When mapped on the equatorial plane, the TEC distribution is similar to the global distribution of the He^+ plasmasphere derived from the IMAGE/EUV images. Because GPS TEC includes contributions from the plasmasphere and the ionosphere, an ambiguity arises because line-of-sight measurements were made at a GPS altitude (20,220 km) and were also made on the ground. This ambiguity was clarified by Yizengaw et al. (2008), who compared the GPS signals received by the low Earth-orbiting satellite JASON 1 (1,335 km altitude) with those received by ground-based stations. They concluded that the plasmasphere contributes significantly to ground-based GPS TEC, especially at night, when its contribution reaches 60% at low latitudes.

The plasmasphere consists of H^+, He^+, O^+, O^{++}, D^+, N^+, N^{++}, and other minor ionic species. Their composition ratios are highly variable (Chappell et al. 1972, 1982, Horwitz et al. 1986, 1990b, Farrugia et al. 1989). The most frequent values given for the He^+/H^+ ratio in the plasmasphere are ~2–6% (Farrugia et al. 1989) and ~20% (Horwitz et al. 1990b), but it has also been indicated that the ratio ranges from ~1% to, on occasion, over 100% (Farrugia et al. 1989). The He^+/H^+ ratio decreases with L (Farrugia et al. 1989). O^+ is in general minor, but the O^+/H^+ ratio occasionally increases to ~100% in the outer plasmasphere during a storm recovery phase (Horwitz et al. 1984, 1986). The N^+/O^+ ratio is ~5–10%, and the N^{++}/N^+ ratio is ~1–5% (Chappell et al. 1982). As understood using a magnetoseismology technique, O^+ becomes important in the plasmatrough (Takahashi et al. 2008), or during a large magnetic storm (Takasaki et al. 2006, Kale et al. 2009).

The temperature of the thermal plasma increases with L (Farrugia et al. 1989). The difference in the thermal structure of the inner and outer regions of the plasmasphere has been pointed out by Kotova et al. (2008). On the basis of data from Interball 2 and Magion 5, they showed that on the nightside, the plasmaspheric temperatures are quite close to the ionospheric temperature at $1.4 < L < 2.8$. At $L > 3$, the plasmaspheric temperature is higher than the ionospheric temperature. They suggested that there is a heating source at high L, particularly in the noon-to-dusk sector.

The field-aligned density distribution of plasmaspheric electrons has also been studied (Reinisch et al. 2009 and references therein). Theoretical studies have predicted that the field-aligned density will obey the hydrostatic assumption if the plasmasphere is in a steady condition. If the temperatures of the plasmaspheric plasma are constant and isotropic along a field line, the density distribution is in an exponential form, which is consistent with the result obtained by time-dependent simulation within ±40° MLAT (Rasmussen et al. 1993). Statistical studies have suggested that the field-aligned density can be well fitted to a power law form on the basis of data from Polar (Goldstein et al. 2001, Denton et al.

2002). Radio sounding of the plasmasphere was performed by a radio plasma imager (RPI) on the IMAGE satellite. Huang et al. (2004) and Tu et al. (2006) suggested a mathematical form in order to explain the field-aligned density profile that was observed remotely by IMAGE/RPI. By measuring Alfvén wave harmonic frequencies, Denton et al. (2009) inferred a field-aligned mass density profile, and fitted to a polynomial function. The physical meaning of these empirically obtained field-aligned distributions of thermal plasma is not well understood.

2.2. Formation of Plasmasphere

It has been suggested that the plasmasphere is formed by three principal processes: (1) the supply of thermal plasma from the ionosphere along a field line (e.g., Singh and Horwitz 1992), (2) pitch angle scattering of the supplied plasma (e.g., Schulz and Koons 1972; Lemaire 1989), and (3) large-scale electric fields that act on the drift motion of thermal plasma (e.g., Nishida, 1966).

The main source of H^+ in the plasmasphere is the reaction $O^+ + H \rightarrow O + H^+$ that takes place in the topside ionosphere. The reverse reaction, $O + H^+ \rightarrow O^+ + H$, also takes place with almost the same speed, which is the main sink for H^+. When the plasmasphere is completely empty, the former process will proceed, and H^+ will be supplied into the magnetosphere with a maximum flux. The limiting flux of H^+ is a weak function of a neutral temperature, but is directly proportional to the neutral hydrogen density and to the O^+ scale height and O^+ density at a lower boundary altitude of the production region (Richards and Torr 1985). The lower boundary altitude increases from 500 km for a solar minimum to 1000 km for a solar maximum because of an increase in the neutral density scale height and O^+ density. When the lower boundary altitude increases, the density of the neutral hydrogen decreases, so that the limiting flux is decreased. Thus, the refilling time is longer at a solar maximum than at a solar minimum. The opposite tendency is expected for He^+, according to the simulation performed by Krall et al. (2008). The refilling of He^+ is more rapid at a solar maximum than at a solar minimum because the He^+ density generally increases with solar activity due to photo ionization. The idea that He^+ density is largely controlled by photo ionization is supported by the diurnal variation in the He^+ density observed by IMAGE/EUV (Galvan et al. 2008).

Based on whistler wave observations in Antarctica, the time required to reach an equilibrium was obtained to be ~1 day at $L = 2.5$ and ~8 days at $L = 4$ (Park 1970, 1974). Using cold ion data from the GEOS-2 satellite at geosynchronous orbit, Song et al. (1988) found that the refilling time constants range from ~3 days to ~7 days with refilling rates depending on the *Dst* index. The first global imaging of refilling dynamics was accomplished by Sandel and Denton (2007) using data from IMAGE/EUV. In the early stage of the refilling process, the interior of the He^+ plasmasphere is structured in azimuth and the plasmapause is diffuse, suggesting that the refilling may take place nonuniformly in azimuth. The

refilling rates were inferred to be ~1 He^+ cm^{-3} h^{-1} at L = 3.3, and ~7 × 10^{-2} He^+ cm^{-3} h^{-1} at L = 6, rates which are consistent with those reported in previous studies.

Electric fields play a major role in the formation of the plasmasphere (Nishida 1966, Brice 1967, Kavanagh et al. 1968, Grebowsky 1970, Chen and Grebowsky 1974). The corotation electric field captures the thermal plasma originating from the ionosphere. The convection electric field peels away the outer layer of the thermal plasma. When the electric fields are stationary, the transition between them is precisely determined by the combination of the corotation and convection electric fields. In other words, the plasmasphere corresponds to a last-closed equipotential. The situation, however, is not as simple as this suggests because the electric fields are never stationary. Major changes in the convection electric field result in the formation of a plasma tail (drainage plume) (Grebowsky, 1970, Chen and Grebowsky, 1974). Even though the large-scale convection electric field is relatively stable, small fluctuations in the convection electric fields result in a leakage of plasma (Matsui et al. 1999, 2000). Additional electric fields driven by magnetosphere-ionosphere coupling also result in deformation of the plasmapause (Goldstein et al. 2003b, 2003c).

The plasmasphere can be used as a diagnostic tool to investigate the magnetosphere's electric fields because its structure is highly sensitive to the electric fields. The strength of the large-scale convection electric field was modeled using the location of the plasmapause (Maynard and Chen, 1975). The degree of shielding was investigated using the shape of the plasmapause (Ejiri 1981; Ebihara and Ejiri 2003). The corotation lag (~10%) was evaluated using a distinguishable structure of the plasmapause (Burch et al. 2004). The response time between the solar wind electric field and the electric field in the inner magnetosphere has been evaluated (Goldstein et al. 2003a). Using two-dimensional images of the plasmasphere, snapshots of its electric fields were obtained for the entire plasmasphere (Gallagher and Adrian, 2007), and also along the plasmapause (Goldstein et al. 2004b).

2.3. Fate of Plasmaspheric Plasma

Erosion is the most drastic large-scale phenomenon in the plasmasphere. The onset of erosion is delayed by ~30 min from the enhancement of the solar wind electric field (Goldstein et al. 2003a). The enhanced convection electric field peels away the outer layer of the plasmaspheric plasma. A plasma tail (Grebowsky, 1970, or Figure 2c) or a drainage plume (Sandel et al. 2001, or Figure 2e) is thought to be a manifestation of the path of the peeled plasma. In the noon-dusk sector, sunward drifting cold ions have already been observed at geosynchronous orbit (Freeman 1969, Borovsky and Denton 2008). Borovsky and Denton (2008) confirmed that the drainage plume plasma moves sunward with flow speeds that decrease as storms progress. The integrated mass fluxes in the plumes are ~2×10^{26}

ions/s in the early stage of magnetic storms. It is estimated that ultimately, a total of ~2×10^{31} ions (34 tons of protons) is drained from the main body of the plasmasphere during a magnetic storm. Plumes exhibit large velocity fluctuations, suggesting a turbulent condition, as was previously suggested by Matsui et al. (1999).

The fate of the drained plasma is not well known. During magnetic storms, cold ions have been observed on, or just outside the magnetopause (e.g., Freeman 1969, Elphic et al. 1996, Borovsky et al. 1997). Foster et al. (2004a) observed a cold plume plasma with its leading edge making contact with a cusp region at the ionospheric altitude. The transport rates of the plasmaspheric material were estimated to be ~10^{26} ions/s (Elphic et al. 1997) and >10^{26} ions/s (Foster et al. 2004a). Recently, McFadden et al. (2008) have shown clear evidence that the cold plume plasma exists in open flux tubes, suggesting that the cold plume plasma participates in the magnetic reconnection at the dayside magnetopause. This observed fact supports the idea that the cold plume plasma changes from a closed field line to an open field line at the dayside magnetopause and moves antisunward through the lobe region (Borovsky et al. 1997, Elphic et al. 1997).

Moore et al. (2008) used the term "plasmaspheric wind" to describe the cold plasma population that originates from the plasmasphere. They investigated the fate of the plasmaspheric wind by test particle simulation under 3-D magnetospheric fields provided by a global MHD simulation. The plasmaspheric wind escapes from the magnetosphere downstream, rather than being recycled through the inner magnetosphere. They found that the contribution from the plasmaspheric wind is negligible in comparison with the solar wind protons for the southward IMF condition but becomes significant for the subsequent northward IMF condition.

The plasmasphere is of importance in the dispersion relations of waves, which lead to scattering of the energetic particles trapped in the inner magnetosphere (e.g., Lam et al. 2007, Shprits et al. 2008b, Varotsou et al. 2008, Gamayunov and Khazanov 2008, Gamayunov et al. 2009, Breneman et al. 2009). Chen et al. (2009) evaluated the path-integrated gain of electromagnetic ion cyclotron (EMIC) waves and found that the minimum cyclotron-resonant electron energy occurs in the plasmaspheric plume. The minimum resonant electron energies are several MeV in plumes and near the plasmapause, and >8 MeV in the low-density trough. See Sects. 6.3.2 and 6.4.2 for a more detailed description in this regard.

3. Warm Plasma

In-situ measurements have shown the presence of a variety of ions whose temperatures ranging between a few eV and hundreds of eV (e.g., DeForest and McIlwain 1971, Comfort and Horwitz 1981, Kaye et al. 1981, Fennell et al. 1981, Olsen 1981, Quinn and Johnson 1982, Sojka et al. 1983, Nagai et al. 1983, Sagawa et al. 1987, Olsen et al. 1987, Collin et al. 1993, Yamauchi et al. 1996).

Chappell et al. (2008) have clarified that the warm plasma represents an intermediate energy population (a few eV to hundreds of eV) that is too high in energy to be a direct upward flow of the ionosphere (0.1 to a few eV) and too low in energy to be accepted as part of the dominant plasma sheet (1–10 keV) or ring current (10–100 keV) populations. The warm plasma population tends to appear in the morning to early afternoon sector, which is called the "warm plasma cloak" (Chappell et al. 2008). The pitch angle distribution of the warm ions is isotropic, bidirectional field-aligned, unidirectional field-aligned, or pancake-like, and their occurrence rates depend on the local time, magnetic activity, and ionic species (Comfort and Horwitz 1981, Nagai et al. 1983, Collin et al. 1993).

The direct source mechanism and development of the warm ions is still a subject of debate. The uncertainty arises from the fact that these ions can be accelerated, heated, and transported by different means. The acceleration mechanisms include quasi-static parallel electric fields in the ionosphere (Mizera and Fennell 1977, Frahm et al. 1986), substorm-associated induction electric fields in the magnetosphere (Quinn and McIlwain 1979), and ion cyclotron waves (Klumpar 1979). The heating mechanism includes cyclotron turbulence near the equatorial plane (Olsen et al. 1987). The transport mechanisms include convection from the nightside (Fennell et al. 1981, Chappell et al. 2008) and substorms (Moore et al. 1981). In addition, it has been suggested that the ring current population becomes warm ions due to its interaction with thermal plasmas, that is, due to Coulomb drag (Jordanova et al. 1996).

It has been pointed out that a field-aligned pitch angle distribution of ions does not always indicate a direct supply from the ionosphere (Nagai et al. 1983). The presence of ions in the loss cone is the best indication of such a direct supply.

Warm ions are sometimes accompanied by a wedge-like energy dispersion in energy vs. time spectrograms. These wedge-like structures have been observed by Viking (Yamauchi et al. 1996, Ebihara et al. 2001), Equator-S (Ebihara et al. 2008b), and Cluster (Yamauchi et al. 2009) when the satellites traverse the inner magnetosphere in the radial direction. The shape of this dispersion is well understood to represent a convective transport from the nightside plasmasphere (Ebihara et al. 2001), and the source population of the warm H^+ is estimated to be ~10 eV in the near-Earth plasma sheet (Ebihara et al. 2008b), which is obviously distinct from the typical plasma sheet population (~keV).

Warm (suprathermal) electrons are also supplied from not only the ionosphere (Petersen et al. 1977; Khazanov et al. 1996) but also the plasma sheet (Khazanov et al. 1996). Bortnik et al. (2007) have shown that fluxes of the warm electrons at all energies increase with increasing magnetic activity. It has been suggested that the warm electrons tend to be more likely associated with ECH emissions and upper-band whistler-mode chorus waves (e.g., Horne et al. 2003; Ni et al. 2008).

4. Ring Current

4.1. Carrier of Ring Current

A complete or incomplete ring-like region where the plasma pressure (energy density) is high is hereinafter termed a ring current. The general expression of the ring current is given by Parker (1957) as follows:

$$\begin{aligned}\mathbf{J}_\perp &= \mathbf{J}_M + \mathbf{J}_B + \mathbf{J}_c \\ &= \frac{\mathbf{B}}{B^2}\times\left[\nabla P_\perp + \left(P_\parallel - P_\perp\right)\frac{\left(\mathbf{B}\cdot\nabla\right)\mathbf{B}}{B^2}\right]\end{aligned} \tag{1}$$

where $\mathbf{J}_M$, $\mathbf{J}_B$, $\mathbf{J}_C$, $P_\perp$, $P_\parallel$, $\mathbf{B}$ are the magnetization current (due to gyration), grad-B drift current, curvature drift current, perpendicular pressure, parallel pressure, and magnetic field, respectively. The inertial current is usually negligible in the inner magnetosphere. The pressure terms are given by

$$P_\perp = \frac{1}{2}\sum_i \int F_i(v,\alpha) m_i v^2 \cos^2\alpha dv d\alpha \tag{2}$$

$$P_\parallel = \sum_i \int F_i(v,\alpha) m_i v^2 \sin^2\alpha dv d\alpha \tag{3}$$

where F, i, m, v, and α are the distribution function of particles, particle species, mass, speed, and pitch angle, respectively. Positively (negatively) charged particles drift westward (eastward) due to the grad-B and curvature drifts. Thus, the drift currents $\mathbf{J}_B$ and $\mathbf{J}_C$ flow westward in the Earth's magnetosphere. For isotropic pressure ($P = P_\perp = P_\parallel$), the contributions from $\mathbf{J}_B$ and $\mathbf{J}_C$ are canceled by a part of $\mathbf{J}_M$, and the resultant electric current is simply expressed as $\mathbf{J}_\perp = \mathbf{B}\times\nabla P/B^2$. Thus, the contribution from $\mathbf{J}_M$ is significant, while the drift currents ($\mathbf{J}_B$ and $\mathbf{J}_C$) are less so. In this particular case, the pressure peak ($dP / dL = 0$) is located along the shear of the electric currents, that is, a westward current in the outer region and an eastward current in the inner region. The idea that "the ring current flows westward because ions drift westward and electrons drift eastward" is incorrect.

In-situ observations have shown that the plasma pressure is primarily sustained by ions with an energy that ranges from ~1 keV to ~a few hundred keV (Frank,

1967, Smith and Hoffman, 1973, Williams, 1981, Daglis et al. 1993). The H^+ ions usually make the greatest contribution to the plasma pressure, though the energy density of O^+ ions occasionally dominates that of H^+ ions during particular magnetic storms (Lundin et al. 1980, Lennartsson et al. 1981, Krimigis et al. 1985, Hamilton et al. 1988, Daglis et al. 1999). Other ionic species such as He^+, He^{++}, O^{++} (Krimigis et al. 1985), N^+ (Liu et al. 2005b), and $O^{\geq+3}$ (Ebihara et al. 2009a), have also been identified in the ring current region. The N^+/O^+ ratio is ~0.314 during quiet times, and it decreases with $F_{10.7}$ (Liu et al. 2005b). $O^{\geq+3}$ and $O^{+,++}$ are almost simultaneously enhanced in the heart of the ring current during magnetic storms (Ebihara et al. 2009a).

He^+ and O^+ ions are thought to originate in the Earth, while He^{++} and $O^{\geq+3}$ ions are thought to originate in the Sun. To better understand the ring current, the essential problem lies in understanding the transport, acceleration, and loss processes of these particles that have different origins.

The contribution of electrons to the ring current is not well understood. During quiet times, ~1–50 keV electrons have been found to contribute to 1% (Liu et al. 2005a) of the ring current. During active times, these electrons have been found to contribute to ~25% (Frank, 1967), and 8–19% (Liu et al. 2005a) of the ring current. A simulation has also predicted that the electrons contribute to and ~2% during quiet times and ~10% during active times (Jordanova and Miyoshi 2005). The reason for their small contribution to the ring current is unknown. The smallness may come from the relatively low temperature of the electrons in the nightside plasma sheet (Baumjohann et al. 1989) or from rapid losses of electrons.

Dessler and Parker (1959) and Sckopke (1966) developed a formula that relates the total energy of trapped particles to the magnetic field perturbation at the center of the Earth. Greenspan and Hamilton (2000) confirmed that this formula holds true on average when using the *Dst* index as a proxy for the magnetic field perturbation at the center of the Earth. On the other hand, Turner et al. (2001) have shown that the ring current ions contribute, on average, half of the *Dst* index.

4.2. Structure of Ring Current

Chapman and Ferraro (1933) predicted the existence of a circular ring of current surrounding the Earth. In our time, a detailed picture of the ring current has been obtained by the following different observational means.

1. *Ground-based measurements of the magnetic deflection induced by the ring current* (e.g., Akasofu and Chapman 1964, Kamide and Fukushima 1971, Kamide 1974, Clauer and McPherron 1980). The averaged magnetic field deflection observed at a geomagnetically low latitude is used to derive the *Dst* index (Sugiura, 1964). The local time asymmetry of the ground magnetic deflection can be used to measure the asymmetry of the ring current (Akasofu

and Chapman 1964, Cahil 1966), though one must be careful to take into account the contribution from the field-aligned current (Ohtani et al. 2007a).

2. *In-situ measurements of energetic particles*. The plasma pressure (energy density of plasma) distribution has been observed (e.g., Frank 1967, Smith and Hoffman, 1973, Lui 1987, Spence et al. 1989, De Michelis et al. 1997, Millilo et al. 2000, 2003, Korth et al. 2000, Ebihara et al. 2002, Lui 2003). The observed pressure is always underestimated because of the finite energy window of the instrument used.
3. *In-situ measurements of the magnetic fields induced by the ring current* (Cahill 1966, Sugiura et al. 1971, Hoffman 1973, Terada et al. 1998, Lui 2003, Le et al. 2004, Vallat et al. 2005, Ohtani et al. 2007a).
4. *Remote sensing of energetic neutral atoms (ENAs) emitted from the ring current* (Jorgensen et al. 1997, Pollock et al. 2001, Brandt et al. 2004, Ohtani et al. 2006, Scime et al. 2006).

On average, the plasma pressure (or the energy density) is fairly symmetric during geomagnetically quiet times (De Michelis et al. 1999, Ebihara et al. 2002, Lui 2003). The plasma pressure (or the energy density) becomes asymmetric during high *AE* (De Michelis et al. 1999), low *Dst* (Ebihara et al. 2002), and high *Kp* (Lui 2003) periods. The H^+ pressure is the highest in the dusk-midnight sector (Lui 2003). Ebihara et al. (2002) found that the degree of the pressure asymmetry depends on the storm phase. During the storm main phase, the energy density of H^+ shows an increase on the nightside and a decrease on the dayside (Ebihara et al. 2002, 2004). During the storm recovery phase, the energy density evolves in the opposite direction and becomes asymmetric. The same tendency has been observed by in-situ particle measurements (Stüdemann et al. 1987, Korth et al. 2000) and by ENA measurements (Brandt et al. 2002a).

On average, the anisotropy of the plasma pressure ($A = P_\perp/P_\parallel - 1$) is large on the dayside (or inner region), and small on the nightside (or outer region) (Lui et al. 1994, De Michelis et al. 1999). At midnight, the anisotropy index A is ~2, ~1, and ~0.5 at L = 3, 4, and 6, respectively (Lui et al. 1994). Thus, the second term in Eq. (1) is important when one evaluates the intensity and force balance of the ring current (Lui et al. 1987, 1994, De Michelis et al. 1999). The pitch angle distribution depends on L and energy (Lyons 1977, Collin et al. 1993, Ganushkina et al. 2005, De Benedetti et al. 2005, Ebihara et al. 2008a).

Tinsley (1981) predicted the existence of a secondary ring current belt that results from ENAs that travel from the core of the ring current. Years later, Søraas et al. (2003) and Sørbø et al. (2006) observed an inner belt of ring current during magnetic storms by using data from the low-altitude satellite NOAA. They termed this inner belt the Storm-Time Equatorial Belt (STEB). The STEB appears at an extremely low L-value near the magnetic equator. Convective transport cannot account for the formation of the STEB. It is plausible that the STEB results from ENAs traveling earthward from the core of the ring current without any influence by the magnetic field. The ENAs can become ions through charge exchange with dense neutral hydrogen and oxygen.

It should be noted that the ring current does not perfectly encircle the Earth as might inferred from the name. The plasma pressure distribution is not axisymmetric with respect to Earth's dipole moment. The asymmetry of the pressure distribution results in uneven current density of the ring current. The rest of the current is thought to flow into/away from the ionosphere along a field line, called field-aligned currents. Electric currents that might be associated with ring current are drawn in Figure 4.

4.3. Transport and Acceleration of Ring Current Particles

4.3.1. Convection

A long-lasting main phase of magnetic storms is associated with a prolonged southward IMF (Kokubun 1972), which results in the enhancement of the large-scale convection (Dungey 1961, Baumjohann and Haerendel 1985, Weimer 2001, 2005, Matsui et al. 2008). A large-scale, dawn-to-dusk convection electric field conveys charged particles from the near-Earth plasma sheet to the dayside magnetopause (Kavanagh et al. 1968). As the particles drift earthward, they gain kinetic energy in order to conserve the first two adiabatic invariants. The first μ and second *J* adiabatic invariants are respectively expressed as (Roederer 1970)

$$\mu = \frac{p^2{}_{\perp}}{2m_0 B}, \tag{4}$$

$$J = \oint p_{\parallel} dl, \tag{5}$$

where m_0 is the rest mass, p is the momentum, and dl is a line element along a field line. If the magnetic field is the dipole, the kinetic energy will be proportional to L^{-3} for an equatorial pitch angle of 90° and to L^{-2} for an equatorial pitch angle of 0° (Ejiri 1978). The ions tend to drift westward due to grad-B and curvature drifts as they gain kinetic energy. As a consequence, the plasma pressure (or the energy density) of ions is increased in the dusk-midnight sector. The convection electric field also conveys the preexisting particles on the dayside to the dayside magnetopause (Ebihara et al. 2002), further developing an asymmetric distribution of the plasma pressure, namely "asymmetric ring current."

It has been confirmed that enhancements of the convection electric field can reasonably account for observations regarding the morphology of the ring current, ion flux enhancements, and observed variations in the *Dst* (Ejiri et al. 1980, Roeder et al. 1999, Korth et al. 2000, Brandt et al. 2002b, Ebihara et al. 2004, Miyoshi and Kataoka 2005, Burke et al. 2007), and numerical simulations (Wolf et al. 1982, Fok et al. 1996, Kozyra et al. 1998a, Ebihara and Ejiri 1998, 2000,

Jordanova et al. 1999, Liemohn et al. 1999, 2001, Brandt et al. 2002b, Garner et al. 2004, Ebihara and Fok, 2004, Liemohn et al. 2005). During the super storm of November 2003, the intensified convection electric field could account for the ion injection deep into $L = 1.5$ (Ebihara et al. 2005a).

When the convection electric field becomes weak during a storm's recovery phase, these particles tend to drift azimuthally, resulting in symmetric distribution of the plasma pressure, namely "symmetric ring current" (Korth et al. 2000, Ebihara et al. 2002).

The rate of increase of kinetic energy due to the electrostatic field is given by $q\mathbf{V}\bullet\mathbf{E}$, where q is charge, $\mathbf{V}$ is the drift velocity, and $\mathbf{E}$ is the electric field. The upper limit of the particle energy to be accelerated is determined by the total electric potential imposed on the magnetosphere. The cross polar cap potential, which is a measure of the net potential, shows saturation for a large solar wind electric field (Reiff et al. 1981, Wygant et al. 1983, Siscoe et al. 2002, Ober et al. 2003, Hairston et al. 2005). DMSP satellite measurements indicate that the saturation limit of the cross polar cap potential was about 260 kV for the severe storms of October–November 2003 (Hairston et al. 2005). This saturation is thought to have resulted from the Region 1 field-aligned current (Siscoe et al. 2002), ionospheric conductance (Merkin et al. 2005), the impedance mismatch between the solar wind and ionosphere (Kivelson and Ridley 2008), and a current-limited voltage generator (Borovsky et al. 2009). Lopez et al. (2009) have proposed a mechanism that explains the nonsaturated behavior of the ring current intensification under a saturated condition.

The details of structure and generation mechanism of the electric field in the inner magnetosphere remain controversial. The electric field measured near the plasmapause is highly variable and its amplitude increases with magnetic activity (Maynard et al. 1983). When averaged, the electric fields are qualitatively in agreement with ionospheric observations (Maynard et al. 1983, Baumjohann and Haerendel, 1985, Rowland and Wygant 1998, Matsui et al. 2008). The cause of fluctuations in the electric fields in the inner magnetosphere has not yet been determined. Hori et al. (2005) have pointed out that no systematic increase was found in plasma sheet electric fields (>9 Re) during a storm's main phase. Their result may introduce ambiguity to the idea that enhanced convection conveys the plasma sheet particles into the inner magnetosphere during the main phase of a storm. A large spike in the amplitude of the poleward electric field has frequently been observed in the magnetosphere at subauroral latitudes (Maynard et al. 1980) and is described in detail in Sect. 4.6.1.

The response time of the inner magnetospheric convection electric field to the solar wind electric field is also uncertain. On the basis of their observation of plasmaspheric erosion, Goldstein et al. (2003a) obtained a response time of ~30 min. They suggested that the propagation time from the magnetopause to the ionosphere takes ~3–15 min, followed by ~10–25 min for complete reconfiguration of the ionospheric convection. Kikuchi et al. (1996, 2008) have shown that the dawn-to-dusk convection electric field is "immediately" transmitted from the polar region to the inner magnetosphere and to the equatorial

ionosphere as well. This suggests that reconfiguration of the ionospheric convection can be effected quickly, at the speed of light, by the TM_0 mode waves in an Earth-ionosphere waveguide (Kikuchi et al. 1978).

4.3.2. Substorm

Impulsive enhancements of particle fluxes have frequently been observed near geosynchronous orbit (Konradi et al. 1967, DeForest and McIlwain, 1971, McIlwain, 1974) and inside the geosynchronous orbit (Reeves et al. 1996, Ohtani et al. 2007b). These enhancements are associated with substorms that are identified by ground magnetic fields (Konradi et al. 1967, DeForest and McIlwain 1971, Kamide and McIlwain 1974). Because of the sudden appearance of particles, this phenomenon is called a "substorm injection."

A "substorm injection" that is not accompanied by energy dispersion is called a "dispersionless" injection. Such an injection has been observed at least at $4 \leq L \leq 8$ (Friedel et al. 1996). After injection, a cloud of the injected particles begins to display energy dispersion due to drift velocities, depending on its energy (DeForest and McIlwain 1971). Mauk and McIlwain (1974) specified a zero-energy boundary of the injected cloud at the geosynchronous orbit, and found that the location of the boundary depends on MLT and *Kp*. They suggested a spiral-shaped boundary of injection, called an injection boundary. Konradi et al. (1975) extended the injection boundary to the morning quadrant by reflecting the spiral-shaped evening boundary about the midnight meridian. As a consequence of the reflection, the injection boundary has a dented form, shaped somewhat like the numeral "3". Following the study of Konradi et al., this 3-shaped boundary is commonly referred to as an injection boundary (e.g., Mauk and Meng 1983, Lopez et al. 1990, Reeves et al. 1996). However, the existence of the 3-shaped boundary is still a controversial subject. Zhang et al. (2009) simulated a plasma bubble ejected by a substorm and demonstrated that the inner edge of the plasma sheet has a 3-shaped boundary.

A "substorm injection" is thought to be caused by the relaxation of the magnetic field associated with a substorm (Walker et al. 1976). In the course of such relaxation (dipolarization), a strong dawn-dusk induction electric field was observed (Aggson et al. 1983). A 2-min envelope of the dawn-dusk electric field having an amplitude of 30 mV/m correlates with that of the inductive fields of the collapsing magnetic field. Low-frequency (10 s) and high-frequency ($t < 1$ s) wave variations were also present throughout the event.

At geosynchronous altitude, the ion temperature increases significantly, while the ion density remains almost constant during the course of a substorm (Birn et al. 1997a). This quite likely suggests that the particles are significantly accelerated. A test particle simulation performed in the three-dimensional MHD field showed that ions with an energy >20 keV are accelerated by the cross-tail electric field under nonadiabatic motion during dipolarization (Birn et al. 1997b). Particles can also be accelerated by a parallel component of the induction electric

field (Quinn and McIlwain 1982), and by magnetic field fluctuations having frequencies that are close to the gyrofrequencies of the ions (Ono et al. 2009). The test particle simulation performed by Birn et al. (1997b) showed that ions with an energy <20 keV are not effectively accelerated by this process because the $E \times B$ drift dominates the cross-tail drifts. A substorm-associated dipolarization event probably results in both a local acceleration (as was observed by Lopez et al. 1990) and the inward transport of particles (as was observed by DeForest and McIlwain 1971, Mauk and McIlwain 1974). Sergeev et al. (1998) have emphasized that one can observe an increase, a decrease, or no variation of flux after a substorm, and that particle flux variation depends on the energy and radial flux gradient.

The net result of a "substorm injection" on the ring current is still being debated. Mitchell et al. (2003) observed intensifications of H^+ and O^+ immediately following substorms. H^+ and O^+ were not simultaneously enhanced, suggesting that a mass-dependent acceleration process probably takes place. Simulations have shown that a substorm results in net intensification of the ring current (Fok et al. 1999, Zhang et al. 2009). Further observations and simulations are awaited that will quantitatively evaluate the overall influence of a substorm on the development of the ring current.

4.3.3. Compression of Magnetosphere

Sometimes the magnetosphere is compressed by an abrupt enhancement of the solar wind dynamic pressure prior to the main phase of a storm. This is called storm sudden commencement (SSC), which is followed by a storm's initial phase. Due to magnetospheric compression, ions having an energy between keV and hundreds-of-keV are increased by ~25–40% due to adiabatic energization (Lee et al. 2007). Due to an azimuthal induction electric field (Shinbori et al. 2004), preexisting particles are expected to drift in the radial direction. The magnetospheric state established in the initial phase may also play an important role in the subsequent development of the ring current during the main phase of a storm.

4.3.4. Wave-Particle Interaction

EMIC waves can be excited by cyclotron resonant instability with anisotropic ring current H^+, leading to heavy ion heating perpendicular to the ambient magnetic field (e.g., Gendrin and Roux 1980, Anderson and Fuselier 1994, Thorne and Horne 1994, Horne and Thorne 1997). This process may be efficient when the concentration of O^+ is significantly enhanced, and contribute to the observed acceleration of O^+ up to the ring current energy. Recently, Pickett et al. (2010) found the triggered emission of EMIC waves in the inner magnetosphere. Omura et al. (2010) developed a nonlinear wave growth theory of this triggered

emissions, which may cause efficient acceleration of ions in the inner magnetosphere.

4.4. Source of Ring Current Particles

The importance of the number density in the plasma sheet has been suggested based on observations (Thomsen et al. 1998, Smith et al. 1999, Liemohn et al. 2008), and simulations (Chen et al. 1994, Kozyra et al. 1998b, Ebihara and Ejiri 1998, 2000, Kozyra and Liemohn 2003, Ebihara et al. 2005a). In stronger storms, the plasma sheet density at geosynchronous altitude becomes high (Liemohn et al. 2008). In super storms, on average, density peaks appear 9 hours before the storm peak, and around the storm peak. For the super storm of November 20, 2003, the enhancement of the plasma sheet density around the storm peak is necessary in order to account for the large development of the ring current (Ebihara et al. 2005a).

On average, the plasma sheet density is fairly well correlated with the solar wind density (Terasawa et al. 1997, Borovsky et al. 1998, Ebihara and Ejiri, 2000). Terasawa et al. (1997) found that the plasma sheet becomes dense and cold when the IMF is northward. The best correlations between the plasma sheet parameters and the IMF is obtained when the solar wind density is averaged over 5–12 h prior to the plasma sheet observations. For given plasma pressure in the plasma sheet, cold-dense plasma sheet results in deeper penetration of the plasma sheet ions (Garner 2003, Lavraud and Jordanova, 2007). At geosynchronous altitude, the density is usually 0.4–2 cm^{-3}, though it sometimes exceeds 2 cm^{-3} (Borovsky et al. 1997, Thomsen et al. 2003, Lavraud et al. 2005). This is called a super dense plasma sheet. A hot and super dense plasma sheet is detected at geosynchronous orbit for ~20 h following the convection onset that is led by high-speed coronal hole streams (CHS) (Denton and Borovsky, 2008).

Some entry processes from the solar wind into the magnetosphere have been suggested: magnetic reconnection near the subsolar point under a southward IMF (Dungey 1961), double lobe reconnection under a northward IMF (Song and Russell 1992, Song et al. 1999), diffusive entry (Terasawa et al. 1997, Fujimoto et al. 1998), Kelvin-Helmholz instability (Hasegawa et al. 2004), and cusp entry (Fritz et al. 2003). Once it has entered, the plasma is transported to the inner magnetosphere by the convection electric field through the plasma sheet (Spence and Kivelson 1993), eddy diffusion (Borovsky et al. 1998), and convection throughout the lobe (Ebihara et al. 2009a).

The Earth's ionosphere is also a significant source of ring current particles, as evidenced by in-situ observations of O^+ in the heart of the ring current (Lundin et al. 1980, Lennartsson et al. 1981, Krimigis et al. 1985, Hamilton et al. 1988, Daglis et al. 1999, Pulkkinen et al. 2001). At least three distinct time scales for the supply of O^+ have been determined: ~10s of minutes (Daglis and Axford 1996, Daglis et al. 2000, Mitchell et al. 2003), ~days (Hamilton et al. 1988, Daglis et al.

1999), and ~years (Young et al. 1982, Pulkkinen et al. 2001, Greenspan and Hamilton, 2002).

On a short time scale (~10s of minutes), the variation of O^+ ions is associated with a substorm expansion. This variation may be attributed to a rapid supply of ions from the ionosphere to the equatorial plane (Daglis and Axford 1996), or to a localized energization of preexisting ions (Mitchell et al. 2003). Mitchell et al. (2003) stressed that the rapid enhancement of O^+ just after substorms cannot be explained by a rapid supply from the ionosphere. Trajectory tracing of O^+ predicts that it usually takes ~1–2 h to reach the equatorial plane from the ionosphere (Cladis and Francis 1992). Nosé et al. (2009a) have presented observational evidence that during magnetic storms, the O^+ outflow commences in the topside ionosphere within several minutes immediately following a substorm, and that subsequently, O^+ is increased in the near-Earth plasma sheet on a time scale of 1 h.

The medium time-scale (~days) variation is associated with a magnetic storm. During magnetic storms, O^+ ions are enhanced in the ring current (Krimigis et al. 1985, Hamilton et al. 1988, Daglis et al. 1999, Pulkkinen et al. 2001). The O^+ concentration is also increased in the plasma sheet (Lennartsson and Sharp 1982), which can be attributed to an enhancement of the auroral and polar outflow of O^+ (Yau et al. 1985a, Abe et al. 1996). In-situ observations have suggested that O^+ can be directly introduced from the ionosphere into the inner magnetosphere during magnetic storms (Kaye et al. 1981, Sheldon et al. 1998, Yao et al. 2008).

The long time scale (~years) variation is associated with variations in the solar cycle. Outflowing O^+ from the topside ionosphere is increased with $F_{10.7}$ (Yau et al. 1985b). O^+ concentration is also increased with increasing $F_{10.7}$ in the plasma sheet in the energy 0.1–16 keV/e (Lennartsson et al. 1989) and 9.4–212.1 keV/e (Nosé et al. 2009b).

Ebihara et al. (2006) emphasized the importance of the thinness of the current sheet in transporting O^+ from the ionosphere to the inner magnetosphere. When outflowing O^+ first encounters the current sheet, it moves in a meandering path and undergoes nonadiabatic acceleration in the current sheet where the gyroradius is close to the curvature radius of a field line (Sergeev et al. 1983, 1993). When the current sheet is thick, the O^+ gains more energy and undergoes grad-B and curvature drifts. When energized too much, O^+ is difficult to drift earthward by the E×B drift (Ebihara and Ejiri 2000, Garner 2003, Lavraud and Jordanova 2007). In order to effectively supply O^+ from the current sheet to the inner magnetosphere, a thin current sheet and strong convection are needed (Ebihara et al. 2006). During magnetic storms, the magnetic field is stretched further (Ohtani et al. 2007a) and the current sheet becomes thin (Sitnov et al. 2008). The storm-time current sheet structure would help the O^+ efficiently propagate into the inner magnetosphere.

4.5. Loss of Ring Current Ions

4.5.1. Charge Exchange

A fast ion captures an electron from a neutral atom to become a fast neutral atom. In the neutral state, a fast atom becomes free of any control by a magnetic field, as has been observed by the IMAGE satellite (e.g., Mitchell et al. 2003). The charge exchange occurs frequently in the region where there is a high concentration of neutral atoms. In the topside ionosphere, oxygen is the dominant neutral species. With increasing altitude, hydrogen becomes dominant (Rairden et al. 1986). The number density of neutral hydrogen is ~500–1000 cm^{-3} at 3 Re, and ~50–100 cm^{-3} at 6 Re (Rairden et al. 1986, Østgaard et al. 2003). The cross sections for the charge exchange have been suggested by Janev et al. (1993) for the H^+–H reaction, by Barnett (1990) for the He^+–H reaction, and by Phanef et al. (1987) for the O^+–H reaction. Because the geocoronal hydrogen is dense at a low altitude, ions with small equatorial pitch angles readily undergo charge exchange. Smith and Bewtra (1976) suggest that the bounce-averaged lifetime is as follows:

$$\langle \tau \rangle = \frac{\cos^{3.5\pm0.2} \lambda_m}{n_H v \sigma_{ch}}, \tag{6}$$

where $<\tau>$, n_H, v, σ_{ch}, and λ_m are the bounce-averaged lifetime, neutral hydrogen density in the equatorial plane, velocity of the ion, charge exchange cross section, and mirror latitude, respectively. The lifetime of H^+ is shorter than that of O^+ for energy less than 45 keV, while it is longer than that of O^+ for energy greater than 45 keV (Fok et al. 1991).

Ebihara and Ejiri (2003) calculated the ring current evolution during weak magnetic storms, and showed that the *Dst* variation is well explained by the ring current simulation with the charge exchange loss. When the charge exchange loss is excluded, the *Dst* variation is obviously different from that observed.

Hamilton et al. (1988) demonstrated a rapid recovery of *Dst* (*e*-folding time scale of ~9.3 h) and a rapid decay of O^+ ions (30–310 keV/e) during the intense storm of February 1986. They suggested that the rapid decay of O^+ could be attributed to the short charge exchange lifetime of O^+. The two-step recovery of *Dst* can be attributed to the rapid decay of O^+ followed by the slow decay of H^+. Fok et al. (1995) simulated the ring current during the February 1986 storm and encountered a problem in the interpretation of the rapid recovery of *Dst*. Kozyra et al. (1998a) pursued the rapid recovery, and suggested that, in addition to charge exchange, precipitation loss plays an important role in the ion loss.

4.5.2. Coulomb Drag

Ions are decelerated by Coulomb collisions with thermal plasma. This is called Coulomb drag. The decay rate has been formulated by Fok et al. (1991) and Jordanova et al. (1996). The Coulomb drag results in redistribution of the ions in the velocity space, and it enhances the low-energy ion precipitating fluxes inside the plasmasphere (Jordanova et al. 1996). The kinetic energy of the ions is transferred to the thermal electrons (Kozyra et al. 1987) and to the ionosphere, contributing emissions at 630 nm. The resultant glow of these emissions manifests in what are termed stable auroral red (SAR) arcs (Cole 1965, Kozyra et al. 1997). Coulomb drag is insignificant in ring current decay because the loss rate is much smaller than that of the charge exchange at energy >10 keV (Fok et al. 1991) and because the plasmasphere shrinks during magnetic storms.

4.5.3. Coulomb Scattering

Ions are scattered by Coulomb collisions with thermal plasma and are precipitated into the ionosphere in what is called Coulomb scattering. Jordanova et al. (1996) found that, in general, the decay rates are small. The decay rates due to Coulomb scattering are much smaller than those due to Coulomb drag by two orders of magnitude.

4.5.4. Wave-Particle Interaction

Ions are scattered by the EMIC waves (e.g., Cornwall 1970, Summers 2005, Summers et al. 2007) that are frequently observed in the inner magnetosphere (e.g., Anderson et al. 1992, Mursula et al. 2001; Engebretson et al. 2007). EMIC waves are primarily caused by the temperature anisotropy of ions with an energy of 10–50 keV (Cornwall 1977). Such temperature anisotropy can be easily established by the charge exchange as represented by Eq.(6), as well as by convective transport. Jordanova et al. (1997) calculated the growth of EMIC waves and the evolution of the ring current with pitch angle diffusion due to wave-particle interaction. They found that EMIC waves are readily developed near the plasmapause on the duskside, resulting in scattering of the ions. The localized precipitation of ions results in the proton auroral emission associated with plumes, and is remotely monitored by an auroral imager onboard the IMAGE satellite (Fuselier et al. 2004, Spasojevic et al. 2005, Jordanova et al. 2007).

Thorne and Horne (1997) showed that the EMIC waves are absorbed efficiently at high magnetic latitudes via cyclotron resonant interactions with energetic O^+. When the fractional composition of ring current O^+ exceeds 60%, cyclotron absorption by resonant O^+ can become so severe to totally suppress wave excitation. The storm-time development of the ring current may be modulated by

the relative composition of energetic O^+ through resonant interaction with EMIC waves.

4.5.5. Adiabatic Loss Cone Loss

When ions drift earthward, their equatorial pitch angle shifts toward 90° due to the conservation of the first two adiabatic invariants. The loss cone angle is also rapidly widended as the ions drift earthward, so that ions with a small pitch angle encounter the loss cone at a certain *L*-value without any pitch angle scattering (c.f., Figure 9 of Ebihara and Ejiri 2003). This is called adiabatic loss cone loss. Jordanova et al. (1996) have suggested that adiabatic loss cone loss is sufficient to explain the ion precipitation observed by satellites. Ebihara and Ejiri (2003) precisely calculated the precipitating ion flux and found that the energy flux of the precipitating flux is much smaller than that observed by the DMSP satellite. The calculated loss rate of the ring current due to the adiabatic loss cone loss is ~1–2% for a weak storm. The importance of the adiabatic loss cone loss is yet to be conclusively determined.

4.5.6. Violation of First Adiabatic Invariant

The first adiabatic invariant of ions is no longer conserved when the ions are situated in a stretched magnetic field line. The pitch angle is scattered and the ions are precipitated into the ionosphere. The characteristics of such scattering due to field line curvature (FLC) have been theoretically studied (Sergeev et al. 1983, Büchner and Zelenyi 1989, Delcourt et al. 1996). The FLC scattering is thought to be responsible for the global precipitation of ions with a pitch angle distribution that is almost isotropic at the topside ionosphere (Sergeev et al. 1993). The equatorward edge of the isotropic precipitation is called the isotropic boundary (IB), whose latitude, they suggest, is a manifestation of the stretching of the magnetic field on the nightside.

4.5.7. Magnetopause Loss

When ions encounter the magnetopause, they are thought to escape from it (Möbius et al. 1986, Zong and Wilken 1999, Christon et al. 2000, Keika et al. 2004). Herein, we refer to two types of magnetopause loss of ring current particles. In Type 1, the plasma sheet density suddenly decreases on the nightside. In Type 2, the dayside magnetopause shrinks.

Type 1. Liemohn et al. (2001) calculated the evolution of the ring current by changing the convection electric field and suggested that most of the main phase ring current is due to the fact that the ions have open drift paths. This implies that under a strong convection electric field, the ions are injected from the plasma

sheet on the nightside and ejected to the dayside magnetopause. The compensation between the inflow and the outflow determines the budget of the total energy of particles within the inner magnetosphere, that is, the ring current. When the plasma sheet density abruptly decreases, this change is transmitted sunward so that the total energy of the particles decreases (Ebihara and Ejiri 1998, 2003, Liemohn et al. 2001, Jordanova et al. 2003). The transit time involved depends entirely on the strength of the convection electric field. When the plasma sheet density and the convection electric field simultaneously decrease, the transit time will be very long and the change in the plasma sheet density is not effectively transmitted into the inner magnetosphere because the last-closed equipotential is expanded (Ejiri 1978). In the case of Type 1, the degree of loss depends on the plasma sheet density on the nightside and the strength of the convection electric field.

Type 2. Keika et al. (2004) have shown that the energetic ions originating from the magnetosphere are frequently observed outside the magnetopause during magnetic storms. The energy flux of outflowing ions is well correlated with the square root of the solar wind dynamic pressure, rather than the solar wind electric field (Keika et al. 2005). The energy flux of outflowing ions during the recovery phase is comparable to that during the main phase. Keika et al. (2005) have suggested that the magnetospheric ions are lost due to magnetic drift, rather than the $E \times B$ drift. In the case of Type 2, the degree of the loss depends on the standoff distance of the dayside magnetopause.

4.6. Influence on Other Regions and Energy Regimes

4.6.1. Ring Current-Ionosphere Coupling

The electric current (ring current) cannot be completely closed in the inner magnetosphere. Vasyliunas (1970) and Wolf (1970) have suggested the following conceptual framework regarding the closure of the electric current. The convection electric field conveys hot plasma into the inner magnetosphere, and enhances the plasma pressure. A remnant of the current must flow into/away from the ionosphere along a field line to complete the closure. To conduct away the space charge deposited by the field-aligned current, an additional electric field must be developed in the ionosphere. This electric field is fed back into the magnetosphere, affecting the $E \times B$ drift velocity of the trapped particles. Thus, the electric field induced by the ring current potentially influences the dynamics of the inner magnetosphere.

The ring current tends to generate a downward (magnetosphere to ionosphere) field-aligned current on the duskside, and an upward (ionosphere to magnetosphere) current on the dawnside. This current system resembles the Region 2 field-aligned current (Iijima and Potemra 1976). The direction of the

resultant electric field is eastward on the nightside, which is opposite to that of the convection electric field. Thus, the resultant electric field is called a shielding electric field, whose existence has been supported by ground-based observations (Fejer et al. 1979, Kelley et al. 1979, Spiro et al. 1988, Kikuchi et al. 2008, 2010, Ebihara et al. 2008c). An overshielding condition can be established immediately following an abrupt decay of the Region 1 current (Spiro et al. 1988, Peymirat et al. 2000, Ebihara et al. 2008c), an abrupt decay of the aurora oval (Ebihara et al. 2004), or an abrupt contraction of the auroral oval (Kikuchi et al. 2008), because the ring current-associated field-aligned current cannot decay as quickly as the Region 1 current.

The shielding electric field may elongate the pattern of the duskside convection cell toward the equatorward of the dawnside convection cell. The resultant convection cell resembles the Harang discontinuity (Erickson et al. 1991, Ebihara et al. 2005a, Gkioulidou et al. 2009). During a storm, the ring current intensifies and the elongation is further developed. Finally, a flow reversal on the dawnside develops (Ebihara et al. 2005a), which was observed by a satellite (Ebihara et al. 2005a) and by HF radar (Kataoka et al. 2007) at subauroral latitudes. It appears that a strong westward electric field is established near the eastern edge of the flow reversal, resulting in the intensification of the tens-of-keV proton fluxes in the inner magnetosphere (Fok et al. 2001, Ebihara and Fok 2004). Such unusual dawnside enhancements of tens-of-keV proton fluxes were first confirmed by IMAGE satellite observations (Brandt et al. 2002b). It has also been suggested that the shielding electric field impedes the development of the ring current (Ebihara et al. 2005b). The intensity of the ring current was previously thought to be simply proportional to the plasma sheet density (N_{ps}) (Chen et al. 1994, Ebihara et al. 1998, 2000, Liemohn et al. 2001), but the shielding may result in the intensity being proportional to the square root of N_{ps} (Ebihara et al. 2004). The degree of the impediment may depend upon the conductivity (Spiro and Wolf 1984, Ebihara et al. 2004).

In the premidnight sector, the downward Region 2 current tends to flow into the ionosphere equatorward of the auroral oval. The upward Region 1 current tends to flow away from the auroral oval. A poleward electric field is then established on the duskside to complete the closure of the Region 1 and Region 2 currents. The conductivity is high in the auroral oval due to the precipitation of energetic particles, while the conductivity is low in the subauroral region. The poleward electric field is strengthened in the subauroral region because of low conductivity, resulting in a rapid, westward plasma flow in the subauroral region (Anderson et al. 1993). This phenomenon has been described by various terms: Polarization Jet (PJ) (Galperin et al. 1973), SubAuroral Ion Drift (SAID) (Spiro et al. 1979), Drift Spike (DS) (Unwin and Cummack, 1980), SubAuroral Electric Field (SAEF) (Maynard et al. 1980, Karlsson et al. 1998), and SubAuroral Polarization Stream (SAPS) (Foster and Vo, 2002). PJ, SAID, and DS probably refer to a subregion of SAPS.

Data from the DMSP satellites shows that the latitude of the SAPS channel decreases with a decrease in the Dst index, suggesting that the SAPS is related to

the ring current (Huang and Foster 2007). Seasonal variations in the SAPS have also been noted. There is a strong correlation between the subauroral integrated conductivity and the latitude of the SAPS channel, and there is a strong anticorrelation between the conductivity and the SAPS velocity (Wang et al. 2008). This suggests that the SAPS is a part of the current system caused by a current generator. The SAPS is intensified after a substorm following a delay of >30 min (Anderson et al. 2001), ~10 min (Mishin and Puhl-Quinn 2007), and ~30 s (Nishimura et al. 2008). If a substorm results in a localized enhancement of the plasma pressure, a blob of the plasma pressure will travel inward under the influence of the convection electric field, enhancing the SAPS speed. When this is the case, the delay time can be explained by the traveling time between the source and the observation point. Quasi-periodic variations in the speed of the SAPS have been observed during a time of disturbance (Foster et al. 2004b, Ebihara et al. 2009b), and these may be interpreted in terms of structured, multiple ring currents moving earthward (Ebihara et al. 2009b). Different types of subauroral flows have recently been reported. One study reported is that a westward flow is sandwiched in between eastward flows, a configuration which was termed a mirror eastward flow channel (Makarevich et al. 2009). A rapid, eastward plasma flow was also found, which was termed an abnormal SAID (Voiculescu and Roth 2008).

4.6.2. Ring Current-Thermosphere Coupling

In the course of the precipitation of energetic protons deep into the atmosphere, the protons undergo electron capture, neutral excitation, and electron loss processes. The hydrogen atoms can be left in an excited state so that Lyman, Balmer, or other H series may be radiated (Vallance Jones 1974). The proton aurora is thus considered to be a direct manifestation of proton precipitation from the magnetosphere. A patch of proton aurora in the subauroral region was first observed by Ono et al. (1987). A similar patch was also observed together with intensification of geomagnetic ULF waves that manifest in bursts, the so-called Pc 1 pulsations (Sakaguchi et al. 2007, 2008, Yahnin et al. 2007, Yahnina et al. 2008). The close relationship between the proton auroral spot and the bursts of Pc 1 pulsations implies that the source of the proton precipitation is probably the EMIC waves excited in the ring current. This excitation of the EMIC waves is stimulated by compression of the dayside magnetosphere (Zhang et al. 2008, Yahnina et al. 2008, Usanova et al. 2008) and convective transport (Jordanova et al. 1997), which causes temperature anisotropy or some other instabilities. Jordanova et al. (2006, 2007) simulated the growth rate of the EMIC waves with the evolving ring current H^+, O^+, and He^+ ion distributions. The global distribution of the simulated proton precipitation is similar to that of the proton aurora taken by IMAGE/FUV.

Hardy et al. (1989) have documented the global distribution of precipitating ions. The hemispheric energy input from the ions is 11–17% of that from the electrons. The precipitating ions, however, are the major source of ionization and

conductance in the evening sector (Senior et al. 1987, Senior 1991, Galand and Richmond, 2001), along with Joule heating, an increase in the *E* and *F* region temperature, and strong neutral winds in the lower thermosphere (Galand et al. 2001).

The ENAs emitted from the ring current are suggested to strike the thermosphere and cause the ionization at low latitudes. Rowe (1974) presented the observation that the electron density in the nightside *E* region at Arecibo was significantly enhanced during magnetic storms. Precipitating ENAs are sufficient to account for the electron density enhancement (Lyons and Richmond 1978). Spectrographic photometers onboard TIMED detected anomalous auroral emissions from the nightside thermosphere at low latitudes during intense magnetic storms (Zhang et al. 2006). The brightness of these anomalous emissions is correlated with |*Dst*|. Zhang et al. (2006) suggest that the source of the anomalous emissions is ENAs.

4.6.3. Ring Current-Plasmasphere Coupling

The ring current interacts with the plasmasphere both directly and indirectly. Theoretically, the inner edge of the ion plasma sheet and the plasmasphere can coexist in the "nose" energy dispersion structure (Ejiri et al. 1980, Kozyra et al. 1993). The energy of the ring current ions is degraded by the Coulomb drag and transferred to the thermal plasma. The heat flux is then propagated to the topside ionosphere along a field line, resulting in a glow of emissions that are called SAR arcs (Cole 1965, Kozyra et al. 1987) (see Sect. 4.5.2). SAR arcs can last for ~28 h (Craven et al. 1982) and can be a very bright (~13 kilo Rayleighs) (Baumgardner et al. 2007).

The ring current induces additional electric fields in the ionosphere, known as SAPS and overshielding (Sect. 4.6.1). The deformation of the ionospheric electric field is transmitted to the magnetosphere, and is also thought to result in deformation of the plasmasphere (Goldstein et al. 2003c, 2004a).

4.6.4. Ring Current-Ring Current Coupling

The electric field deformed by the ring current can also deform the ring current itself. Post-midnight enhancements of tens-of-keV ions (Brandt et al. 2002b) can be explained by the electric potential deformed by the ring current (Fok et al. 2003, Ebihara and Fok 2004). The convection electric field is weakened by the ring current, and the strength of the ring current is no longer proportional to the plasma sheet density (Spiro et al. 1984, Ebihara et al. 2004). For a detailed explanation, see Sect. 4.6.1.

Lyons and Williams (1976) have shown that during the main phase of a storm, the flux of the equatorially mirroring ions at >200 keV decreases. Lyons (1977) found that the pitch angle distribution of the ions shows a butterfly pattern having

a minimum flux at a 90° pitch angle in association with a reduction in the equatorial magnetic field. They have attributed the decrease in the 90° ions to adiabatic deceleration (betatron deceleration). Ebihara et al. (2008a) have demonstrated that during the main phase of a storm, the H^+ flux at >80 keV at pitch angles near 90° decreases, while the H^+ flux at near 0° and 180° increases. Ebihara et al. (2008a) have suggested that these variations can be explained by a combination of the betatron deceleration (due to a depression of the equatorial magnetic fields), and Fermi acceleration (due to a shortening of the distance between mirror points). Zaharia et al. (2006) have predicted that the pressure anisotropy ($A = P_\perp / P_\parallel - 1$) is reduced mainly due to the Fermi acceleration under the magnetic field that is depressed by the ring current.

4.6.5. Ring Current-Radiation Belt Coupling

Relativistic trapped particles sometimes show an abrupt decrease during magnetic storms (McIlwain 1966, Williams et al. 1968), in what is called a *Dst* effect, or a ring current effect. The *Dst* effect may be understood, in part, as energy deceleration due to the betatron deceleration and radial displacement due to the conservation of the third invariant (Dessler and Karplus 1961). This process may be valid when the field deformation proceeds slowly enough (Northrop and Teller 1960). For a detailed explanation, see Sect. 6.4.1.

EMIC waves generated from the ring current ions cause pitch angle scattering of the radiation belt electrons (see Sect. 6.4.2), which is another example of ring current-radiation belt coupling. ULF waves driven by ring current ions also have an impact on the radial transport and energization of radiation belt electrons (Ozeke and Mann 2008).

5. Proton Radiation Belt

5.1 Time Variation of Proton Radiation Belt

The inner part of the proton belt, $L < 2.0$, is very stable. Secular changes in the Earth's magnetic field may gradually increase the proton intensity by a factor of 10 due to contacting drift shells (Selesnick et al. 2007). Therefore, the reduction of the Earth's intrinsic magnetic field exerts an impact upon the proton belt. During solar cycles, solar activity causes expansion of the scale height of upper atmosphere, and the collision rate increases at a low altitude. The proton flux shows solar cycle variations that are anti-correlated with solar activities (Miyoshi et al. 2000).

In the outer part of the proton belt ($L > 2$), dramatic variations have been observed, especially during strong interplanetary shocks. For example, during the recorded SSC event on March 24, 1991, a new proton belt was formed within just 3 min (Blake et al. 1992). A similar shock-associated enhancement of the proton belt was observed in 2003 (Looper et al. 2005).

5.2 Source and Loss of Relativistic Protons

It has been though that Cosmic Ray Albedo Neutron Decay (CRAND) is mainly responsible for energies >100 MeV protons. In CRAND, the cosmic ray flux on the atmosphere is backscattered as neutrons which decay into protons and electrons trapped in the inner magnetosphere. Solar protons during proton events are a source of protons of the radiation belt (Hudson et al. 1995, 2004, Kress et al. 2005). The inward transport of protons by radial diffusion is important for their acceleration (Albert et al. 1998, Jordanova and Miyoshi 2005). The dominant causes of loss of protons are Coulomb collisions with plasmaspheric thermal plasma and atmospheric absorption, which have been modeled in a three-dimensional Fokker-Planck simulation for the proton radiation belt (Beutierer et al. 1995). The precipitation into the ionosphere due to the pitch angle scattering is also important.

In the outer part of the proton belt, shock-related compression of the magnetosphere can accelerate solar protons to energies of more than tens of MeV on timescales of tens of seconds (Hudson et al. 1995).

6. Electron Radiation Belt

6.1. Time Variation of Electron Radiation Belt

In the inner belt, the electron flux is usually stable, while the electron flux sometimes increases in association with large magnetic storms. During the strong SSC event on March 24, 1991, injections and drift echoes of tens of MeV electrons were observed at $L = 2$ (Blake et al. 1992, Li et al. 1993, Gannon et al. 2005).

In the slot region and the outer belt, the electron flux shows dynamical time variations on various scales. Electron flux variations in the radiation belts are the result of achieving a balance between source (transport/acceleration) and loss processes (Reeves et al. 2003). Different processes for acceleration/transportation and loss occur simultaneously during storms (see Figure 2 of Reeves 2007; and

reviews Friedel et al. 2002, Millan and Thorne 2007, Shprits et al. 2008a b, Hudson et al. 2008 and references therein).

6.1.1. Storm-Time Variations

Typically, the outer belt flux decreases/disappears during the main phase of a storm then returns to its prestorm level during the early recovery and recovery phases (e.g., Baker et al. 1986, Nagai 1988, Reeves et al. 2003, Miyoshi and Kataoka 2005, Li et al. 2005). The flux sometimes increases to a degree that is higher than its prestorm level. The typical time scale for the flux enhancement of the outer belt is a few days (Nagai 1988, Reeves et al. 1998), depending on the L-shell (e.g., Li et al. 1997, Vassiliadis et al. 2003, 2005), while it has been observed that rapid flux enhancement in the inner portion of the outer belt and in the slot region takes place within a few hours (Baker et al. 1998b, Nagai et al. 2006). As will be discussed later, the decrease and increase in the electrons of the outer radiation belt frequently occur not only in storms but also associated with solar wind disturbances.

Magnetic storms are caused by large scale interplanetary structures. Coronal Mass Ejections (CMEs) and Corotating Interaction Regions (CIRs) have intense electric fields that can drive magnetic storms, though there are several differences between CME- and CIR-driven storms (Borovsky and Denton 2006). CMEs have a strong magnetic field in the sheath as well as the ejecta and exert an interplanetary shock that causes the sudden commencement of the storm. CIRs have a strong magnetic field that is the interface between slow and fast streams, and they are followed in time by CHS. All intense storms ($Dst < -150$ nT) are driven by CMEs during solar cycle 23. Therefore, it is expected that the outer belt will respond differently to CME- vs. CIR-driven storms. Note that the outer belt flux variation is independent of the storm size as measured by the *Dst* index (Reeves et al. 2003). CIR-driven storms are more effective than CME-driven storms for the large flux enhancement of MeV electrons in the outer portion as well as at geosynchronous orbit (Miyoshi and Kataoka 2005). Large flux enhancements of MeV electrons occur at geosynchronous orbit in 80% of intense CIR-driven storms ($Dst < -100$ nT), and in ~50% of CME-driven storms (Kataoka and Miyoshi 2006). On the other hand, large flux enhancement in the inner portion and the slot region occur during CME-driven great-storms of $Dst < -150$ nT (Miyoshi and Kataoka 2005). These findings are consistent with the peak *L*-shell dependence on the storm amplitude (e.g., Tverskaya et al. 2002, O'Brien et al. 2003).

It is noteworthy that a large number of multiple storms occur during the solar maximum. The size of these multiple storms tends to be large and sometimes exceeds –400 nT (Kataoka and Miyoshi 2006). For example, the largest flux enhancement observed was in the inner portion and the slot region in the famous Halloween event, which occurred in October 2003 (Baker et al. 2004, Horne et al. 2005b, Loto'aniu et al. 2006). The largest flux enhancement during solar cycle 23

at geosynchronous orbit was observed in July 2004 during the recovery phase of intense multiple storms driven by a series of CMEs (Kataoka and Miyoshi 2008a b). These multiple storms might not have any notable effect on the solar cycle variations of the outer belt since subsequent solar wind structures produce new variations in the outer belt. In the inner belt, however, long-lasting flux enhancements which persist for more than a few years have been observed following intense multiple storms triggered by events such as those of March 1991 and October/November 2003 (Li and Temerin 2001, Looper et al. 2005).

6.1.2. Semiannual Variations

Besides variations ranging from a few days to a week, there are other timescales for flux variation of the radiation belts. During the solar declining phase, recurrent flux variations of 27 days and 13.5 days are significantly associated with the arrival of recurrent high-speed CHS. There are also semiannual variations in which the flux increases in the spring and autumn (Baker et al. 1999, Li et al. 2001, Miyoshi et al. 2004). The origin of this semiannual variation in the radiation belts is geomagnetic activities that are driven by the Russell-McPherron effect (Russell and McPherron 1973, Baker et al. 1999, Miyoshi et al. 2004).

6.1.3. Solar Cycle Variations

The outer belt and slot region vary with the solar cycle (Miyoshi et al. 2004, Li et al. 2006, Fung et al. 2006, Maget et al. 2007, Baker and Kanekal 2008). During the solar declining phase, the flux in the outer portion of the outer belt tends to increase in association with small storms (and also with no storms), while the flux in the inner portion of the outer belt and the slot region tends to decrease. During the solar active period, the flux tends not to increase in the outer portion, and vice versa in the inner portion. These long-term variations in each position correspond to long-term structural shifts of the outer belt; the outer belt moves outward during the solar declining phase and moves inward during the solar active period (Miyoshi et al. 2004). These long-term structural variations are the result of occurrence variations of CME-driven great storms and high-speed coronal hole streams. That is, CME-driven great storms tend to increase electrons in the inner portions, while CHS causes a large flux enhancement in the outer portion (Miyoshi and Kataoka 2005, Baker and Kanekal 2008).

In the inner belt ($L < 2$), energetic electrons increase during the solar active period at $L > 1.4$ (Abel et al. 1994, Miyoshi et al. 2004), while they decrease at $L < 1.3$ (Abel et al. 1994).

6.2. Response to Solar Wind and IMF

6.2.1. Solar Wind Speed

Solar wind speed is a primary driver of the large flux enhancement of the outer belt (e.g., Paulikas and Blake 1979). Since ULF pulsations in the Pc 5 range have been well correlated with solar wind speed (e.g., Mathie and Mann 2001) through Kelvin-Helmhorz instability (Claudepierre et al. 2008) and/or fluctuations in the solar wind dynamic pressure (Takahashi and Ukhorskiy 2007), correlations between the solar wind speed and MeV electron flux enhancement may indicate that radial diffusion is a dominant process in flux enhancement (see Sect. 6.3.1).

6.2.2. IMF

Because the outer belt electrons do not always increase greatly when high-speed streams arrive at the Earth (e.g., Kim et al. 2006), there must be parameters other than solar wind speed that control flux enhancement.

Flux enhancement tends to occur during the predominantly southward IMF (Blake et al. 1998, Iles et al. 2002, Miyoshi et al. 2007). Statistical studies focused upon CHS have shown that the large flux enhancement of MeV electrons depends on the Russell-McPherron effect; that is, the flux tends to increase largely in the southward Bz dominant CHS (Miyoshi and Kataoka 2008a b, McPherron et al. 2009). It should be noted that the average amplitude of the minimum *Dst* in the coronal hole stream is small, greater than –50 nT, which means that intense flux enhancements at GEO occur regardless of whether or not a magnetic storm takes place (Kim et al. 2006, Miyoshi and Kataoka 2008a). A statistical survey revealed that 90% (50%) of the fast CHSs (average solar wind speed faster than 500 km/s) display a large flux enhancement at geosynchronous orbit when the southward (northward) Bz is dominant (Miyoshi and Kataoka 2008b).

6.2.3. Solar Wind Density and Dynamic Pressure

The enhancement of solar wind dynamic pressure causes the adiabatic acceleration of the energetic particles due to the compression of the background magnetic field. On the other hand, flux decreases at the outer portion of the outer belt (e.g., geosynchronous orbit) tend to occur in large dynamic pressure (Onsager et al. 2007, Ohtani et al. 2009). Same tendency about flux decrease has been found in the solar wind density (Lyatsky and Khazanov, 2008).

6.3. Transport and Acceleration of Relativistic Electrons

6.3.1. Radial Diffusion

Since the typical energy of radiation belt particles exceeds the upper limit of the particle energy to be accelerated by the convection electric field (Sect. 4.3.1), radiation belt particles are usually not affected by the convection electric field.

Radial diffusion is regarded as one of the plausible mechanisms that could cause flux enhancement of the radiation belts. The elemental process of radial diffusion is a "drift resonance" that occurs between electrons drifting around the Earth and fluctuations in the electric/magnetic field. Considering the typical electron drift period, the ULF pulsation in the Pc 5 frequency range (~a few minutes) is the most plausible driver for electron diffusion (e.g., Elkington et al. 1999, 2003, 2006, Perry et al. 2005, Sarris et al. 2006). The origin of Pc-5 ULF waves has been variously attributed to Kelvin-Helmhorz instability (e.g., Chen and Hasegawa 1974), fluctuations in the solar wind dynamic pressure (e.g., Takahashi and Ukhorskiy 2007), and the drift-bounce resonance of ring current ions (e.g., Southwood et al. 1969). In radial diffusion, the first two adiabatic invariants (Eqs. (4) and (5)), μ and J, are always conserved, so the electron energy and pitch angle must change when the electrons move in a radial direction. The particle energy increases and the pitch angle of a particle shifts to 90° when a particle moves earthward and vice versa when a particle moves outward.

Since a random resonance with fluctuations has been assumed, the following Fokker-Planck equation has been used to describe radial diffusion (e.g., Schulz and Lanzerotti 1974, Schulz 1991, Shprits et al. 2008a and references therein):

$$\frac{\partial f}{\partial t} = L^2 \frac{\partial}{\partial L}\left(\frac{D_{LL}}{L^2} \frac{\partial f}{\partial L} \right) + Source - Loss, \tag{7}$$

where f is the phase space density of electrons, D_{LL} is the radial diffusion coefficient, t is time, and L indicates the L-shell. As shown in this equation, the direction of particle flow is determined entirely by the particle distribution, following Fick's law, and is independent of the mechanism given by the radial diffusion coefficient. If there is no source inside the radiation belts, the phase space density for any μ and J in the plasma sheet will be larger than that in the radiation belts, thus producing flux enhancements. Therefore, the positive gradient of the phase space density will be observed. In contrast to the diffusive model, coherent resonance with narrow-band waves has also been studied (Degeling et al. 2008).

Drift-resonance acceleration has been confirmed by observation (Tan et al. 2004). Many studies have shown a correlation between flux enhancement and the ULF Pc 5 power (e.g., Rostoker et al. 1998, Baker et al. 1998a b, O'Brien et al.

2001, Mathie and Mann 2001, Green and Kivelson 2001, Kim et al. 2006, Sarris et al. 2007).

6.3.2 In-Situ Accelerations by Wave-Particle Interactions

There are other mechanisms that produce relativistic electrons in the radiation belts: Some plasma waves; whistler, magnetosonic, free-space mode waves such as auroral kirometric radiation; and fast MHD waves can resonate with electrons by violation of adiabatic invariants, causing an acceleration (Horne and Thorne, 1998, Summers et al. 1998, 2000, 2001, Horne et al. 2007, Xiao et al. 2007, 2010). A recirculation process (Nishida 1976) driven by both radial transport and pitch angle scattering, which causes a violation of all adiabatic invariants, has been applied for the energization of electrons (Fujimoto and Nishida 1990, Liu et al. 1999). Here, we focus on whistler-mode wave particle interactions, which are thought to be the mechanism responsible for producing MeV electrons.

Whistler-mode chorus waves generated outside the plasmapause can accelerate the electrons of the outer radiation belt by Doppler-shifted cyclotron resonance (e.g., Horne and Thorne 1998, Summers et al. 1998, Horne 2002, Shprits et al. 2008b and references therein). The resonance condition of relativistic electrons can be given by

$$\omega - kv = n\frac{\Omega}{\gamma}, \tag{8}$$

where ω is the wave-frequency, k is the wave number vector, v is the particle velocity, n is the harmonic number, Ω is the electron gyro-frequency, and γ is the relativistic factor. Since a faster phase speed is required to effectively accelerate electrons, the low plasma density outside the plasmapause provides an environment that is conducive to this acceleration.

In this process, plasma/particles with different energy ranges are coupled to generate chorus waves and subsequent electron accelerations. Whistler-mode chorus waves are generated by the temperature anisotropy of injected plasma sheet electrons of a few tens of keV, and are then amplified largely due to the subsequent nonlinear process (Santolik et al. 2003, Katoh and Omura 2007a, Omura et al. 2008). A global simulation has successfully reproduced chorus enhancement during the storm (Jordanova et al. 2010). Generated whistler-mode chorus waves can resonate with subrelativistic electrons that might be coming from the plasma sheet and accelerate these electrons to the level of relativistic energies. Therefore, the chorus wave acts as a mediating agent by absorbing a small fraction of the power of the low-energy electrons, which results in wave growth, and then, its transfer to the acceleration of high-energy electrons. Since the wave-dispersion relations as well as the resonance condition are strongly affected by the ambient plasma density and magnetic field, the variations in thermal plasma density greatly changes the electron acceleration. That is, the cross-energy coupling of particles whose energies differ by more than 6 orders is

essential to produce relativistic electrons of the outer belt in regard to the internal acceleration (Miyoshi et al. 2003, 2007, Bortnik and Thorne 2007, Horne 2007).

The acceleration process of wave-particle interactions as well as pitch angle scattering has been often described by the Fokker-Planck equations in the velocity space.

$$\frac{\partial f}{\partial t} = \frac{1}{v \sin\alpha} \frac{\partial}{\partial \alpha} \sin\alpha \left(D_{\alpha\alpha} \frac{1}{v} \frac{\partial f}{\partial \alpha} + D_{\alpha v} \frac{\partial f}{\partial v} \right) + \frac{1}{v^2} \frac{\partial}{\partial v} v^2 \left(D_{v\alpha} \frac{1}{v} \frac{\partial f}{\partial \alpha} + D_{vv} \frac{\partial f}{\partial v} \right), \tag{9}$$

where α is the pitch angle. The diffusion coefficients D_{vv}, $D_{\alpha\alpha}$, $D_{\alpha v}$, and $D_{v\alpha}$ are given by the quasi-linear theory, considering the resonance condition of a given wave spectrum (e.g., Lyons 1974, Albert 1999). Based upon a detailed estimation of the diffusion coefficients (e.g., Horne et al. 2005a, Li et al. 2007) in the realistic plasma environment during storms, electron acceleration caused by wave-particle interaction is considered to be possible.

Over the last few years, several research efforts have supported the concept of accelerations being caused by wave-particle interactions. Chorus wave power is most intense outside the plasmapause at midnight and is distributed to the dawn sector and early afternoon sector. In this region, the cold plasma density is low, which fulfills the condition required for efficient electron diffusion (e.g., Meredith et al. 2003b, Li et al. 2008, 2009). The large flux enhancement of the outer belt occurs concurrently with chorus wave enhancement (e.g., Meredith et al. 2001, 2003a, Miyoshi et al. 2003, 2007, Kasahara et al. 2009), and recent comprehensive numerical simulations and the modeling of diffusion coefficients using the observed plasma parameters have accounted for electron acceleration on the order of 1–2 days, which is comparable to the observed times scale for acceleration (e.g., Miyoshi et al. 2003, Varotsou et al. 2005, 2008, Fok et al. 2008, Albert et al. 2009, Shprits et al. 2009, Xiao et al. 2010, Subbotin et al. 2010). The flat-top pitch angle distributions that are predicted by the wave-particle interaction process have been observed during storms (Horne et al. 2003). Some of the solar wind parameter dependence of the outer belt electrons (Sect. 6.2) can be explained by acceleration via wave-particle interactions.

Although most studies of local acceleration processes have focused on the whistler-mode chorus waves using quasi-linear diffusion theory, strong nonlinear interactions with individual chorus elements (Katoh and Omura 2007b, Omura et al. 2007, Katoh et al. 2008, Bortnik et al. 2008) are also important for the acceleration.

6.3.3 Which Mechanism Is Important?

From the standpoint of radial diffusion, the close correlation between solar wind speed and the MeV electron flux enhancement as described in Sect. 6.2 supports

the idea that radial diffusion is a primary mechanism for the flux enhancement of the outer belt (e.g., Rostoker et al. 1998, Baker et al. 1998a b, O'Brien et al. 2001, Mathie and Mann 2001, Green and Kivelson 2001, Mann et al. 2004, Kim et al. 2006, Sarris et al. 2006), because the solar wind speed is the main driver for the Pc 5 ULF activities in the magnetosphere. During a CHS, the plasma sheet temperature is high (Borovsky et al. 1997, Denton et al. 2006), so that seed populations with a large magnetic moment may be stored in the plasma sheet. These electrons may be diffused inward by continuous enhanced radial diffusion to produce large flux enhancements during a CHS.

From the standpoint of the internal acceleration by VLF waves, the dependence on solar wind speed and IMF described in Sect. 6.2 can be understood as follows. The acceleration by VLF waves is especially effective when a continuous source of hot electrons can be maintained to produce a chorus for the several-day period required to accelerate electrons to relativistic energies. This suggests that a prolonged period of enhanced convection/substorms is required for acceleration (Meredith et al. 2002, Miyoshi et al. 2003, Bortonik and Thorne 2007, Horne 2007). The southward IMF and high-speed solar wind causes continuous substorm/convection activities (the so-called HILDCAAs: High Intensity Long Duration Continuous AE Activities, e.g., Tsurutani et al. 2006) in which continuous hot electron injections from the plasma sheet into the inner magnetosphere can be seen (Obara et al. 2000, Denton et al. 2006).

The close relationship between CHS and accelerations by VLF waves was conducted in two CIR storms in November 1993 by polar-orbit satellites. Observations showed that the outer belt electron flux increased largely during the recovery phase of the first storm when the Russell-McPherron effect was at work and did not increase during the recovery phase of the second storm when it was not at work. The differences in hot electrons, subrelativistic electrons, VLF waves, and substorm/convection activities are consistent with the scenario according to which the internal acceleration by VLF waves is important to flux enhancement (Miyoshi et al. 2007). Some observations (Lyons et al. 2005, 2009) have shown the correlations between VLF waves measured on the ground and MeV electron flux enhancement during CHS, which can be explained by this scenario.

Observations of the phase space density profile are critical for discriminating between radial diffusion and internal accelerations. Equation (7) shows that the phase space density gradient should be possible if the inward radial diffusion contributes to flux enhancement, because the direction of particle movement is determined by the slope of the phase space density. On the other hand, the appearance of local peaks and the subsequent local evolution of the phase space density indicate that the internal acceleration process contributes to flux enhancement (see Figure 2 of Green and Kivelson 2004). Equation (7) is described in variables of the first and second adiabatic invariants and L-value, so that it is essential to obtain the accurate phase space density at a certain μ and J.

There are several observational reports of local peaks of the phase space density inside the outer belt, which suggests an internal acceleration (e.g., Brautingam and Albert 2000, Selesnick and Blake 2000, Miyoshi et al. 2003,

Green and Kivelson 2004, Iles et al. 2006, Chen et al. 2006, 2007, Fennell and Roeder, 2008). Some studies have reported the positive gradient of the phase space density, suggesting that radial diffusion is the primary mechanism of flux enhancement during a storm (e.g., Hilmer et al. 2000, Onsager et al. 2004). Due to certain problems that are addressed below, the subject of phase space density profiles during a storm is still being debated. However, it may be natural to consider that both radial diffusion and in-situ acceleration contribute to flux enhancement, though during a storm, one process might play a more dominant role than the other.

It should be noted here that some problems attend the derivation of accurate phase space density values (see also Green and Kivelson 2004). The magnetic field model is necessary in order to derive the second adiabatic invariant and L* (Roederer, 1970). The results of the phase space density profile depend largely on the magnetic field model that is used for the calculation (Selesnick and Blake, 2000, Ni et al. 2009a). Since the interesting period about the large flux variation is often magnetic storms, a strong distortion of the magnetic field is to be expected, which in turn makes it more difficult to derive an accurate phase space density profile. Another problem in the calculation of phase space density is the coverage of the equatorial pitch angle. It has been reported that flux variations depend on the pitch angle (Seki et al. 2005) and that the phase space density profile depends on the second adiabatic invariant even when the first adiabatic invariant is the same (Fennell and Roeder 2008). Therefore, a reliable empirical and physical magnetic field model that can be applied in intense magnetic storms is one of the keys to an accurate phase space density profile. Moreover, observations around the magnetic equator that can cover a wide range of equatorial pitch angles, that is, a wide range of the second invariant, are important and necessary for future missions.

Note that the data assimilation technique for the radiation belt studies has recently developed, which couples the radial diffusion model (Eq. 7) with the satellite data, to derive more accurate phase space density profile and specify the physical processes that cause the flux enhancement (e.g., Koller et al. 2007, Kondrashov et al. 2007, Shprits et al. 2007, Ni et al. 2009 a b). The data assimilation would become useful and important tool for better understanding of radiation belt physics.

6.4. Loss of Relativistic Electrons

6.4.1. Adiabatic Effect

Electron fluxes decrease in a certain *L*-shell in a fixed energy window during magnetic storms (McIlwain 1966, Kim and Chan 1997). This is the so-called the

Dst effect or ring current effect (Sect. 4.6.5), which causes no change in the phase space density in the adiabatic coordinate space. This process causes flux reduction during the main phase and subsequent flux recovery to the prestorm level if only adiabatic processes take place. Due to the ring current effect, the pitch angle distribution of electrons conserving the first and second adiabatic invariants exhibits butterfly distribution due to betatron acceleration (Lyons et al. 1977) and a combination of betatron acceleration and Fermi acceleration (Ebihara et al. 2008a).

In about a quarter of magnetic storms, however, the flux of the outer belt electrons does not recover to the prestorm level (Reeves et al. 2003), in which case other nonadiabatic loss processes must occur (see Millan and Thorne 2007 and references therein).

6.4.2. Precipitation into Atmosphere

Pitch angle scattering with plasma waves causes the precipitation of particles into the atmospheric loss cone, which is one of the important processes in outer belt electron loss. This precipitation of MeV electrons depletes ozone through the enhancement of NOx (Thorne 1977), which may affect the climate (e.g., Rozanov et al. 2005).

Pitch angle scattering has been described by the first term of Eq.(9). Whistler-mode waves such as plasmaspheric hiss and chorus resonate with radiation belt electrons (Kennel and Petschek 1966, Lyons et al. 1972). Whistler-mode hiss waves are responsible for the formation of the slot region. The equilibrium structure of the radiation belts—the inner belt, outer belt, and slot region—has been successfully reproduced considering the wave-particle interactions with plasmaspheric hiss (Lyons et al. 1972, Lyons and Thorne 1973, Albert 1994, 1999, Abel and Thorne 1998a b). The measured decay rates following storms show good agreement with the estimated life times (Albert 2000, Meredith et al. 2006) and a one-dimensional radial diffusion simulation (e.g., Lam et al. 2007). The top-hat shape of the pitch angle distribution is another piece of evidence that attests to the pitch angle scattering by hiss waves (e.g., West et al. 1973, Lyons et al. 1975a b, Morioka et al. 2001). The close correlation between the plasmapause and the outer belt position also supports the idea that whistler-mode hiss is an important loss process (O'Brien et al. 2003, Miyoshi et al. 2004, Goldstein et al. 2005, Li et al. 2006). Lightning whistler becomes more important, as do the VLF transmitters at lower L (Abel and Thorne 1998 a b) and the outer belt (Bortnik et al. 2006a b).

Another kind of wave for the pitch angle scattering of relativistic electrons is EMIC waves in the region where the plasmasphere overlaps with the ring current (e.g., Cornwall et al. 1970, Jordanova et al. 1997). The rapid pitch angle scattering by EMIC waves when electron energies become relativistic has been predicted theoretically, (Thorne and Kennel 1971, Lyons et al. 1972, Summers and Thorne 2003, Albert 2003). There have also been several observations that suggest EMIC-

relativistic electron interactions (e.g., Foat et al. 1995, Lorentzen et al. 2000, Millan et al. 2002, Meredith et al. 2003c, Sandanger et al. 2007). In addition, recent satellite-ground conjunction observations as well as theoretical checks have identified that EMIC waves actually cause the coincident precipitation of tens of keV ions and MeV electrons into the ionosphere near the plasmapause (Miyoshi et al. 2008). A self-consistent simulation that included convection, radial diffusion, and pitch angle scattering by whistlers and EMIC waves showed that EMIC waves cause the pitch angle scattering of both ring current ions and MeV electrons, but the dominant process in the global loss of the outer belt during the main phase is the outward diffusion, as shown in Sect 6.4.3 (Jordanova et al. 2008).

Outside the plasmapause, whistler-mode chorus causes the pitch angle scattering of electrons as well as acceleration (Thorne et al. 2005). It has been suggested that the microbursts of MeV electrons that occur on the dawn-side between L = 4–6 (e.g., Nakamura et al. 1995, 2000, Lorentzen et al. 2001) are the result of scattering by whistler-mode chorus waves. Microbursts occur frequently during the storm recovery phase, but losses are much stronger during the main phase, and are capable of emptying the outer belt in one day or less (O'Brien et al. 2004).

6.4.3 Magnetopause Loss

It has been suggested that electron loss from the magnetopause is the mechanism responsible for electron flux dropouts. Three-dimensional test particle simulations (Kim et al. 2008, Saito et al. 2010) showed that magnetopause shadowing (MPS) causes the abrupt loss of the outer portion of the outer belt and changes in the trapping boundary. Two-dimensional test particle simulations showed that the storm-time partial ring current produces a nightside depression of the magnetic field, causing an outward expansion of the outer belt and the loss of electrons in the outer portion (Ukhorskiy et al. 2006). If the phase space density of the outer portion decreases due to MPS, then electrons move outward due to the outward diffusion (Eq.(7)). Some simulation studies (Brautingam and Albert, 2000, Miyoshi et al. 2003, 2006, Jordanova and Miyoshi 2005, Shprits et al. 2006) found that the outward diffusion triggered by the flux decrease in the outer portion leads to changes in the lower L-shells, which in turn contributes to the flux decrease during the main phase. Recently, Ohtani et al. (2009) have shown observational evidence that some flux loss observed at geosynchronous orbit can be explained by MPS (see Sect. 6.2.3). It is worthwhile to note that such outward diffusion also occurs through the negative phase space density gradient when the internal acceleration causes the peak phase space density inside the outer radiation belt (Shprits et al. 2009).

6.4.4 Which Mechanism Is Important?

During the time of a storm, it is understood that the various loss processes take place simultaneously, but it has not been quantitatively understood which process predominates in the net loss of the outer belt. Different processes work at different L-shell and local times. Green et al. (2004) suggest that precipitation may account for a part of the precipitation, rather than MPS, but they do not identify the exact mechanism by which this takes place. Bortnik et al. (2006c) indicated that both MPS (for high *L*) and precipitation by EMIC waves (for low *L*) may have been active in the November 2003 storm. The effective solar wind parameters that would cause a loss have been debated. Onsager et al. (2007) found that the onset of southward IMF is an important cause of flux dropouts, while Ohtani et al. (2009) showed that dynamic pressure enhancement is also essential, due to MPS. Borovsky and Denton (2009) showed that the onset of the flux dropouts associated with CIRs tends to occur after the crossing of the IMF sector boundary, and they investigated how the pitch angle scattering by EMIC waves inside the drainage plumes could be an important factor. Quantitative physics-based models that take into consideration both of these mechanisms would be necessary in order to quantitatively identify this mechanism.

6.5. Cross-Energy Couplings for Acceleration of Relativistic Electrons

Figure 5 summarizes these transport/acceleration mechanisms in the *L*-energy diagram of the inner magnetosphere. In radial diffusion (indicated by blue lines), the electrons move earthward with increasing energy due to the conservation of the first two adiabatic invariants. In this process, the ULF waves that are driven by solar wind and ring current instability are essential for driving the particle transport. The ambient plasma density has an effect on the condition of the drift-bounce resonance (Ozeke and Mann, 2008). On the other hand, in the in-situ acceleration by waves (indicated by red lines), subrelativistic electrons are accelerated to MeV energies by whistler-mode waves that are generated by the plasma instability of the ring current electrons. In this process, the thermal plasma density plays an essential role as the ambient medium. Because the transport of ring current electrons and thermal plasma are predominantly controlled by convective electric fields (see. Sects. 2, 3, and 4), the process of convection may affect the relativistic electron dynamics in this process. In the loss process, different energy electrons and ions affect the dynamics of the relativistic electrons through wave-particle interactions. Therefore, the formation of the radiation belt including both flux enhancement and decrease is one of the manifestations of cross-energy/cross-regional couplings in the inner magnetosphere.

7. Concluding Remarks

The physical processes involved in the structure and dynamics of the inner magnetosphere are schematically summarized in Figure 6. While the diagram is admittedly incomplete, it provides an essential context for understanding the inner magnetosphere and magnetic storms. Each element is directly or indirectly coupled with one another, so that the inner magnetosphere should be treated as a nonlinear, compound system. Once studied a particular element in detail, one should take into account its physical connection with the others as a system network.

During magnetic storms, each element is activated and the network of the inner magnetospheric system is dynamically stimulated. The following processes are expected to occur simultaneously:

1. The convection electric field is enhanced by southward IMF and fast solar wind.
2. Plasma sheet particles are transported into the inner magnetosphere by the convection electric field.
3. The ring current is developed on the nightside, and the plasmasphere shrinks.
4. The inner magnetospheric magnetic field is inflated by the ring current, resulting in deformation of the ring current and the radiation belt.
5. The inner magnetospheric electric field is deformed by the ring current, resulting in further deformation of the ring current and the plasmasphere.
6. Waves are excited, resulting in the acceleration and scattering of particles.
7. Magnetic and electric fields fluctuate greatly, enhancing the radial diffusion of energetic particles.
8. The ionospheric conductivity is enhanced by the precipitation of protons, electrons and ENAs.
9. The ionosphere is heated by the ring current, resulting in the glow of a SAR arc.
10. Various types of auroras are excited by the precipitating protons, electrons and ENAs.

The inner magnetosphere is so dynamic and complicated that only a system-based approach can promise to offer an overall understanding of the inner magnetosphere and the Sun-Earth connection. To achieve a comprehensive understanding of the dynamics of the inner magnetosphere, several interesting missions are now in progress and are being planned. An international fleet of inner magnetosphere exploration satellites will consist of THEMIS (US), RBSP (US), ORBITALS (Canada), RESONANCE (Russia), and ERG (Japan) around the next solar maximum. Well-networked ground-based observations by instruments such as the magnetometer and SuperDARN HF-radar are powerful remote-sensing tools for exploring the inner magnetosphere. Simulations that can comprehend cross region and cross energy couplings, such as the Radiation Belt Environment (RBE) model (Fok et al. 2008) and the ring current-atmosphere interactions

model (RAM) (Jordanova et al. 2010), are also valid to investigate the tightness of the coupling and the manner in which basic laws of physics lead to a certain observed effect.

References

Abe, T., Watanabe, S., Whalen, B.A., Yau, A.W., Sagawa, E.: Observations of polar wind and thermal ion outflow by Akebono/SMS. J. Geomagn. Geoelectr. **48**, 319–325 (1996)

Abel, B., Thorne, R.M., Vampola, A.L.: Solar cycle behavior of trapped energetic electrons in Earth's radiation belt. J. Geophys. Res. **99**, 19427–19431 (1994)

Abel, B., Thorne, R.M.: Electron scattering loss in the Earth's inner magnetosphere, 1. Dominant physical processes. J. Geophys. Res. **103**, 2385–2396 (1998a)

Abel, B., Thorne, R.M.: Electron scattering loss in the Earth's inner magnetosphere, 2. Sensitivity to model parameters. J. Geophys. Res. **103**, 2397–2407 (1998b)

Aggson, T.L., Heppner, J.P., Maynard, N.C.: Observations of large magnetospheric electric fields during the onset phase of a substorm, J. Geophys. Res. **88**, 3981–3990 (1983)

Akasofu, S.-I., Chapman, S.: On the asymmetric development of magnetic storm fields in low and middle latitudes, Planet. Space Sci. **12**, 607–626 (1964)

Albert, J.M.: Quasi-linear pitch angle diffusion coefficients: Retaining high harmonics. J. Geophys. Res. **99**, 23741–23745 (1994)

Albert, J.M., Ginet, G., Gussenhoven, M.: CRRES observations of radiation belt protons 1. Data overview and steady state radial diffusion. J. Geophys. Res. **103**, 9261–9273 (1998)

Albert, J.M.: Analysis of quasi-linear diffusion coefficients. J. Geophys. Res. **104**, 2429–2441 (1999)

Albert, J.M.: Pitch angle diffusion as seen by CRRES, Adv. Space Res. **12**, 2343–2346 (2000)

Albert, J.M.: Evolution of quasi-linear diffusion coefficients for EMIC waves in a multispecies plasma. J. Geophys. Res. (2003). doi:10.1029/2002JA009792

Albert, J.M., Meredith, N.P., Horne, R.B.: Three‐dimensional diffusion simulation of outer radiation belt electrons during the 9 October 1990 magnetic storm, J. Geophys. Res.(2009). doi:10.1029/2009JA014336.

Anderson, B.J., Erlandson, R.E., Zanetti, L.J.: A statistical study of pc 1–2 magnetic pulsations in the equatorial magnetosphere, 1. Equatorial occurrence distributions, J. Geophys. Res. **97**, 3075–3088 (1992)

Anderson, P.C., Hanson, W.B., Heelis, R.A., Craven, J.D., Baker, D.N., Frank, L.A.: A proposed production model of rapid subauroral ion drifts and their relationship to substorm evolution, J. Geophys. Res. **98**, 6069–6078 (1993)

Anderson, B.J. Fuselier, S.A.: Response of thermal ions to electromagnetic ion cyclotron waves, J. Geophys. Res., **99**, 19413-19425 (1994)

Anderson, P.C., Carpenter, D.L., Tsuruda, K., Mukai, T., Rich, F.J. : Multisatellite observations of rapid subauroral ion drifts (SAID), J. Geophys. Res., **106**, 29,585–29,599 (2001). doi:10.1029/2001JA000128

Anderson, P.C., Johnston, W.R., Goldstein, J.: Observations of the ionospheric projection of the plasmapause, Geophys. Res. Lett. (2008). doi:10.1029/2008GL033978

Barnett, C.F.: Atomic data for fusion, vol. I, Collisions of H, H2, He and Li atoms and ions with atoms and molecules, Tech. Rep. ORNL–6086/VI}, Oak Ridge Natl. Lab., Oak Ridge, Tenn. (1990)

Baker, D.N., Blake, J.B., Klebesadel, R.W., Higbie, P.R.: Highly relativistic electrons in the Earth's outer magnetosphere, 1. Lifetimes and temporal history 1979-1984. J. Geophys. Res. **91**, 4265–4276 (1986)

Baker, D.N., Pulkkinen, T., Li, X., Kanekal, S., Blake, J.B., Selesnick, R.S., Henderson, M.G., Reeves, G.D., Spence, H.E., Rostoker, G.: Coronal mass eiection, magnetic clouds, and relativistic electron events: ISTP. J. Geophys. Res. **103**, 17279–17291 (1998a)

Baker, D.N., Pulkkinen, T.I., Li, X., Kanekal, S.G., Ogilivie, K.W., Lepping, R.P., Blake, J.B., Callis, L.B., Rostoker, G., Singer, H.J., Reeves, G.D.: A strong CME-related magnetic cloud interaction with the Earth's magnetosphere: ISTP observations of rapid relativistic electron acceleration on May 15, 1997. Geophys. Res. Lett. **25**, 2975–2978 (1998b)

Baker, D.N., Kanekal, S.G., Pulkkinen, T.I., Blake, J.B.: Equinoctial and solstitial averages of magnetospheric relativistic electrons: A strong semiannual modulation. Geophys. Res. Lett. **26**, 3163–3196 (1999)

Baker, D.N., Kanekal, S.G., Li, X., Monk, S.P., Goldstein, J., Burch, J.L.: An extreme distortion of the Van Allen belt arising from the "Halloween" solar storm in 2003, Nature **432**, 878–881 (2004)

Baker, D.N., Kanekal, S.G.: Solar cycle changes, geomagnetic variations, and energetic particle properties in the inner magnetosphere. J. Atm. Solar-Terr. Phys. **70**, 195–206 (2008)

Barnett, C.F., Atomic data for fusion, vol. I, Collisions of H, H2, He and Li atoms and ions with atoms and molecules, Tech. Rep. ORNL-6086 V5, Oak Ridge Natl. Lab.,Oak Ridge, Tenn. (1990)

Baumgardner, J., Wroten, J., Semeter, J., Kozyra, J., Buonsanto, M., Erickson, P., and Mendillo, M.: A very bright SAR arc: Implications for extreme magnetosphere-ionosphere coupling, Ann. Geophys. **25**, 2593–2608 (2007)

Baumjohann, W., Haerendel, G.: Magnetospheric convection observed between 0600 and 2100 LT: Solar wind and IMF dependence, J. Geophys. Res. **90**, 6370–6378 (1985)

Baumjohann, W., Paschmann, G., Cattell, C.A.: Average plasma properties in the central plasma sheet, J. Geophys. Res. **94**, 6597 (1989)

Beutier, T., Boscher, D., France, M.: SALAMMBO: A three-dimensional simulation of the proton radiation belt. J. Geophys. Res. **100**, 17181–17188 (1995)

Birn, J., Thomsen, M.F., Borovsky, J.E., Reeves, G.D., McComas, D.J., Belian, R.D.: Characteristic plasma properties during dispersionless substorm injections at geosynchronous orbit, J. Geophys. Res. **102**, 2309–2324 (1997a)

Birn, J., Thomsen, M.F., Borovsky, J.E., Reeves, G.D., McComas, D.J., Belian, R.D, Hesse, M.: Substorm ion injections: Geosynchronous observations and test particle orbits in three-dimensional dynamic MHD fields, J. Geophys. Res. **102**, 2325–2341 (1997b)

Blake, J.B., Kolasinski, W.A., Fillius, R.W., Mullen, E.G.: Injection of electrons and protons with energies of tens of MeV into L < 3 on 24 March 1991. Geophys. Res. Lett. **19**, 821–824 (1992)

Blake, J.B., Kolasinski, W.A., Fillius, R.W., Mullen, E.G.: Injection of electrons and protons with energies of tens of MeV into L<3 on March 24, 1991. Geophys. Res. Lett. **19**, 821–824 (1992)

Borovsky, J.E., Thomsen, M.F., McComas, D.J.: The superdense plasma sheet: Plasmaspheric origin, solar wind origin or ionospheric origin?, J. Geophys. Res. **102**, 22089–22097 (1997)

Borovsky, J.E., Thomsen, M.F., Elphic, R.C.: The driving of the plasma sheet by the solar wind, J. Geophys. Res. **103**, 17617–17639 (1998)

Borovsky, J.E., Denton, M.H.: Differences between CME-driven storms and CIR-driven storms. J. Geophys. Res. (2006). doi:10.1029/2005JA011447

Borovsky, J.E., Denton, M.H.: A statistical look at plasmaspheric drainage plumes, J. Geophys. Res. (2008). doi:10.1029/2007JA012994

Borovsky, J.E., Denton, M.H.: Relativistic-electron dropouts and recovery: A superposed epoch study of the magnetosphere and the solar wind. J. Geophys. Res. (2009). doi:10.1029/2008JA013128

Borovsky, J.E., Lavraud, B., Kuznetsova, M.M.: Polar cap potential saturation, dayside reconnection, and changes to the magnetosphere. J. Geophys. Res. (2009). doi:10.1029/2009JA014058

Bortnik, J., Inan, U.S., Bell, T.F.: Temporal signatures of radiation belt electron precipitation induced by lightning-generated MR whistler waves: 1. Methodology, J. Geophys. Res. (2006a). doi:10.1029/2005JA01182

Bortnik, J., Inan, U.S., Bell, T.F.: Temporal signatures of radiation belt electron precipitation induced by lightning-generated MR whistler waves: 2. Global signatures, J. Geophys. Res. (2006b). doi:10.1029/2005JA011398

Bortnik, J., Thorne, R.M., O'Brien, T.O., Green, J.C., Strangeway, R.J., Shprits, Y.Y., Baker, D.N.: Observation of two distinct rapid loss-mechanisms during the November 20, 2003 radiation belt dropout event. J. Geophys. Res. (2006c). doi:10.1029/2006JA011802

Bortnik, J., Thorne, R.M.: The dual role of ELF/VLF chorus waves in the acceleration and precipitation of radiation belt electrons. J. Atm. Solar-Terr. Phys. **69**, 378–376 (2007)

Bortnik, J., Thorne, R.M., Inan, U.S.: Nonlinear interaction of energetic electrons with large amplitude chorus. Geophys. Res. Lett. (2008). doi:10.1029/2008GL035500

Bortnik, J., Thorne, R.M., Meredith, N.P.: Modeling the propagation characteristics of chorus using CRRES suprathermal electron fluxes, J. Geophys. Res. (2007). doi:10.1029/2006JA012237

Brandt, P.C., Mitchell, D.G., Ebihara, Y., Sandel, B.R., Roelof, E.C., Burch, J.L., Demajistre, R.: Global IMAGE/HENA observations of the ring current: Examples of rapid response to IMF and ring current-plasmasphere interaction, J. Geophys. Res. (2002a). doi:10.1029/2001JA000084

Brandt, P.C., Ohtani, S., Mitchell, D.G., Fok, M.-C., Roelof, E.C., Demajistre, R.: Global ENA observations of the storm mainphase ring current: Implications for skewed electric fields in the inner magnetosphere, Geophys. Res. Lett. (2002b). doi:10.1029/2002GL015160

Brandt, P.C., Roelof, E.C., Ohtani, S., Mitchell, D.G., Anderson, B.: IMAGE/HENA: pressure and current distributions during the 1 October 2002 storm, Adv. Space Res. **33**, Streamers, slow solar wind, and the dynamics of the magnetosphere, 719–722 (2004)

Brandt, P.C., Y. Zheng, T.S. Sotirelis, K.Oksavik, F.J. Rich: The linkage between the ring current and the ionosphere system, in "Midlatitude ionospheric dynamics and disturbances", edited by P.M. Kintner, A.J. Coster, T. Fuller-Rowell, A.J. Mannucci, M. Mendillo, and R. Heelis, AGU Geophys. Monogra. Ser. 181, 135–143 (2008)

Brautigam, D.H., Albert, J.M: Radial diffusion analysis of outer radiation belt electrons during the October 9, 1990, magnetic storm. J. Geophys. Res. **105**, 291–309 (2000)

Breneman, A.W., Kletzing, C.A., Pickett, J., Chum, J., Santolik, O.: Statistics of multispacecraft observations of chorus dispersion and source location, J. Geophys. Res. (2009). doi:10.1029/2008JA013549

Brice, N.M.: Bulk Motion of the Magnetosphere. J. Geophys. Res. **72**, 5193–5211(1967)a

Carpenter, D.L., Anderson, R.R., Calvert, W., Moldwin, M.B.: CRRES observations of density cavities inside the plasmasphere. J. Geophys. Res. 105, 23323–23338 (2000)

Burch, J.L., et al.: Views of the Earth's magnetosphere with the IMAGE satellite, Science 291, 619 (2001)

Burch, J.L., Goldstein, J., Sandel, B.R.: Cause of plasmasphere corotation lag, Geophys. Res. Lett. (2004). doi:10.1029/2003GL019164

Burke, W.J., Gentile, L.C., Huang, C.Y.: Penetration electric fields driving main phase Dst, J. Geophys. Res. (2007). doi:10.1029/2006JA012137

Büchner, J., Zelenyi, L.: Regular and chaotic charged particle motion in magnetotaillike field reversals, 1. Basic theory of trapped motion, J. Geophys. Res. **94**, 11821–11842 (1989)

Cahill, L.Jr.: Inflation of the inner magnetosphere during a magnetic storm, J. Geophys. Res. **71**, 4505–4519 (1966)

Carpenter, D.L.: Whistler evidence of a 'knee' in the magnetospheric ionization density profile, J. Geophys. Res. **68**, 1675–1682 (1963)

Carpenter, D.L.: Whistler studies of the plasmapause in the magnetosphere 1. Temporal variations in the position of the knee and some evidence on plasma motions near the knee, J. Geophys. Res. **71**, 693–709 (1966)

Carpenter, D.L., Anderson, R.R.: An ISEE/whistler model of equatorial electron density in the magnetosphere, J. Geophys. Res. **97**, 1097–1108 (1992)

Carpenter, D.L., Lemaire, J.: Erosion and recovery of the plasmasphere in the plasmapause region, Space Sci. Rev. **80**, 153–179 (1997)

Carpenter, D.L., Anderson, R.R., Calvert, W., Moldwin, M.B.: CRRES observations of density cavities inside the plasmasphere, J. Geophys. Res., **105**, 23323–23338 (2000)

Carpenter, D.L., Lemaire, J.: The plasmasphere boundary layer, Ann. Geophys. **22,** 4291–4298 (2004)

Chappell, C.R., Harris, K.K., Sharp, G.W.: A study of the influence of magnetic activity on the location of the plasmapause as measured by OGO 5, J. Geophys. Res. **75**, 50–56 (1970)

Chappell, C.R.: Recent satellite measurements of the morphology and dynamics of the plasmasphere, Rev. Geophys. **10**, 951–979 (1972)

Chappell, C.R.: Detached plasma regions in the magnetosphere, J. Geophys. Res. **79**, 1861–1870 (1974)

Chappell, C.R., Olsen, R.C., Green, J.L., Johnson, J.F.E., Waite, J.H.Jr.: The discovery of nitrogen ions in the Earth's magnetosphere, Geophys. Res. Lett. **9**, 937–940 (1982)

Chappell, C.R., Huddleston, M.M., Moore, T.E., Giles, B.L., Delcourt, D.C.: Observations of the warm plasma cloak and an explanation of its formation in the magnetosphere, J. Geophys. Res. (2008). doi:10.1029/2007JA012945

Chapman, S., Ferraro, V.C.A.: A new theory of magnetic storms, Terr. Magn. Atmos. Electr. **38**, 79–96 (1933)

Chen, A.J., Grebowsky, J.M.: Plasma tail interpretations of pronounced detached plasma regions measured by Ogo 5, J. Geophys. Res. **79**, 3851–3855 (1974)

Chen, L., Hasegawa, A. (1974): A theory of long-period magnetic pulsations: Impulse excitation of surface eigenmode. J. Geophys. Res. **79**, 1033–1037 (1974)

Chen, M., Lyons, L., Schulz, M.: Simulations of phase space distributions of storm time proton ring current, J. Geophys. Res. **99**, 5745–5759 (1994)

Chen, Y., Friedel, R.H.W., Reeves, G.D.: Phase space density distributions of energetic electrons in the outer radiation belt during two Geospace Environment Modeling Inner Magnetosphere/Storms selected storms. J. Geophys. Res. (2006). doi:10.1029/2006JA011703

Chen, Y., Reeves, G.D., Friedel, R.H.W., The energization of relativistic electrons in the outer Van Allen radiation belt. Nature Physics (2007). doi:10.1038/nphys655

Chen, L., Thorne, R.M., Horne, R.B.: Simulation of EMIC wave excitation in a model magnetosphere including structured high-density plumes, J. Geophys. Res. (2009). doi:10.1029/2009JA014204

Christon, S.P., Desai, M.I., Eastman, T.E., Gloeckler, G., Kokubun, S., Lui, A.T.Y., McEntire, R.W., Roelof, E.C., Williams, D.J.: Low-charge-state heavy ions upstream of Earth's bow shock and sunward flux of ionospheric O+1, N+1, and O+2 ions: Geotail observations, Geophys. Res. Lett. **27**, 2433–2436 (2000)

Cladis, J.B., Francis, W.E.: Distribution in magnetotail of O+ ions from cusp/cleft ionosphere: A possible substorm trigger, J. Geophys. Res. **97**, 123–130 (1992)

Claudepierre, S.G., Elkington, S.R., Wiltberger, M.: Solar wind driving of magnetospheric ULF waves: Pulsations driven by velocity shear at the magnetopause. J. Geophys. Res. (2008). doi:10.1029/2007JA012890

Clauer, C.R., McPherron, R.L.: The relative importance of the interplanetary electric field and magnetospheric substorms on partial ring current development, J. Geophys. Res. **85**, 6747–6759 (1980)

Cole, K.D.: Stable auroral red arcs, Sinks for energy of Dst main phase, J. Geophys. Res. **70**, 1689–1706 (1965)

Collin, H.L., Quinn, J.M., Cladis, J.B.: An empirical static model of low energy ring current ions, Geophys. Res. Lett. **20**, 141–144 (1993)

Comfort, R.H., Horwitz, J.L.: Low energy ion pitch angle distributions observed on the dayside at geosynchronous altitudes, J. Geophys. Res. **86**, 1621–1627 (1981)

Cornwall, J.M., Coroniti, F.V., Thorne, R.M.: Turbulent loss of ring current protons. J. Geophys. Res. **75**, 4699–4709 (1970)

Cornwall, J.M.: On the role of charge exchange in generating unstable waves in the ring current, J. Geophys. Res. **82**, 1188–1196 (1977)

Craven, J.D., Frank, L.A., Ackerson, K.L.: Global observations of a SAR arc, Geophys. Res. Lett. **9**, 961–964 (1982)

Daglis, I.A., Sarris, E.T., Wilken, B.: AMPTE/CCE CHEM observations of the ion population at geosynchronous altitudes, Ann. Geophys. **11**, 685 (1993)

Daglis, I.A., Axford, W.I.: Fast ionospheric response to enhanced activity in geospace: Ion feeding of the inner magnetotail, J. Geophys. Res. **101**, 5047–5065 (1996)

Daglis, I.A., Kasotakis, G., Sarris, E.T., Kamide, Y., Livi, S., Wilken, B.: Variations of the ion composition during an intense magnetic storm and their consequences , Phys. Chem. Earth, **24**, 229–232 (1999)

Daglis, I.A., Kamide, Y., Monikis, C., Reeves, G.D., Sarris, E.T., Shiokawa, K., Wilken, B.: 'Fine structure' of the storm-substorm relationship: Ion injections during DST decrease, Adv. Space Res. **25**, 2369–2372 (2000)

Darrouzet, F, Décréau, P.M.E., De Keyser, J., Masson, A., Gallagher, D.L., Santolik, O., Sandel, B.R., Trotignon, J.G., Rauch, J.L., Le Guirriec, E., Canu, P., Sedgemore, F., Andr´e, M., Lemaire, J.F.: Density structures inside the plasmasphere: Cluster observations, Ann. Geophys. **22**, 2577–2585 (2004)

De Benedetti, J., Milillo, A., Orsini, S., Mura, A., De Angelis, E., Daglis, I.A.: Empirical model of the inner magnetosphere H+ pitch angle distributions (eds.) Pulkkinen, T.I., Tsyganenko, N.A., Friedel, R.H.W., The Inner Magnetosphere: Physics and Modelling, Geophysical Monogra. Ser. 38, 283–291, AGU, Washington, D.C. (2005)

DeForest, S.E., McIlwain, C.E.: Plasma clouds in the magnetosphere, J. Geophys. Res. **76**, 3587 (1971)

Degeling, A.W., Ozeke, L.G., Rankin, R., Mann, I.R., Kabin, K.: Drift resonance generation of peaked relativistic electron distributions by Pc5 ULF waves. J. Geophys. Res. (2008). doi:10.1029/2007JA012411

Delcourt, D., Sauvaud, J.-A., Martin Jr., R., Moore, T.: On the nonadiabatic precipitation of ions from the near-Earth plasma sheet, J. Geophys. Res. **101**, 17409–17418 (1996)

De Michelis, P., Daglis, I.A., Consolini, G.: Average terrestrial ring current derived from AMPTE/CCE–CHEM measurements, J. Geophys. Res. **102**, 14103–14111 (1997)

De Michelis, P., Daglis, I.A., Consolini, G.: An average image of proton plasma pressure and of current systems in the equatorial plane derived from AMPTE/CCE-CHEM measurements, J. Geophys. Res. **104**, 28615–28624 (1999)

Denton, R.E., Goldstein, J., Menietti, J.D.: Field line dependence of magnetospheric electron density, Geophys. Res. Lett. (2002). doi:10.1029/2002GL015963

Denton, M.H., Borovsky, J.E., Skoug, R.M., Thomsen, M.F., Lavraud, B., Henderson, M.G., McPherron, R.L., Zhang, J.C., Liemohn, M.W.: Geomagnetic storms driven by ICME- and CIR-dominated solar wind. J. Geophys. Res. (2006). doi:10.1029/2005JA011436

Denton, M.H., Borovsky, J.E.: Superposed epoch analysis of high-speed-stream effects at geosynchronous orbit: Hot plasma, cold plasma, and the solar wind, J. Geophys. Res. (2008). doi:10.1029/2007JA012998

Denton, R.E., Décréau, P., Engebretson, M.J., Darrouzet, F., Posch, J.L., Mouikis, C., Kistler, L.M., Cattell, C.A., Takahashi, K., Schäfer, S., Goldstein, J.: Field line distribution of density at L = 4.8 inferred from observations by CLUSTER. Ann. Geophys. **27**, 705–724 (2009).

Dessler, A.J., and Parker, E.N.: Hydromagnetic theory of geomagnetic storms, J. Geophys. Res., **64**, 2239–2252 (1959).

Dessler, A.J., Karplus, R.: Some effects of diamagnetic ring currents on Van Allen radiation, J. Geophys. Res. **66**, 2289–2295 (1961)

Dungey, J.W.: Interplanetary magnetic field and the auroral zones. Phys. Rev. Lett. **6**, 47–48 (1961)

Ebihara, Y., Ejiri, M.: Modeling of solar wind control of the ring current buildup: A case study of the magnetic storms in April 1997, Geophys. Res. Lett. **25,** 3751–3754 (1998)

Ebihara, Y., Ejiri, M.: Simulation study on fundamental properties of the storm-time ring current, J. Geophys. Res. **105**, 15843–15859 (2000)

Ebihara, Y., Yamauchi, M., Nilsson, H., Lundin, R., Ejiri, M.: Wedge-like dispersion of sub-keV ions in the dayside magnetosphere: Particle simulation and Viking observation, J. Geophys. Res., **106**, 29571–29584 (2001)

Ebihara, Y., Ejiri, M., Nilsson, H., Sandahl, I., Milillo, A., Grande, M., Fennell, J.F., Roeder, J.L.: Statistical distribution of the storm–time proton ring current: POLAR measurements, Geophys. Res. Lett. (2002). doi:10.1029/2002GL015430

Ebihara, Y., Ejiri, M.: Numerical simulation of the ring current: Review, Space Sci. Rev. **105**, 377– 452(2003)

Ebihara, Y., Ejiri, M. Sandahl, I. Nilsson, H. Grande, M. Fennell, J.F. Roeder, J.L. Ganushkina, N.Yu. and Milillo, A.: Structure and dynamics on the proton energy density in the inner magnetosphere, Adv. Space Res., **33**, 711–718, (2004)

Ebihara, Y., Fok, M.-C.: Postmidnight storm–time enhancements of tens-of-keV proton flux, J. Geophys. Res. (2004). doi:10.1029/2004JA010523

Ebihara, Y., Fok, M.-C., Wolf, R.A., Immel, T.J., Moore, T.E.: Influence of ionosphere conductivity on the ring current, J. Geophys. Res. (2004). doi:10.1029/2003JA010351

Ebihara, Y., Fok, M.-C., Sazykin, S., Thomsen, M.F., Hairston, M.R., Evans, D.S., Rich, F.J., Ejiri, M.: Ring current and the magnetosphere–ionosphere coupling during the super storm of 20 November 2003, J. Geophys. Res. (2005a). doi:10.1029/2004JA010924

Ebihara, Y., Fok, M.-C., Wolf, R.A., Thomsen, M.F., Moore, T.E.: Nonlinear impact of the plasma sheet density on the ring current, J. Geophys. Res. (2005b). doi:10.1029/2004JA010435

Ebihara Y., Yamada, M., Watanabe, S., Ejiri, M.: Fate of outflowing suprathermal oxygen ions that originate in the polar ionosphere, J. Geophys. Res. (2006). doi:10.1029/2005JA011403

Ebihara, Y., Fok, M.-C., Blake, J.B., Fennell, J.F.: Magnetic coupling of the ring current and the radiation belt, J. Geophys. Res. (2008a). doi:10.1029/2008JA013267

Ebihara Y., Kistler, L.M., Eliasson, L.: Imaging cold ions in the plasma sheet from the Equator-S satellite, J. Geophys. Res. Lett. (2008b). doi:10.1029/2008GL034357

Ebihara, Y., Nishitani, N., Kikuchi, T., Ogawa, T., Hosokawa, K., Fok, M.-C.: Two-dimensional observations of overshielding during a magnetic storm by the

Super Dual Auroral Radar Network (SuperDARN) Hokkaido radar, J. Geophys. Res. (2008c). doi:10.1029/2007JA012641

Ebihara Y., Kasahara, S., Seki, K., Miyoshi, Y., Fritz, T.A., Chen, J., Grande, M., Zurbuchen, T.H.: Simultaneous entry of oxygen ions originating from the Sun and Earth into the inner magnetosphere during magnetic storms, J. Geophys. Res. (2009a). doi:10.1029/2009JA014120

Ebihara, Y., Nishitani, N., Kikuchi, T., Ogawa, T., Hosokawa, K., Fok, M.-C., Thomsen, M.F.: Dynamical property of storm time subauroral rapid flows as a manifestation of complex structures of the plasma pressure in the inner magnetosphere, J. Geophys. Res. (2009b). doi:10.1029/2008JA013614

Ejiri, M.: Trajectory traces of charged particles in the magnetosphere, J. Geophys. Res. **83**, 4798–4810 (1978)

Ejiri, M., Hoffman, R.A. and Smith, P.H. :Energetic particle penetrations into the inner magnetosphere, J. Geophys. Res., 85(A2), 653–663 (1980).

Ejiri, M.: Shielding of the magnetospheric convection electric field and energetic charged particle penetrations towards the Earth, Magnetospheric dynamics, Proc. of ISAS symposium on magneto–ionosphere, 113 (1981)

Elkington, S.R., Hudson, M.K., Chan, A.A.: Acceleration of relativistic electrons via drift-resonant interaction with toroidal-mode Pc-5 ULF oscillations. Geophys. Res. Lett. **26**, 3273–3276 (1999)

Elkington, S.R., Hudson, M.K., Chan, A.A.: Resonant acceleration and diffusion of outer zone electrons in an asymmetric geomagnetic field. J. Geophys. Res. (2003). doi:10.1029/2001JA009202

Elkington, S.R.: A review of ULF interactions with radiation belt electrons. In: Takahashi, K., Chi, P.J., Denton, R.E., Lysak, R.L. (eds.) Magnetospheric ULF waves: Synthesis and New directions, pp. 177–193, AGU, Washington D.C. (2006)

Elphic, R.C., Weiss, L.A., Thomsen, M.F., McComas, D.J., Moldwin, M.B.: Evolution of plasmaspheric ions at geosynchronous orbit during times of high geomagnetic activity, Geophys. Res. Lett. **23**, 2189–2192 (1996)

Elphic, R.C., Thomsen, M.F., Borovsky, J.E.: The fate of the outer plasmasphere, Geophys. Res. Lett. **24**, 365–368 (1997)

Engebretson, M.J., et al.: Cluster observations of Pc 1-2 waves and associated ion distributions during the October and November 2003 magnetic storms, Planet. Space Sci., **55**, 829–848 (2007)

Erickson, G.M., Spiro, R.W. and Wolf, R.A.: The physics of the Harang discontinuity, J. Geophys. Res. **96**, 1633–1645 (1991)

Farrugia, C.J., Young, D.T., Geiss, J., Balsiger, H.: The Composition, temperature, and density structure of cold ions in the quiet terrestrial plasmasphere: GEOS 1 Results, J. Geophys. Res. **94**, 11865–11891 (1989)

Fejer, B.G., Gonzales, C.A., Farley, D.T., Kelley, M.C., Woodman, R.F.: Equatorial electric fields during magnetically disturbed conditions, 1. The effect of the interplanetary magnetic field, J. Geophys. Res. **84**, 5797–5802 (1979)

Fennell, J.F., Croley, D.R.Jr., Kaye, S.M.: Low-energy ion pitch angle distribution in the magnetosphere: Ion zipper distributions, J. Geophys. Res. **86**, 3375–(1981)

Fennell, J. F., Roeder, J.L.: Storm time phase space density radial profiles of energetic electrons for small and large K values: SCATHA results. J. Atm. Solar-Terr. Phys. **70**, 1760–1773 (2008)

Foat, J.E., Lin, R.P., Smith, D.M., F. Fenrich, Millan, R., Roth, I., Lorentzen, K.R., McCarthy, M.P., Parks, G.K., Treilhou, J.P.: First detection of a terrestrial MeV X-ray burst. Geophys. Res. Lett. **25**, 4109–4112 (1995)

Fok, M.-C., Kozyra, J.U., Nagy, A., Cravens, T.: Lifetime of ring current particles due to coulomb collisions in the plasmasphere, J. Geophys. Res. **96**, 7861–7867 (1991)

Fok, M.-C., Moore, T.E., Kozyra, J.U., Ho, G.C., Hamilton, D.C.: Three-dimensional ring current decay model, J. Geophys. Res. **100**, 9619–9632 (1995)

Fok, M.-C., Moore, T.E. Greenspan, M.E.: Ring current development during storm main phase, J. Geophys. Res. **101**, 15311–15322 (1996)

Fok, M.-C., Moore, T.E., Delcourt, D.C.: Modeling of inner plasma sheet and ring current during substorms, J. Geophys. Res. **104**, 14557–14569 (1999)

Fok, M.-C., Wolf, R.A., Spiro, R.W., Moore, T.E.: Comprehensive computational model of Earth's ring current, J. Geophys. Res. **106**, 8417–8424 (2001)

Fok, M.-C., et al.: Global ENA image simulations, Space Sci. Rev. **109**, 77–103 (2003)

Fok, M.-C., Horne, R.B., Meredith, N.P., Glauert, S.A.: Radiation Belt Environment model: Application to space weather nowcasting. J. Geophys. Res. (2008). doi:10.1029/2007JA012558

Foster, J.C., Vo, H.B.: Average characteristics and activity dependence of the subauroral polarization stream, J. Geophys. Res. (2002). doi:10.1029/2002JA009409

Foster, J.C., Coster, A.J., Erickson, P.J., Rich, F.J., Sandel, B.R.: Stormtime observations of the flux of plasmaspheric ions to the dayside cusp/magnetopause, Geophys. Res. Lett. (2004a). doi:10.1029/2004GL020082

Foster, J.C., Erickson, P.J. Lind, F.D. and Rideout, W.:Millstone Hill coherent-scatter radar observations of electric field variability in the sub-auroral polarization stream, Geophys. Res. Lett. (2004b). doi:10.1029/2004GL021271

Frahm, R.A., Reiff, P.H., Winningham, J.D., Burch, J.L.: Banded ion morphology: Main and recovery storm phases, in ion acceleration in the magnetosphere and ionosphere, Geophys. Monogr. Ser. **38**, Chang, T. et al. (eds), pp. 98–107, AGU, Washington D.C. (1986)

Frank, L.A.: On the extraterrestrial ring current during geomagnetic storms, J. Geophys. Res. **72**, 3753–3767 (1967)

Freeman Jr., J .W.: Magnetospheric wind, Science **63**, 1061– 1062 (1969)

Friedel, R.H.W., Korth, A., Kremser, G.: Substorm onsets observed by CRRES: Determination of energetic particle source regions, J. Geophys. Res. **101**, 13137–13154 (1996)

Friedel, R.H., Reeves, G.D., Obara, T.: Relativistic electron dynamics in the inner magnetosphere -a review. J. Atm. Solar-Terr. Phys. **64**, 265–282 (2002)

Fritz, T.A., Chen, J., Siscoe, G.L.: Energetic ions, large diamagnetic cavities, and Chapman-Ferraro cusp, J. Geophys. Res. (2003). doi:10.1029/2002JA009476

Fujimoto, M. Nishida, A.: Energization and anisotropization of energetic electrons in the Earth's radiation belt by the recirculation process. J. Geophys. Res. **95**, 4265–4270 (1990)

Fujimoto, M., Terasawa, T., Mukai, T., Saito, T., Yamamoto, T., Kokubun, S.: Plasma entry from the flanks of the near-Earth magnetotail: Geotail observations. J. Geophys. Res. **103**, 4391-4408 (1998)

Fung, S.F., Shao, X., Tan, L.C.: Long-term variations of the electron slot region and global radiation belt structure. Geophys. Res. Lett. (2006). doi:10.1029/2005GL024891

Fuselier, S.A., Gary, S.P., Thomsen, M.F., Claflin, E.S., Hubert, B., Sandel, B. R., Immel, T.: Generation of transient dayside subauroral proton precipitation, J. Geophys. Res. (2004). doi:10.1029/2004JA010393

Galperin, Y.I., Ponomarev, V.N., Zosimova, A.G.: Direct measurements of drift rate of ions in upper atmosphere during a magnetic storm. II. Results of measurements during magnetic storm of November 3, 1967, Cosmic Res., Engl. Transl. **11**, 249–258 (1973)

Galvan, D.A., Moldwin, M.B., Sandel, B.R.: Diurnal variation in plasmaspheric He inferred from extreme ultraviolet images, J. Geophys. Res. (2008). doi:10.1029/2007JA013013

Gamayunov, K.V., Khazanov, G.V.: Crucial role of ring current H+ in electromagnetic ion cyclotron wave dispersion relation: Results from global simulations, J. Geophys. Res. (2008). doi:10.1029/2008JA013494

Gamayunov, K.V., Khazanov, G.V., Liemohn, M.W., Fok, M.-C., Ridley, A.J.: Self–consistent model of magnetospheric electric field, ring current, plasmasphere, and electromagnetic ion cyclotron waves: Initial results, J. Geophys. Res. (2009). doi:10.1029/2008JA013597

Ganushkina, N.Yu., Pulkkinen, T.I., Kubyshkina, M.V., Sergeev, V.A., Lvova, E.A., Yahnina, T.A., Yahnin, A.G., Fritz, T.A.: Proton isotropy boundaries as measured on mid- and low-altitude satellites, Ann. Geophys. **23**, 1839–1847 (2005)

Garner, T.W.: Numerical experiments on the inner magnetospheric electric field, J. Geophys. Res. (2003). doi:10.1029/2003JA010039

Garner, T.W., Wolf, R.A., Spiro, R.W., Burke, W.J., Fejer, B. G., Sazykin, S., Roeder, J. L., Hairston, M. R.: Magnetospheric electric fields and plasma sheet injection to low L-shells during the 4-5 June 1991 magnetic storm: Comparison between the Rice Convection Model and observations, J. Geophys. Res. (2004). doi:10.1029/2003JA010208

Galand, M., Fuller-Rowell, T.J., Codrescu, M.V.: Response of the upper atmosphere to auroral protons, J. Geophys. Res. **106**, 127–139 (2001)

Galand, M., Richmond, A.D.: Ionospheric electrical conductances produced by auroral proton precipitation, J. Geophys. Res. **106**, 117–125 (2001)

Gallager, D.L., Adrian, M.L.: Two-dimensional drift velocities from the IMAGE EUV plasmaspheric imager, J. Atmos. Solar-Terr. Phys. **69**, 341–350 (2007)

Gannon, J.L., Li, X., Temerin, M.: Parametric study of shock-induced transport and energization of relativistic electrons in the magnetosphere. J. Geophys. Res. (2005). doi:10.1029/2004JA010679

Gendrin, R., Roux, A.: Energization of Helium ions by proton-induced hydromagnetic waves, J. Geophys. Res. **85**, 4577–4586 (1980)

Gkioulidou, M., Wang, C.-P., Lyons, L.R., and Wolf, R.A.: Formation of the Harang reversal and its dependence on plasma sheet conditions: Rice convection model simulations, J. Geophys. Res. (2009). doi:10.1029/2008JA013955

Goldstein, J., Denton, R.E., Hudson, M.K., Miftakhova, E.G., Young, S.L., Menietti, J.D., Gallagher, D.L.: Latitudinal density dependence of magnetic field lines inferred from Polar plasma wave data, J. Geophys. Res. **106**, 6195–6201 (2001)

Goldstein, J., Sandel, B.R., Forrester, W.T., Reiff, P.H.: IMF-driven plasmasphere erosion of 10 July 2000, Geophys. Res. Lett. (2003a). doi:10.1029/2002GL016478

Goldstein, J., Sandel, B.R., Hairston, M.R., Reiff, P.H.: Control of plasmaspheric dynamics by both convection and sub-auroral polarization stream, Geophys. Res. Lett. (2003b). doi:10.1029/2003GL018390

Goldstein, J., Spiro, R.W., Sandel, B.R., Wolf, R.A., Su, S.-Y., Reiff, P.H.: Overshielding event of 28-29 July 2000, Geophys. Res. Lett. (2003c). doi:10.1029/2002GL016644

Goldstein, J., Sandel, B.R., Hairston, M.R., Mende, S.B.: Plasmapause undulation of 17 April 2002, Geophys. Res. Lett. (2004a). doi:10.1029/2004GL019959

Goldstein, J., Wolf, R.A., Sandel, B.R., Reiff, P.H.: Electric fields deduced from plasmapause motion in IMAGE EUV images, Geophys. Res. Lett. (2004b). doi:10.1029/2003GL018797

Goldstein, J., Kanekal, S.G., Baker, D.N., Sandel, B.R.: Dynamic relationship between the outer radiation belt and the plasmapause during March-May 2001. Geophys. Res. Lett. (2005). doi:10.1029/2005GL023431

Green, J.C., Kivelson, M.G.: A tale of two theories: How the adiabatic response and ULF waves affect relativistic electrons. J. Geophys. Res. **106**, 25777–25791 (2001)

Green, J.L., Reinisch, B.W.: An overview of results from RPI on IMAGE, Space Sci. Rev. **145**, 231–261 (2002)

Green, J.C., Kivelson, M.G.: Relativistic electrons in the outer radiation belt: Differentiating between acceleration mechanisms. J. Geophys. Res. (2004). doi:10.1029/2003JA010153

Green, J.C., Onsager, T.G., O'Brien, T.P., Baker, D.N.: Testing loss mechanisms capable of rapidly depleting relativistic electron flux in the Earth's outer radiation belt. J. Geophys. Res. (2004). doi:10.1029/2004JA010579

Green, J.L., Fung, S.F.: Advances in inner magnetosphere passive and active wave research. In: Pulkkinen, T.I., Tsyganenko, N.A., Friedel, H.W. (eds.) The inner magnetosphere Physics and modeling. doi:10.1029/155GM21 (2005), AGU, Washington D.C.

Greenspan, M. E., and D. C. Hamilton: A test of the Dessler-Parker-Sckopke relation during magnetic storms, J. Geophys. Res. **105,** 5419–5430 (2000)

Greenspan, M.E., Hamilton, D.C.: Relative contributions of H^+ and O^+ to the ring current energy near magnetic storm maximum, J. Geophys. Res. (2002). doi:10.1029/2001JA000155

Grebowsky, J.M.: Model study of plasmapause motion, J. Geophys. Res. **75**, 4329–4333 (1970)

Grebowsky, J.M., Maynard, N.C., Tulunay, Y.K., Lanzerotti, L.J.: Coincident observations of ionospheric troughs and the equatorial plasmapause, Planet. Space Sci. **24**, 1177–1185 (1976)

Grebowsky, J.M., Benson, R.F., Webb, P.A., Truhlik, V., Bilitza, D.: Altitude variation of the plasmapause signature in the main ionospheric trough, J. Atm. Solar-Terr. Phys. **71**, 1669–1676 (2009)

Hamilton, D.C., Gloeckler, G., Ipavich, F.M., Stüdemann, W., Wilken, B., Kremser, G.: Ring current development during the great geomagnetic storm of February 1986, J. Geophys. Res. **93**, 14343–14355 (1988)

Hairston M.R., Drake, K.A., Skoug, R.: Saturation of the ionospheric polar cap potential during the October-November 2003 superstorms, J. Geophys. Res. (2005). doi:10.1029/2004JA010864

Hardy, D.A., Gussenhoven, M.S., Brautigam, D.: A statistical model of auroral ion precipitation, J. Geophys. Res. **94**, 370–392 (1989)

Hasegawa, H., et al.: Rolled-up Kelvin-Helmholtz vortices and associated solar wind entry at Earth's magnetopause, Nature **430**, 755–758 (2004)

Hilmer, R.V., Ginet, G.P., Cayton, T.E.: Enhancement of equatorial energetic electron fluxes near L=4.2 as a result of high speed solar wind streams. J. Geophys. Res. **105**, 23311–23322 (2000)

Hoffman, R.A.: Particle and field observations from Explorer 45 during the December 1971 magnetic storm period, J. Geophys. Res. **78**, 4771–4777 (1973)

Hori, T. et al.: Storm-time convection electric field in the near - Earth plasma sheet, J. Geophys. Res. (2005). doi:10.1029/2004JA010449

Horne, R.B., Thorne, R.M.: Wave heating of He+ by electromagnetic ion cyclotron waves in the magnetosphere: Heating near the H^+ - He^+ bi-ion resonance frequency, J. Geophys. Res. **102**, 11457–11471 (1997)

Horne, R.B., Thorne, R.M.: Potential waves for relativistic electron scattering and stochastic acceleration during magnetic storms. Geophys. Res. Lett. **25**, 3011–3014 (1998)

Horne, R.B.: The contribution of wave-particle interactions to electron loss and acceleration in the earth's radiation belts during geomagnetic storms, In: Stone, W.R. (eds.) Rev. of Radio Sci., 1999-2002, pp. 801–829, Wiley (2002)

Horne, R.B., Meredith, N.P., Thorne, R.M., Heynderickx, D., Iles, R.H.A., Anderson, R.R.: Evolution of energetic electron pitch angle distributions during storm time electron acceleration to megaelectronvolt energies. J. Geophys. Res. (2003). doi:10.1029/2001JA009165

Horne, R.B., Thorne, R.M., Glauert, S.A., Albert, J.M., Meredith, N.P., Anderson, R.R.: Timescale for radiation belt electron acceleration by whistler mode chorus waves. J. Geophys. Res. (2005a). doi:10.1029/2004JA010811

Horne, R.B., Thorne, R.M., Shprits, Y.Y., Meredith, N.P., Glauert, S.A., Smith, A.J., Kanekal, S.G., Baker, D.N., Engebretson, M.J., Posch, J.L., Spasojevic, M., Inan, U.S., Pickett, J.S., Decreau, P.M.M.: Wave acceleration of electrons in the Van Allen radiation belts. Nature **437**, 227–230 (2005b)

Horne, R.B.: Plasma astrophysics: Acceleration of killer electrons. Nature Phys. **3**, 590–591 (2007)

Horne, R.B., Thorne, R.M., Glauert, S.A., Meredith, N.P., Pokhotelov, D., Santolik, O.: Electron acceleration in the Van Allen radiation belts by fast magnetosonic waves. Geophys. Res. Lett. (2007). doi:10.1029/2007GL030267

Horwitz, J.L., Comfort, R.H., Chappell, C.R.: Thermal ion composition measurements of the formation of the new outer plasmasphere and double

plasmapause during storm recovery phase, Geophys. Res. Lett. **11**, 701–704 (1984)

Horwitz, J., Brace, L., Comfort, R., Chappell, C.: Dual-spacecraft measurements of plasmasphere-ionosphere coupling, J. Geophys. Res. **91**, 11203–11216 (1986)

Horwitz, J.L., Comfort, R.H., Chappell, C.R.: A statistical characterization of plasmasphere density structure and boundary locations, J. Geophys. Res. **95**, 7937–7947 (1990a)

Horwitz, J.L., Comfort, R.H., Richards, P.G., Chandler, M.O., Chappell, C.R., Anderson, P., Hanson, W.B., Brace, L.H.: Plasmasphere-ionosphere coupling, 2. ion composition measurements at plasmaspheric and ionospheric altitudes and comparison with modeling results, J. Geophys. Res. **95**, 7949–7959 (1990b)

Huang, X., Reinisch, B.W., Song, P., Green, J.L., Gallagher, D.L.: Developing an empirical density model of the plasmasphere using IMAGE/RPI observations, Adv. Space Res. **33**, 829–832 (2004)

Huang, C.-S., Foster, J.C.: Correlation of the subauroral polarization streams (SAPS) with the Dst index during severe magnetic storms, J. Geophys. Res. **112,** (2007). doi:10.1029/2007JA012584

Hudson, M.K., Kotelnikov, A.D., Li, X., Roth, I., Temerin, M., Wygant, J., Blake, J.B., Gussenhoven, M.S.: Simulation of proton radiation belt formation during the March 24, 1991 SSC. Geophys. Res. Lett. **22**, 291–294 (1995)

Hudson, M.K., Kress, B.T., Mazur, J.E., Perry, K.L., Slocum, P.L.: 3D modeling of shock-induced trapping of solar energetic particles in the Earth's magnetosphere. J. Atm. Solar-Terr. Phys. **66**, 1389–1397 (2004)

Hudson, M.K., Kress, B.T., Mueller, H.-R., Zastrow, J.A., Blake, J. B.: Relationship of the Van Allen radiation belts to solar wind drivers. J. Atm. Solar-Terr. Phys. **70**, 708–729 (2008)

Iijima, T., Potemra, T.A.: The amplitude distribution of field-aligned currents at northern high latitudes observed by Triad, J. Geophys. Res. **81**, 2165–2174 (1976)

Iles, R.H., Meredith, N.P., Fazakerley, A.N., Horne, R.B.: Phase space density analysis of the outer radiation belt energetic electron dynamics. J. Geophys. Res., (2006). doi:10.1029/2005JA011206

Janev, R.K., Smith, J.J.: Cross sections for collision processes of hydrogen atoms with electrons, protons, and multiply-charged ions, in Atomic and Plasma-Material Interaction Data for Fusion, Int. At. Energ. Agency. **4**, 1–80 (1993)

Jordanova, V.K., Kistler, L.M., Kozyra, J.U, Khazanov, G.V., Nagy, A.F.: Collisional losses of ring current ions, J. Geophys. Res. **101**, 111–126 (1996)

Jordanova, V.K., Kozyra, J.U., Nagy, A.F., Khazanov, G.V.: Kinetic model of the ring current-atmosphere interactions, J. Geophys. Res. **102**, 14279–14291 (1997)

Jordanova, V.K., Farrugia, C.J., Quinn, J.M., Torbert, R.B., Borovsky, J.E., Sheldon R.B., Peterson, W.K.: Simulation of off-equatorial ring current ion spectra measured by Polar for a moderate storm at solar minimum, J. Geophys. Res. **104**, 429–436 (1999)

Jordanova, V.K., Kistler, L.M., Thomsen, M.F., Mouikis, C.G.: Effects of plasma sheet variability on the fast initial ring current decay. Geophys. Res. Lett.(2003). doi:10.1029/2002GL016576

Jordanova, V.K., Miyoshi,Y.: Relativistic model of ring current and radiation belt ions and electrons: Initial results. Geophys. Res. Lett. (2005). doi:10.1029/2005GL023020

Jordanova, V.K., Miyoshi, Y., Zaharia, S., Thomsen, M.F., Reeves, G.D., Evans, D.S., Moukis, C.G., Fennell, J.F: Kinetic simulations of ring current evolution during the Geospace Environment Modeling challenging events. J. Geophys. Res. (2006). doi:10.1029/2006JA011644.

Jordanova V.K., Spasojevic, M., Thomsen, M.F.: Modeling the electromagnetic ion cyclotron wave-induced formation of detached subauroral proton arcs, J. Geophys. Res. (2007). doi:10.1029/2006JA012215

Jordanova, V.K., Albert, J., Miyoshi, Y.: Relativistic electron precipitation by EMIC waves from self-consistent global simulations. J. Geophys. Res. (2008). doi:10.1029/2008JA013239

Jordanova, V.K., Thorne, R.M., Li, W., Miyoshi, Y.: Excitation of whistler-mode chorus from global ring current simulations. J. Geophys. Res. (2010). doi:10.1029/2009JA014810

Jorgensen, A.M., Spence, H.E., Henderson, M.G., Reeves, G.D., Sugiura, M. and Kamei, T.: Global energetic neutral atom (ENA) measurements and their association with the Dst index, Geophys. Res. Lett. **24**, 3173–3176 (1997)

Kamide, Y., Fukushima, N.: Analysis of magnetic storms with DR indices for equatorial ring-current field, Radio Sci. **6**, 277–278 (1971)

Kamide, Y.: Association of DP and DR fields with the interplanetary magnetic field variation, J. Geophys. Res. **79**, 49–55 (1974)

Kamide, Y., McIlwain, C.E.: The onset time of magnetospheric substorms determined from ground and synchronous satellite records, J. Geophys. Res. **79**, 4787–4790 (1974)

Kale, Z.C., Mann, I.R., Waters, C.L., Vellante, M., Zhang, T.L., Honary, F.: Plasmaspheric dynamics resulting from the Hallowe'en 2003 geomagnetic storms, J. Geophys. Res. **114**, (2009). doi:10.1029/2009JA014194

Karlsson, T., Marklund, G., Blomberg, L., Mälkki, A.: Subauroral electric fields observed by the Freja satellite: A statistical study, J. Geophys. Res. **103**, 4327–4341 (1998)

Kasahara, Y., Miyoshi, Y., Omura, Y., Berkhoglyadova, O., Nagano, I., Kimura, I., Tsurutani, B.: Simultaneous satellite observations of VLF chorus, hot and relativistic electrons in a magnetic storm "recovery phase". Geophys. Res. Lett. (2009). doi:10.1029/2008GL036454

Kataoka, R., Miyoshi, Y.: Flux enhancement of radiation belt electrons during geomagnetic storms driven by coronal mass ejections and corotating interaction regions. Space Weather (2006). doi:10.1029/2005SW000211

Kataoka, R., Nishitani, N., Ebihara, Y., Hosokawa, K., Ogawa, T., Kikuchi, T., Miyoshi, Y.: Dynamic variations of a convection flow reversal in the subauroral postmidnight sector as seen by the SuperDARN Hokkaido HF radar, Geophys. Res. Lett. (2007). doi:10.1029/2007GL031552

Kataoka, R., Miyoshi, Y.: Magnetosphere inflation during the recovery phase of geomagnetic storms as an excellent magnetic confinement of killer electrons. Geophys. Res. Lett. (2008a). doi:10.1029/2007GL031842

Kataoka, R., Miyoshi, Y.: Average profiles of the solar wind and outer radiation belt during the extreme flux enhancement of relativistic electrons at geosynchronous orbit. Ann. Geophys. **26**, 1335–1339 (2008b)

Katoh, Y., Omura, Y.: Computer simulation of chorus wave generation in the Earth's inner magnetosphere. Geophys. Res. Lett. (2007a). doi:10.1029/2006GL028594

Katoh, Y., Omura, Y.: Relativistic particle acceleration in the process of whistler-mode chorus wave generation. Geophys. Res. Lett. (2007b). doi:10.1029/2007GL029758

Katoh, Y., Omura, Y., Summers, D.: Rapid energization of radiation belt electrons by nonlinear wave trapping. Ann. Geophys. **26**, 3451–3456 (2008)

Kavanagh Jr., L.D., Freeman Jr., J.W., Chen, A.J.: Plasma flow in the magnetosphere, J. Geophys. Res. **73**, 5511–5519 (1968)

Kaye, S.M., Shelley, E.G., Sharp, R.D., Johnson, R.G.: Ion composition of zipper events, J. Geophys. Res. **86**, 3383–3388 (1981)

Keika, K., Nosé, M., Christon, S.P., McEntire, R.W.: Acceleration sites of energetic ions upstream of the Earth's bow shock and in the magnetosheath: Statistical study on charge states of heavy ions, J. Geophys. Res. **(**2004). doi:10.1029/2003JA009953

Keika, K., Nosé, M., Ohtani, S.-I., Takahashi, K., Christon, S.P., McEntire, R.W.: Outflow of energetic ions from the magnetosphere and its contribution to the decay of the storm time ring current, J. Geophys. Res. (2005). doi:10.1029/2004JA010970

Kelley, M.C., Fejer, B.G., Gonzales, C.A.: An explanation for anomalous equatorial ionospheric electric fields associated with a northward turning of the interplanetary magnetic field, Geophys. Res. Lett. **6**, 301–304 (1979)

Kennel, C., Petschek, H.: Limit on stably trapped particle fluxes. J. Geophys. Res. **71**, 1–28 (1966)

Khazanov, G.V., Moore, T.E., Liemohn, M.W., Jordanova, V.K., Fok, M.-C.: Global, collisional model of high-energy photoelectrons, Geophys. Res. Lett. **23**, 331–334 (1996)

Kikuchi, T., Araki, T., Maeda, H., Maekawa, K.: Transmission of polar electric fields to the equator, Nature **273**, 650–651 (1978)

Kikuchi, T., Lühr, H., Kitamura, T., Saka, O., Schlegel, K.: Direct penetration of the polar electric field to the equator during a DP 2 event as detected by the auroral and equatorial magnetometer chains and the EISCAT radar, J. Geophys. Res. **101**, 17161–17173 (1996)

Kikuchi, T., Hashimoto, K.K., Nozaki, K.: Penetration of magnetospheric electric fields to the equator during a geomagnetic storm, J. Geophys. Res. (2008). doi:10.1029/2007JA012628

Kikuchi, T., Ebihara, Y., Hashimoto, K., Kataoka, R., Hori, T., Watari, S., Nishitani, N.: Penetration of the convection and overshielding electric fields to the equatorial ionosphere during a quasi-periodic DP2 geomagnetic fluctuation event, J. Geophys. Res. (2010). doi:10.1029/2008JA013948

Kim, H.-J., Chan, A.A.: Fully adiabatic changes in storm time relativistic electron fluxes. J. Geophys. Res. **102**, 22107–22116 (1997)

Kim, H.-J., Kim, K.C., Lee, D.-Y., Rostoker, G.: Origin of geosynchronous relativistic electron events. J. Geophys. Res. (2006). doi:10.1029/2005JA011469

Kim, K.C., Lee, D.-Y. , Kim, H.-J., Lyons, L.R., Lee, E.S., Ozturk, M.K., Choi, C.R.: Numerical calculations of relativistic electron drift loss effect. J. Geophys. Res. (2008). doi:10.1029/2007JA013011

Kivelson, M.G., Ridley, A.J.: Saturation of the polar cap potential: Inference from Alfvén wing arguments. J. Geophys. Res. (2008). doi:10.1029/2007JA012302

Klumpar, D.M.: Transversely accelerated ions: An ionospheric source of hot magnetospheric ions, J. Geophys. Res. **84**, 4229–4237 (1979)

Kokubun, S.: Relationship of interplanetary magnetic field structure with development of substorm and storm main phase, Planet. Space Sci. **20**, 1033–1049 (1972)

Koller, J., Chen, Y., Reeves, G.D., Friedel, R.H.W., Cayton, T.E., Vrugt, J.A.: Identifying the radiation belt source region by data assimilation, J. Geophys. Res. (2007). doi:10.1029/2006JA012196.

Kondrashov, D., Shprits, Y., Ghil, M., Thorne, R.: A Kalman filter technique to estimate relativistic electron lifetimes in the outer radiation belt, J. Geophys. Res. (2007). doi:10.1029/2007JA012583.

Konradi, A.: Proton events in the magnetosphere associated with magnetic bays, J. Geophys. Res. **72**, 3829–3841 (1967)

Konradi, A., Semar, C.L., Fritz, T.A.: substorm-injected protons and electrons and the injection boundary model, J. Geophys. Res. **80**, 543–552 (1975)

Koons, H.C.: Observations of large-amplitude, Whistler mode wave ducts in the outer plasmasphere, J. Geophys. Res. **94**, 15393–15397 (1989)

Korth, A., Friedel, R.H.W., Mouikis, C.G., Fennell, J.F., Wygant, J.R., Korth, H.: Comprehensive particle and field observations of magnetic storms at different local times from the CRRES spacecraft, J. Geophys. Res. **105**, 18729–18740 (2000)

Kotova, G., Bezrukikh, V., Verigin, M., Smilauer, J.: New aspects in plasmaspheric ion temperature variations from INTERBALL 2 and MAGION 5 measurements, J. Atm. Solar-Terr. Phys. **70**, 399–406 (2008)

Kozyra, J.U., Shelley, E.G., Comfort, R H., Brace, L.H., Cravens, T.E., Nagy, A.F.: The role of ring current O^+ in the formation of stable auroral red arcs, J. Geophys. Res. **92**, 7487–7502 (1987)

Kozyra, J. U., Chandler, M.O., Hamilton, D.C. Peterson, W.K., Klumpar, D.M., Slater, D.W., Buonsanto, M.J., and Carlson, H.C.: The role of ring current nose events in producing stable auroral red arc intensifications during the main phase: Observations during the September 19-24, 1984, equinox transition study, J. Geophys. Res. **98**, 9267–9283 (1993)

Kozyra, J.U., Nagy, A F., Slater, D.W.: High-Altitude energy source(s) for stable auroral red arcs, Rev. Geophys. **35**, 155–190 (1997)

Kozyra, J.U., Fok, M.-C., Sanchez, E.R., Evans, D.S., Hamilton, D.C., Nagy, A.F.: The role of precipitation losses in producing the rapid early recovery phase of the great magnetic storm of February 1986, J. Geophys. Res. **103**, 6801– 6814 (1998a)

Kozyra, J.U., Jordanova, V.F, Borovsky, J.E, Thomsen, M.F, Knipp, D., Evans, D.S., McComas, D., Cayton, T.: Effects of a high-density plasma sheet on ring current development during the November 2-6, 1993, magnetic storm, J. Geophys. Res. **103**, 26285–26305 (1998b)

Kozyra, J.U., Liemohn, M.W.: Ring current energy input and decay, Space Sci. Rev. **109**, 105–131 (2003)

Krall, J., Huba, J.D., Fedder, J.A.: Simulation of field-aligned H+ and He+ dynamics during late-stage plasmasphere refilling, Ann. Geophys. **26**, 1507–1516 (2008)

Kress, B.T., Hudson, M.K., Slocum, P.L.: Impulsive solar energetic ion trapping in the magnetosphere during geomagnetic storms. Geophys. Res. Lett. (2005). doi:10.1029/2005GL022373

Krimigis, S.M., Gloeckler, G., McEntire, R.W., Potemra, T.A., Scarf, F.L., Shelley, E.G.: Magnetic storm of September 4, 1984: A systhesis of ring current spectra and energy densities measured with AMPTE/CCE, Geophys. Res. Lett. **12**, 329–332 (1985)

Lam, M.M., Horne, R.B., Meredith, N.P., Glauert, S.A.: Modeling the effects of radial diffusion and plasmaspheric hiss on outer radiation belt electrons, Geophys. Res. Lett. **34,** (2007). doi:10.1029/2007GL031598

Lavraud, B., Denton, M. H., Thomsen, M. F., Borovsky, J. E., Friedel, R. H. W.: Superposed epoch analysis of dense plasma access to geosynchronous orbit, Ann. Geophys., 23, 2519-2529 (2005), doi:10.5194/angeo-23-2519-2005.

Lavraud, B., Jordanova, V.K.: Modeling the effects of cold-dense and hot-tenuous plasma sheet on proton ring current energy and peak location. Geophys. Res. Lett.(2007), doi:10.1029/2006GL027566.

Le, G., Russell, C.T., Takahashi, K.: Morphology of the ring current derived from magnetic field observations, Ann. Geophys. **22**, 1267–1295 (2004)

Lee, D.-Y., Ohtani, S., Brandt, P.C., Lyons, L.R.: Energetic neutral atom response to solar wind dynamic pressure enhancements, J. Geophys. Res. (2007). doi:10.1029/2007JA012399

Lemaire, J.: Plasma distribution models in a rotating magnetic dipole and refilling of plasmaspheric flux tubes, Phys. Fluids **B1**, 1519–1525 (1989).

Lemaire, J.: The formation of the light ion trough and peeling off the plasmasphere, J. Atmos. Terr. Phys. **63**, 1285–1291 (2001)

Lennartsson, W., Sharp, R.D., Shelley, E.G., Johnson, R.G., Balsiger, H.: Ion composition and energy distribution during 10 magnetic storms, J. Geophys. Res. **86**, 4628–4638 (1981)

Lennartsson, W., Sharp, R.D.: A comparison of the 0.1-17 keV/e ion composition in the near equatorial magnetosphere between quiet and disturbed conditions, J. Geophys. Res. **87**, 6109–6120 (1982)

Lennartsson, W.: Energetic (0.1- to 16-keV/e) magnetospheric ion composition at different levels of Solar F10.7, J. Geophys. Res. **94**, 3600–3610 (1989)

Li, X., Roth, I., Temerin, M., Wygant, J.R., Hudson, M.K., Blake, J.B.: Simulation of the prompt energization and transport of radiation belt particles during the March 24, 1991 SSC. Geophys. Res. Lett. **20**, 2423–2426(1993)

Li, X., Baker, D.N., Temerin, M., Cayton, T.E., Reeves, G.D., Christensen, R.A., Blake, J.B., Looper, M.D., Nakamura, R., Kanekal, S.G.: Multisatellite observations of the outer zone electron variation during the November 3-4, 1993, magnetic storm. J. Geophys. Res. **102**, 14123–14140 (1997)

Li, X., Temerin, M.A.: The electron radiation belt. Space Sci. Rev. **95**, 569–580 (2001)

Li, X., Baker, D.N., Kanekal, S.G., Looper, M., Temerin, M.: Long term measurements of radiation belts by SAMPEX and their variations. Geophys. Res. Lett. **28**, 3827–3830 (2001)

Li, X., Baker, D.N., Temerin, M., Reeves, G., Friedel, R., Shen, C.: Energetic electrons, 50 keV to 6 MeV, at geosynchronous orbit: Their responses to solar wind variations. Space Weather (2005). doi:10.1029/2004SW000105

Li, X., Baker, D.N., O'Brien, T.P., Xie, L., Zong, Q.G.: Correlation between the inner edge of outer radiation belt electrons and the innermost plasmapause location. Geophys. Res. Lett. (2006). doi:10.1029/2006GL026294.

Li, W., Shprits, Y.Y., Thorne, R.M.: Dynamic evolution of energetic outer zone electrons due to wave-particle interactions during storms. J. Geophys. Res. (2007). doi:10.1029/2007JA012368

Li, W., Thorne, R.M., Meredith, N.P., Horne, R.B., Bortnik, J., Shprits, Y.Y., Ni, B.: Evaluation of whistler mode chorus amplication during an injection event observed on CRRES, J. Geophys. Res. (2008), doi:10.1029/2008JA013129

Liemohn, M.W., Kozyra, J.U., Jordanova, V.K., Khazanov, G.V., Thomsen, M.F., Cayton, T.E.: Analysis of early phase ring current recovery mechanisms during geomagnetic storms, Geophys. Res. Lett. **26**, 2845–2848 (1999)

Liemohn, M.W., Kozyra, J.U., Thomsen, M.F., Roeder, J.L., Lu, G., Borovsky, J.E., Cayton, T.E.: Dominant role of the asymmetric ring current in producing the stormtime Dst*, J. Geophys. Res. **106**, 10883–10904 (2001)

Liemohn, M.W., Ridley, A.J., Brandt, P.C., Gallagher, D.L., Kozyra, J.U., Mitchell, D.G., Roelof, E.C., DeMajistre, R.: Parametric analysis of nightside conductance effects on inner magnetospheric dynamics for the 17 April 2002 storm, J. Geophys. Res. (2005). doi:10.1029/2005JA011109

Liemohn, M.W., Zhang, J.-C., Thomsen, M.F., Borovsky, J.E., Kozyra, J.U., Ilie, R.: Plasma properties of superstorms at geosynchronous orbit: How different are they?, Geophys. Res. Lett. (2008). doi:10.1029/2007GL031717

Liu, W., Rostoker, G., Baker, D.: Internal acceleration of relativistic electrons by large-amplitude ULF pulsations. J. Geophys. Res. **104**, 17391–17407 (1999)

Liu, S., Chen, M.W., Roeder, J.L., Lyons, L.R., Schulz, M.: Relative contribution of electrons to the stormtime total ring current energy content, Geophys. Res. Lett. (2005a). doi:10.1029/2004GL021672

Liu, W.L., Fu, S.Y., Zong, Q.-G., Pu, Z.Y., Yang, J., Ruan, P.: Variations of N+/O+ in the ring current during magnetic storms, Geophys. Res. Lett. (2005b). doi:10.1029/2005GL023038

Looper, M.D., Blake, J.B., Mewaldt, R.A.: Response of the inner radiation belt to the violent Sun-Earth connection events of October-November 2003. Geophys. Res. Lett. (2005). doi:10.1029/2004GL021502

Lopez, R.E., Sibeck, D.G., McEntire, R.W., Krimigis, S.M.: The energetic ion substorm injection boundary, J. Geophys. Res. **95**, 109–117 (1990)

Lopez, R.E., Lyon, J.G. Mitchell, E. Bruntz, R. Merkin, V.G. Brogl, S. Toffoletto, F. and Wiltberger, M.: Why doesn't the ring current injection rate saturate?, J. Geophys. Res. (2009). doi:10.1029/2008JA013141.

Lorentzen, K.R., McCarthy, M.P., Parks, G.K., Foat, J.E., Millan, R.M., Smith, D.M., Lin, R.P., Treilhou, J.P.: Precipitation of relativistic electrons by interaction with electromagnetic ion cyclotron waves. J. Geophys. Res. 5381–5389 (2000)

Lorentzen, K.R., Blake, J.B., Inan, U.S., Bortnik, J.: Observations of relativistic electron microbursts in association with VLF chorus. J. Geophys. Res. **106**, 6017–6027 (2001)

Loto'aniu, T.M., Mann, I.R., Ozeke, L.G., Chan, A.A., Dent, Z.C., Milling, D.K.: Radial diffusion of relativistic electrons into the radiation belt slot region during the 2003 Halloween geomagnetic storms. J. Geophys. Res. (2006). doi:10.1029/2005JA011355

Lui, A.T.Y., McEntire, R.W., Krimigis, S.M.: Evolution of the ring current during two geomagnetic storms, J. Geophys. Res. **92**, 7459–7470 (1987)

Lui, A.T.Y., Spence, H.E., Stern, D.P.: Empirical Modeling of the quiet time nightside magnetosphere, J. Geophys. Res. **99**, 151–157 (1994)

Lui, A.T.Y.: Inner magnetospheric plasma pressure distribution and its local time asymmetry, Geophys. Res. Lett. (2003). doi:10.1029/2003GL017596

Lundin, R., Lyons, L.R., Pissarenko, N.: Observations of the ring current composition at L < 4, Geophys. Res. Lett. **7**, 425–428 (1980)

Lyatsky, W. Khazanov, G.V.: Effect of solar wind density on relativistic electrons at geosynchronous orbit, Geophys. Res. Lett. (2008), doi:10.1029/2007GL032524

Lyons, L.R., Thorne, R.M.: Parasitic pitch angle diffusion of radiation belt particles by ion cyclotron waves. J. Geophys. Res. **77**, 5608–5616 (1972)

Lyons, L.R., Thorne, R.M., Kennel, C.F.:, Pitch-angle diffusion of radiation belt electrons within the plasmasphere. J. Geophys. Res. 77, 3455–3474 (1972)

Lyons, L.R., Thorne, R.M.: Equilibrium structure of radiation belt electrons. J. Geophys Res. **78**, 2142–2149 (1973)

Lyons, L.R.: General relations for resonant particle diffusion in pictcn angle and decay. J. Plasma Phys. **12**, 45–49 (1974)

Lyons, L. R., Williams, D.J.: The quiet time structure of energetic (35-560 keV) radiation belt electrons. J. Geophys. Res. **80**, 943–950 (1975a)

Lyons, L. R., Williams, D.J.: The storm and poststorm evolution of energetic (35-560 keV) radiation belt electron distributions. J. Geophys. Res. **80**, 3985–3994 (1975b)

Lyons, L., Williams, D.: Storm-associated variations of equatorially mirroring ring current protons, 1-800 keV, at constant first adiabatic invariant, J. Geophys. Res. **81**, 216–220 (1976)

Lyons, L.R.: Adiabatic evolution of trapped particle pitch angle distributions during a storm main phase. J. Geophys. Res. **82**, 2428–2432 (1977)

Lyons, L.R., Richmond, A.D.: Low-latitude E region ionization by energetic ring current particles, J. Geophys. Res. **83**, 2201–2204 (1978)

Lyons L.R., Williams, D.: Quantitative aspects of magnetospheric physics, D. Reidel, Norwell, Mass. (1984)

Lyons, L.R., Lee, D.-Y., Thorne, R.M., Horne, R.B., Smith, A.J.: Solar wind–magnetosphere coupling leading to relativistic electron energization during high–speed streams. J. Geophys. Res. (2005). doi:10.1029/2005JA011254

Lyons, L.R., Lee, D.-Y., Kim, H.-J., Hwang, J.A., Thorne, R.M., Horne, R.B., Smith, A.J.: Solar-wind-magnetosphere coupling, including relativistic electron energization, during high-speed streams. J. Atm. Solar-Terr. Phys. **71**, 1059–1072 (2009)

Maget, V., Bourdarie, S., Boscher, D., Friedel, R.H.W.: Data assimilation of LANL satellite data into the Salammbo electron code over a complete solar cycle by direct insertion. Space Weather (2007). doi:10.1029/2007SW000322

Makarevich R.A., Kellerman, A.C., Bogdanova, Y.V., Koustov, A.V.: Time evolution of the subauroral electric fields: A case study during a sequence of two substorms, J. Geophys. Res. (2009). doi:10.1029/2008JA013944

Mann, I.R., O'Brien, T.P., Milling, D.K: Correlations between ULF wave power, solar wind speed, and relativistic electron flux in the magnetosphere: solar cycle dependence. J. Atm. Solar-Terr. Phys. **66**, 187–198 (2004)

Mathie, R.A., Mann, I.R.: On the solar wind control of Pc5 ULF pulsation power at mid-latitudes: Implications for MeV electron acceleration in the outer radiation belt. J. Geophys. Res. **106**, 29783–29796 (2001)

Matsui, H., Mukai, T., Ohtani, S., Hayashi, K., Elphic, R.C., Thomsen, M.F., Matsumoto, H.: Cold dense plasma in the outer magnetosphere, J. Geophys. Res. **104**, 25077–25095 (1999)

Matsui, H., Nakamura, M., Terasawa, T., Izaki, Y., Mukai, T., Tsuruda, K., Hayakawa, H., Matsumoto, H.: Outflow of cold dense plasma associated with variation of convection in the outer magnetosphere, Journal of Atmospheric and Solar–Terrestrial Physics **62**, 521–526 (2000)

Matsui, H., Puhl-Quinn, P.A., Jordanova, V.K., Khotyaintsev, Y., Lindqvist, P.-A., Torbert, R.B.: Derivation of inner magnetospheric electric field (UNH–IMEF) model using Cluster data set, Ann. Geophys. **26**, 2887–2898 (2008)

Mauk, B.H., McIlwain, C.E.: Correlation of Kp with the substorm-injected plasma boundary, J. Geophys. Res. **79**, 3193–3196 (1974)

Mauk, B.H., Meng, C.-I.: Characterization of geostationary particle signatures based on the 'injection boundary' model, J. Geophys. Res. **88**, 3055–3071 (1983)

Maynard, N.C., Chen, A.J.: Isolated cold plasma regions: Observations and their relation to possible production mechanisms, J. Geophys. Res. **80**, 1009–1013 (1975)

Maynard, N. C., T. L. Aggson, and J. P. Heppner: Magnetospheric observation of large sub‐auroral electric fields, Geophys. Res. Lett. **7**, 881–884 (1980)

Maynard, N.C., Aggson, T.L., Heppner, J.P.: The plasmaspheric electric field as measured by ISEE 1, J. Geophys. Res. **88**, 3991–4003 (1983)

McFadden, J.P., Carlson, C.W., Larson, D., Bonnell, J., Mozer, F.S., Angelopoulos, V., Glassmeier, K., Auster, U.: Structure of plasmaspheric plumes and their participation in magnetopause reconnection: First results from THEMIS, Geophys. Res. Lett. (2008). doi:10.1029/2008GL033677

McIlwain, C.E.: Ring current effects on trapped particles, J. Geophys. Res. **71**, 3623–3628 (1966)

McIlwain, C.E.: Substorm injection boundaries, in Magnetospheric Physics, McComac, B.M. (ed.) P. 143, D. Reidel, Hingham, Mass. (1974)

McPherron, R.L., Baker, D.N., Crooker, N.U.: Role of the Russell-McPherron effect in the acceleration of relativistic electrons. J. Atm. Solar-Terr. Phys. **71**, 1032–1044 (2009)

Meredith, N.P., Horne, R.B., Anderson, R.R.: Substorm dependence of chorus amplitudes: Implications for the acceleration of electrons to relativistic energies. J. Geophys. Res. **106**, 13165–13178 (2001)

Meredith, N.P., Horne, R.B., Summers, D., Thorne, R.M., Iles, R.H.A., Heynderickx, D., Anderson, R.R.: Evidence for acceleration of outer zone electrons to relativistic energies by whistler mode chorus. Ann. Geophys. **20**, 967–979 (2002)

Meredith, N.P., Cain, M., Horne, R.B., Thorne, R. M., Summers, D., Anderson, R.R.: Evidence for chorus-driven electron acceleration to relativistic energies from a survey of geomagnetically disturbed periods. J. Geophys. Res. (2003a). doi:10.1029/2002JA009764

Meredith, N.P., Horne, R.B., Thorne, R.M., Anderson, R.R.: Favored regions for chorus-driven electron acceleration to relativistic energies in the Earth's outer radiation belt. Geophys. Res. Lett. (2003b). doi:10.1029/2003GL017698

Meredith, N.P., Thorne, R.M., Horne, R.B., Summers, D., Fraser, B.J., Anderson, R.R.: Statistical analysis of relativistic electron energies for cyclotron resonance with EMIC waves on CRRES, J. Geophys. Res. (2003c). doi:10.1029/2002JA009700

Meredith, N.P., Horne, R.B., Glauert, S.A., Thorne, R.M., Summers, D., Albert, J.M., Anderson, R.R.: Energetic outer zone electron loss timescales during low geomagnetic activity. J. Geophys. Res. (2006). doi:10.1029/2005JA011516

Merkin, V.G., Sharma, A.S., Papadopoulos, K. Milikh, G., Lyon, J., Goodrich, C.: Global MHD simulations of the strongly driven magnetosphere: Modeling of the transpolar potential saturation, J. Geophys. Res. (2005). doi:10.1029/2004JA010993.

Milillo, A., Orsini, S., Daglis, I.A.: Empirical model of proton fluxes in the equatorial inner magnetosphere: Development, J. Geophys. Res. **106**, 25713–25729 (2001)

Milillo, A., Orsini, S., Delacourt, D.C., Mura, A., Massetti, S., De Angelis, E., Ebihara, Y.: Empirical model of proton fluxes in the equatorial inner magnetosphere: 2. Properties and applications, J. Geophys. Res. (2003). doi:10.1029/2002JA009581

Millan, R.M., Lin, R.P., Smith, D.M., Lorentzen, K.R., McCarthy, M.P.: X-ray observations of MeV electron precipitation with a balloon-borne germanium spectrometer. Geophys. Res. Lett. (2002). doi:10.1029/2002GL015922.

Millan, R.M., Thorne, R.M.: Review of radiation belt electron losses. J. Atm. Solar-Terr. Phys. **69**, 362–377 (2007)

Mishin, E.V., Puhl-Quinn, P.A.: SAID: Plasmaspheric short circuit of substorm injections, Geophys. Res. Lett. (2007). doi:10.1029/2007GL031925

Mitchell, D.G., Brandt, P.C., Roelof, E.C., Hamilton, D.C., Retterer, K.C., Mende, S.: Global imaging of O^+ from IMAGE/HENA, Space Sci. Rev. **109**, 63–75(2003)

Miyoshi, Y., A.Morioka, Misawa,H.: Long term modulation of low altitude proton radiation belt by the Earth's atmosphere. Geophys. Res. Lett. **27**, 2169–2172 (2000)

Miyoshi, Y., A.Morioka, Obara, T., Misawa, H., Nagai, T., Kasahara, Y.: Rebuilding process of the outer radiation belt during the November 3, 1993, magnetic storm - NOAA and EXOS-D observations. J. Geophys. Res. (2003). doi:10.1029/2001JA007542

Miyoshi, Y., Jordanova, V.K., Morioka, A., Evans, D.S.: Solar cycle variations of the electron radiation belts: Observations and radial diffusion simulation. Space Weather (2004). doi:10.1029/2004SW000070

Miyoshi, Y., Kataoka, R.: Ring current ions and radiation belt electrons during geomagnetic storms driven by coronal mass ejections and corotating interaction regions. Geophys. Res. Lett. (2005). doi:10.1029/2005GL024590

Miyoshi, Y. S., Jordanova, V.K., Morioka. A., Thomsen, M.F., Reeves, G.D., Evans, D.S., Green, J.C.: Observations and modeling of energetic electron dynamics during the Oct. 2001 storm. J. Geophys. Res. (2006). doi:10.1029/2005JA011351

Miyoshi, Y., Morioka, A., Kataoka, R., Kasahara, Y., Mukai, T.: Evolution of the outer radiation belt during the November 1993 storms driven by corotating interaction regions. J. Geophys. Res. (2007). doi:10.1029/2006JA012148

Miyoshi, Y., Kataoka, R.: Flux enhancement of the outer radiation belt electrons after the arrival of stream interaction regions. J. Geophys. Res. (2008a). doi:10.1029/2007JA012506

Miyoshi, Y., Kataoka, R.: Probabilistic space weather forecast of the relativistic electron flux enhancement at geosynchronous orbit. J. Atm. Solar-Terr. Phys. **70**, 475–481 (2008b)

Miyoshi, Y., Sakaguchi, K., Shiokawa, K., Evans, D., Albert, J., Connors, M., Jordanova V.: Precipitation of radiation belt electrons by EMIC waves,

observed from ground and space. Geophys. Res. Lett. (2008). doi:10.1029/2008GL035727

Mizera, P.F., Fennell, J.F.: Signatures of electric fields from high and low altitude farticles distributions, Geophys. Res. Lett. **4**, 311–314 (1977)

Moldwin, M.B., Downward, L., Rassoul, H.K., Amin, R., Anderson, R.R.: A new model of the location of the plasmapause: CRRES results, J. Geophys. Res. (2002). doi:10.1029/2001JA009211

Moore, T.E., Arnoldy, R.L., Feynman, J., Hardy, D.A.: Propagating substorm injection fronts, J. Geophys. Res. **86**, 6713–6726 (1981)

Moore, T.E., Fok, M.-C., Delcourt, D.C., Slinker, S.P., Fedder, J.A.: Plasma plume circulation and impact in an MHD substorm, J. Geophys. Res. (2008). doi:10.1029/2008JA013050

Morgan, M.G., Maynard, N.C.: Evidence of dayside plasmaspheric structure through comparisons of ground-based whistler data and Explorer 45 plasmapause data, J. Geophys. Res. **81,** 3992–3998 (1976)

Morioka, A., Misawa, H., Miyoshi, Y., Oya, H., Iizima, M., Nagai, T.: Pitch angle distribution of relativistic electrons in the inner radiation belt and its relation to equatorial plasma wave turbulence phenomena. Geophys. Res. Lett. **28**, 931–934 (2001)

Möbius, D., Hovestadt, D., Klecker, B., Scholer, M., Ipavich, F.M., Carlson, C.W., Lin, R.P.: A burst of energetic O^+ ions during an upstream particle event, Geophys. Res. Lett. **13**, 1372–1375 (1986)

Murakami, K., Yoshikawa, I., Obana, Y., Yoshikawa, K., Ogawa, G., Yamazaki, A., Kagitani, M., Taguchi, M., Kikuchi, M., Kameda, S., Nakamura, M.: First sequential images of the plasmasphere from the meridian perspective observed by KAGUYA, Earth Planet. Space **62**, e9–e13 (2010)

Mursula, K., Braysy, T., Niskala, K, Russell, C.T.: Pc1 pearls revisited: Structured electromagnetic ion cyclotron waves on Polar satellite and on the ground, J. Geophys. Res. **106**, 29543–29533 (2001)

.

Nagai, T., Johnson, J.F.E., Chappell, C.R.: Low-energy (less than 100 eV) ion pitch angle distributions in the magnetosphere by ISEE 1, J. Geophys. Res. **88**, 6944–6960 (1983)

Nagai, T.: “Space Weather Forecast”: Prediction of relativistic electron intensity at synchronous orbit. Geophys. Res. Lett. **15**, 425–428 (1988)

Nagai, T., Yukimatu, A.S., Matsuoka, A., Asai, K.T., Green, J.C., Onsager, T.G., Singer, H.J.: Timescales of relativistic electron enhancements in the slot region. J. Geophys. Res. (2006). doi:10.1029/2006JA011837

Nakamura, M., Yoshikawa, I., Yamazaki, A., Shiomi, K., Takizawa, Y., Hirahara, M., Yamashita, K., Saito, Y., Miyake, W.: Terrestrial plasmaspheric imaging by an Extreme Ultraviolet Scanner on Planet-B, Geophys. Res. Lett. **27**, 141–144 (2000)

Nakamura, R., Baker, D.N., Blake, J.B., Kanekal, S., Klechker, B., Hovestadt, D.: Relativistic electron precipitation enhancements near the outer edge of the radiation belt. Geophys. Res. Lett. **22**, 1129–1132 (1995)

Nakamura, R., Isowa, M., Kamide, Y., Baker, D.N., Blake, J.B., Looper, M.: SAMPEX observations of precipitation bursts in the outer radiation belt. J. Geophys. Res. **105**, 15875–15885 (2000)

Ni, B., Thorne, R.M., Shprits, Y.Y., Bortnik, J.: Resonant scattering of plasma sheet electrons by whistler-mode chorus: Contribution to diffuse auroral precipitation. Geophys. Res. Lett. **35** (2008). doi:10.1029/2008GL034032.

Ni, B., Shprits, Y., Thorne, R., Friedel, R., Nagai, T.: Reanalysis of relativistic radiation belt electron phase space density using multisatellite observations: Sensitivity to empirical magnetic field models. J. Geophys. Res. (2009a). doi:10.1029/2009JA014438

Ni, B., Shprits, Y., Nagai, T., Thorne, R., Chen, Y., Kondrashov, D., Kim, H.-J.: Reanalysis of the radiation belt electron phase space density using nearly equatorial CRRES and polar-orbiting Akebono satellite observations. J. Geophys. Res. (2009b), doi:10.1029/2008JA013933

Nishida, A.: Formation of plasmapause, or magnetospheric plasma knee, by the combined action of magnetospheric convection and plasma escape from the tail, J. Geophys. Res. **71**, 5669–5679 (1966)

Nishida, A.: Outward diffusion of energetic particles from the Jovian radiation belt. J. Geophys. Res. **81**, 1771-1773 (1976)

Nishimura, Y., Wygant, J., Ono, T., Iizima, M., Kumamoto, A., Brautigam, D., Friedel, R.: SAPS measurements around the magnetic equator by CRRES, Geophys. Res. Lett. (2008). doi:10.1029/2008GL033970

Northrop, T.G., Teller, E.: Stability of the adiabatic motion of charged particles in the Earth's field, Phys. Rev. **117**, 215–225 (1960)

Nosé, M., Ieda, A., Christon, S.P.: Geotail observations of plasma sheet ion composition over 16 years: On variations of average plasma ion mass and O+

triggering substorm model, J. Geophys. Res. (2009a). doi:10.1029/2009JA014203

Nosé, M., Taguchi, S., Christon, S.P., Collier, M.R., Moore, T.E., Carlson, C.W., McFadden, J.P.: Response of ions of ionospheric origin to storm time substorms: Coordinated observations over the ionosphere and in the plasma sheet, J. Geophys. Res. (2009b). doi:10.1029/2009JA014048

Obara, T., Nagatsuma, T., Den, M., Miyoshi, Y., Morioka, A.: Main–phase creation of "seed" electrons in the outer radiation belt. Earth Planets Space **52**, 41–47 (2000)

Ober, D.M., Horwitz, J.L., Gallagher, D.L.: Formation of density troughs embedded in the outer plasmasphere by subauroral ion drift events, J. Geophys. Res. **102**, 14595–14602 (1997)

Ober, D.M., Maynard, N.C., Burke, W.J.: Testing the Hill model of transpolar potential saturation, J. Geophys. Res. (2003). doi:10.1029/2003JA010154

O'Brien, T.P., McPherron, R.L., Sornette, D., Reeves, G.D., Friedel, R., Singer, H.J.: Which magnetic storms produce relativistic electrons at geosynchronous orbit?, J. Geophys. Res. **106**, 15533–15544 (2001)

O'Brien, T.P., Lorentzen, K.R., Mann, I.R., Meredith, N.P., Blake, J.B., Fennell, J.F., Looper, M.D., Milling, D.K., Anderson, R.R.: Energization of relativistic electrons in the present of ULF power and MeV microbursts: Evidence for dual ULF and VLF acceleration. J. Geophys. Res. (2003). doi:10.1029/2002JA009784

O'Brien, T.P., Looper, M.D., Blake, J.B.: Quantification of relativistic electron microburst losses during the GEM storms. Geophys. Res. Lett. (2004). doi:10.1029/2003GL018621

Ohtani, S., Brandt, P.C., Singer, H.J., Mitchell, D.G. , Roelof, E.C.: Statistical characteristics of hydrogen and oxygen ENA emission from the storm-time ring current, J. Geophys. Res. (2006). doi:10.1029/2005JA011201

Ohtani, S., Ebihara, Y., Singer, H.J.: Storm-time magnetic configurations at geosynchronous orbit: Comparison between the main and recovery phases, J. Geophys. Res. (2007a). doi:10.1029/2006JA011959

Ohtani, S., et al.: Cluster observations in the inner magnetosphere during the 18 April 2002 sawtooth event: Dipolarization and injection at r = 4.6 RE, J. Geophys. Res. (2007b). doi:10.1029/2007JA012357

Ohtani, S., Miyoshi, Y., Singer, H., Weygand, J.: On the loss of relativistic electrons at geosynchronous altitude: its dependence on magnetic

configurations and external conditions. J. Geophys. Res. (2009). doi:10.1029/2008JA013391

Olsen, R.C.: Equatorially Trapped plasma populations, J. Geophys. Res. **86**, 11235–11245 (1981)

Olsen, R.C., Shawhan, S.D., Gallagher, D.L., Green, J.L., Chappell, C.R., Anderson, R.R.: Plasma observations at the Earth's magnetic equator, J. Geophys. Res. **92**, 2385–2407 (1987)

Omura, Y., Furuya, N., Summers, D.: Relativistic turning acceleration of resonant electrons by coherent whistler mode waves in a dipole magnetic field. J. Geophys. Res. (2007). doi:10.1029/2006JA012243

Omura, Y., Katoh, Y., Summers, D.: Theory and simulation of generation of whistler-mode chorus. J. Geophys. Res. (2008). doi:10.1029/2007JA012622

Omura, Y., Pickett, J., Grison, B., Santolik, O., Dandouras, I., Engebretson, M., Décréau, P.M.E., Masson, A.: Theory and observation of electromagnetic ion cyclotron triggered emissions in the magnetosphere, J. Geophys. Res. (2010). doi:10.1029/2010JA015300

Ono, T., Hirasawa, T., Meng, C.I.: Proton auroras observed at the equatorward edge of the duskside auroral oval, Geophys. Res. Lett. **14**, 660–663 (1987)

Ono, Y., Nosé, M., Christon, S.P., Lui, A.T.Y.: The role of magnetic field fluctuations in nonadiabatic acceleration of ions during dipolarization, J. Geophys. Res. (2009). doi:10.1029/2008JA013918

Onsager, T.G., Chan, A.A., Fei, Y., Elkington, S.R., Green, J.C., Singer, H.J.: The radial gradient of relativistic electrons at geosynchronous orbit. J. Geophys. Res. (2004). doi:10.1029/2003JA010368

Onsager, T.G., Green, J.C., Reeves, G.D., Singer, H.J.: Solar wind and magnetospheric conditions leading to abrupt loss of outer radiation belt electrons. J. Geophys. Res. (2007). doi:10.1029/2006JA011708

Oya, H., Ono, T.: Stimulation of plasma waves in the magnetosphere using satellite JIKIKEN (EXOS B) Part II: plasma density across the plasmapause, J. Geomag. and Geoel. **39**, 591–607 (1987)

Ozeke, L.G., Mann, I.R.: Energization of radiation belt electrons by ring current ion driven ULF waves. J. Geophys. Res. (2008). doi:10.1029/2007JA012468

Park, C.G.: Whistler observations of the interchange of ionization between the ionosphere and the protonosphere, J. Geophys. Res. **75**, 4249–4260 (1970)

Park, C.G.: Some features of plasma distribution in the plasmasphere deduced from Antarctic whistlers, J. Geophys. Res., **79**, 169–173 (1974)

Parker, E.N.: Newtonian development of the dynamical properties of ionized gases of low density, Phys. Rev. **107**, 924–933 (1957)

Paulikas, G.A., Blake, J.B.: Effects of the solar wind on magnetospheric dynamics: Energetic electrons at the synchronous orbit, In: Olson, W.P. (eds.) Quantitative modeling of magnetosphereic processes, pp. 180–202. AGU, Washington, D. C. (1979)

Perry, K.L., Hudson, M.K., Elkington, S.R.:Incorporating spectral characteristic of Pc5 waves into three-dimesional radiation belt modeling and the diffusion of relativistic electrons. J. Geophys. Res. (2005). doi:10.1029/2004JA010760

Peterson, W.K., Doering, J.P., Potemra, T.A., McEntire, R.W., Bostrom, C.O.: Conjugate photoelectron fluxes observed on Atmosphere Explorer C, Geophys. Res. Lett. **4**, 109–112 (1977)

Peymirat, C., Richmond, A.D., Kobea, A.T.: Electrodynamic coupling of high and low latitudes: Simulations of shielding/overshielding effects, J. Geophys. Res. **105**, 22991–23003 (2000)

Phaneuf, R.A., Janev, R.K., Pindzola, M.S.: Atomic data for fusion, vol. V, Collisions of carbon and oxygen ions with electrons, H, H_2 and He, Tech. Rep. ORNL–6090/V5, Oak Ridge Natl. Lab., Oak Ridge, Tenn. (1987)

Pickett, J.S., Grison, B., Engebretson, M.J., Dan douras, I., Masson, A., Adrian, M.L., Decreau, P.M.E., Cornilleau-Wehrlin, N., Constantinescu, D.: Cluster observations of EMIC triggered emissions in association with Pc1 waves near Earth's plasmapause, *Geophys. Res. Lett.*, 37, L09104, (2010), doi:10.1029/2010GL042648.

Pollock, C.J., et al.: First medium energy neutral atom (MENA) Images of Earth's magnetosphere during substorm and storm‐time, Geophys. Res. Lett. **28**, 1147–1150 (2001)

Pulkkinen, T.I., Ganushkina, N.Yu., Baker, D.N., Turner, N.E., Fennell, J.F., Roeder, J., Fritz, T.A., Grande, M., Kellett, B., Kettmann, G.: Ring current ion composition during solar minimum and rising solar activity: Polar/CAMMICE/MICS results, J. Geophys. Res. **106**, 19131–19147 (2001)

Quinn, J.M., McIlwain, C.E.: Bouncing ion clusters in the Earth's magnetosphere, J. Geophys. Res. **84**, 7365–7370 (1979)

Quinn, J.M., Johnson, R.G.: Composition measurements of warm equatorially trapped ions near geosynchronous orbit, Geophys. Res. Lett. **9**, 777–780 (1982)

Quinn, J.M., Southwood, D.J.: Observations of parallel ion energization in the equatorial region, J. Geophys. Res. **87**, 10536–10540 (1982)

Rairden, R.L., Frank, L.A., Craven, J.D.: Geocoronal imaging with Dynamics Explorer, J. Geophys. Res. **91**, 13613–13630 (1986)

Rasmussen, C.E., Guiter, S.M., Thomas, S.G.: A two-dimensional model of the plasmasphere: refilling time constants, Planet. Space Sci. **41**, 35–43 (1993)

Reeves, G.D., Henderson, M.G., McLachlan, P.S., Belian, R.D., Friedel, R.H.W., Korth, A.: Radial propagation of substorm injections, in Proceedings of the Third International Conference on Substorms, Versailles, France, 12-17 May 1996, Eur. Space Agency Spec. Publ., ESA SP–389, 579–584 (1996)

Reeves, G., Friedel, R., Belian, R., Meier, M., Henderson, M., Onsager, T., Singer, H., Baker, D., Li, X., Blake, J.: The relativistic electron response at geosynchronous orbit during the January 1997 magnetic storm. J. Geophys. Res. **103**, 17559–17570 (1998)

Reeves, G.D., McAdams, K.L., Friedel, R.H.W., O'Brien, T.P.: Acceleration and loss of relativistic electrons during geomagnetic storms. Geophys. Res. Lett. (2003). doi:10.1029/2002GL016513

Reeves, G.D.: Radiation belt storm probes: A new mission for space weather forecasting. Space Weather (2007). doi:10.1029/2007SW000341

Reiff, P.H., Spiro, R.W., Hill, T.W.: Dependence of polar cap potential drop on interplanetary parameters, J. Geophys. Res. **86**, 7639–7648 (1981)

Reinisch, B.W., Moldwin, M.B., Denton, R.E., Gallagher, D.L., Matsui, H., Pierrard, V., Tu, J.: Augmented empirical models of plasmaspheric density and electric field using IMAGE and CLUSTER Data, Space Sci. Rev. **145**, 231–261 (2009)

Richards, P.G., Torr, D.G.: Seasonal, diurnal, and solar cyclical variations of the limiting H+ flux in the Earth's topside ionosphere, J. Geophys. Res. **90**, 5261–5268 (1985)

Roeder, J.L. Fennell, J.F., Grande, M. Livi, S. Sheldon, R.: Ring current response to interplanetary magnetic cloud events, Physics and Chemistry of the Earth, Part C: Solar, Terr. Planet. Sci. **24**, 83–87 (1999).

Roederer, J. G: Dynamics of Geomagnetically Trapped Radiation, SpringerVerlag, New York (1970)

Roelof, E.C.: Remote sensing of the ring current using energetic neutral atoms, Adv. Space. Res. **9**, 195–203 (1989)

Roelof, E.C., Skinner, A.J.: Extraction of ion distributions from magnetospheric ENA and EUV images, Space Sci. Rev. **91**, 437–459 (2000)

Rostoker, G., Skone, S., Baker, D.N.: On the origin of relativistic electrons in the magnetosphere associated with some geomagnetic storms. Geophys. Res. Lett. **25**, 3701–3704 (1998)

Rowe, Jr. J.F: Magnetic activity variations of the nighttime E region at Arecibo. Radio Sci. **9**, 175–182 (1974)

Rowland, D., Wygant, J.: Dependence of the large-scale, inner magnetospheric electric field on geomagnetic activity, J. Geophys. Res. **103**, 14959–14964 (1998).

Rozanov, E., Callis, L., Schlesinger, M., Yang, F., Andronova, N., Zubov, V.: Atmospheric response to NOy source due to energetic electron precipitation. Geophys. Res. Lett. (2005). doi:10.1029/2005GL023041

Russell, C.T., McPherron, R.L.: Semiannual variation of geomagnetic activity. J. Geophys. Res. **78**, 92–108 (1973)

Sagawa, E., Yau, A.W., Whalen, B.A., Peterson, W.K.: Pitch angle distributions of low-energy ions in the near-Earth magnetosphere, J. Geophys. Res. **92**, 12241–12254 (1987)

Saito, S., Miyoshi, Y., Seki, K.: A split in the outer radiation belt by magnetopause shadowing: Test particle simulations. J. Geophys. Res. (2010). doi:10.1029/2009JA014738

Sakaguchi, K., Shiokawa, K., Ieda, A., Miyoshi, Y., Otsuka, Y., Ogawa, T., Connors, M., Donovan, E.F., Rich, F.J.: Simultaneous ground and satellite observations of an isolated proton arc at subauroral latitudes, J. Geophys. Res. (2007). doi:10.1029/2006JA012135

Sakaguchi, K., Shiokawa, K., Miyoshi, Y., Otsuka, Y., Ogawa, T., Asamura, K., Connors, M.: Simultaneous appearance of isolated aurora arcs and Pc1 geomagnetic pulsations at subauroral latitudes. J. Geophys. Res. (2008). doi:10.1029/2007JA012888

Sandanger, M., Søraas, F., Aarsnes, K., Oksavik, K., Evans, D.S.: Loss of relativistic electrons: Evidence for pitch angle scattering by electromagnetic ion cyclotron waves excited by unstable ring current protons, J. Geophys. Res. (2007), doi:10.1029/2006JA012138

Sandel, B.R., Goldstein, J., Gallagher, D.L., Spasojevic, M.: Extreme ultraviolet imager observations of the structure and dynamics of the plasmasphere, Space Sci. Rev. **109**, 25–46 (2003)

Sandel, B.R., Denton, M.H.: Global view of refilling of the plasmasphere, Geophys. Res. Lett. (2007). doi:10.1029/2007GL030669

Santolik, O., Gurnett, D.A., Pickett, J.S., Parrot, M., Cornilleau-Wehrlin, N.: Spatio-temporal structure of storm-time chorus. J. Geophys. Res. (2003). doi:10.1029/2002JA009791

Sarris, T.E., Li, X., Temerin, M.: Simulating radial diffusion of energetic (MeV) electrons through a model of fluctuating electric and magnetic fields. Ann. Geophys. **24**, 1–16 (2006)

Sarris, T.E., Loto'aniu, T.M., Li, X., Singer, H.J.: Observations at geosynchronous orbit at a persistent Pc5 geomagnetic pulsation and energetic electron flux modulations. Ann. Geophys. **25**, 1653–1667 (2007)

Schulz, M., Koons, H.C.: Thermalization of colliding ion streams beyond the plasmapause, J. Geophys. Res. **77**, 248–254 (1972)

Schulz, M., Lanzerotti, L.J.: Particle diffusion in the radiation belts, Sprinter, Heidelberg, Germany (1974)

Schulz, M.: The magnetosphere, In: Jacobs, J.A. (eds.) Geomagnetism, pp. 87–293. Academic press, London (1991)

Scime, E.E., Keesee, A.M. Jahn, J., Kline, J.L., Pollock, C.J., Thomsen, M.F.: Remote ion temperature measurements of Earth's magnetosphere: Medium energy neutral atom (MENA) images (2002). doi:10.1029/2001GL013994

Sckopke, N.: A general relation between the energy of trapped particles and the disturbance field near the Earth, J. Geophys. Res. **71**, 3125–3135 (1966)

Seki, K., Miyoshi, Y., Summers, D., Meredith, N.P.: Comparative study of outer-zone relativistic electrons observed by Akebono and CRRES. J. Geophys. Res. (2005). doi:10.1029/2004JA010655

Selesnick, R.S., Blake, J.B.: On the source location of radiation belt electrons, J. Geophys. Res. **105**, 2607–2624 (2000)

Selesnick, R.S., Looper, M.D., Mewaldt, R.A.: A theoretical model of the inner proton radiation belt. Space Weather (2007). doi:10.1029/2006SW000275

Senior, C., Sharber, J.R., de la Beaujardière, O., Heelis, R.A., Evans, D.S., Winningham, J.D., Sugiura, M., Hoegy, W.R.: E and F region study of the evening sector auroral oval: A Chatanika/Dynamics Explorer 2/NOAA 6 comparison, J. Geophys. Res. **92**, 2477–2494 (1987)

Senior, C.: Solar and particle contributions to auroral height integrated conductivities from EISCAT data: A statistical study, Ann. Geophys. **9**, 449–460 (1991)

Sergeev, V.A., Sazhina, E.M., Tsyganenko, N.A., Lundblad, J.Å, Søraas, F.: Pitch-angle scattering of energetic protons in the magnetotail current sheet as the dominant source of their isotropic precipitation into the nightside ionosphere, Planet. Space Sci. **31**, 1147–1155 (1983)

Sergeev, V.A., Malkov, M., Mursula, K.: Testing the isotropic boundary algorithm method to evaluate the magnetic field configuration in the tail, J. Geophys. Res. **98**, 7609–7620 (1993)

Sergeev, V.A., Shukhtina, M.A., Rasinkangas, R., Korth, A., Reeves, G.D., Singer, H.J., Thomsen, M.F., Vagina, L.I.: Event study of deep energetic particle injections during substorm, J. Geophys. Res. **103**, 9217–9234 (1998)

Sheldon, R.B., Spence, H.E., Fennell, J.F.: Observation of the 40 keV field-aligned ion beams, Geophys. Res. Lett. **25**, 1617– 16i20 (1998)

Shinbori, A., Ono, T., Iizima, T., Kumamoto, A.: SC related electric and magnetic field phenomena observed by the Akebono satellite inside the plasmasphere, Earth Planet. Space **56**, 269–282 (2004).

Shprits, Y.,Y., Thorne, R.M., Friedel, R., Reeves, G.D., Fennell, J., Baker, D.N., Kanekal S.G.: Outward radial diffusion driven by losses at magnetopause J. Geophys. Res. (2006). doi:10.1029/2006JA011657

Shprits, Y., Kondrashov, D., Chen, Y., Thorne, R., Ghil, M. Friedel, R., Reeves, G.: Reanalysis of relativistic radiation belt electron fluxes using CRRES satellite data, a radial diffusion model, and a Kalman filter, J. Geophys. Res. (2007). doi:10.1029/2007JA012579.

Shprits, Y.Y., Elkington, S.R., Meredith, N.P., Subbotin, D.A.: Review of modeling of losses and sources of relativistic electrons in the outer radiation belt I: Radial transport. J. Atm. Solar-Terr. Phys. **70**, 1679–1693 (2008a)

Shprits, Y.Y., Subbotin, D.A., Meredith, N.P., Elkington, S.R.: Review of modeling of losses and sources of relativistic electrons in the outer radiation belt II: Local acceleration and loss. J. Atm. Solar-Terr. Phys. **70**, 1694–1713 (2008b)

Shprits, Y.Y., Subbotin, D.A., Ni, B.: Evolution of electron fluxes in the outer radiation belt computed with the VERB code, J. Geophys. Res. **114** (2009), doi:10.1029/2008JA013784.

Singh, N., Horwitz, J.L.: Plasmasphere refilling: Recent observations and modeling, J. Geophys. Res. **97**, 1049–1079 (1992)

Siscoe, G.L., Crooker, N.U., Siebert, K.D.: Transpolar potential saturation: Roles of region 1 current system and solar wind ram pressure, J. Geophys. Res. (2002). doi:10.1029/2001JA009176

Sitnov, M.I., Tsyganenko, N.A., Ukhorskiy, A.Y., Brandt, P.C.: Dynamical data-based modeling of the storm-time geomagnetic field with enhanced spatial resolution, J. Geophys. Res. (2008) doi:10.1029/2007JA013003

Smith, P.H., Hoffman, R.A.: Ring current particle distributions during the magnetic storms of December 16-18, 1971, J. Geophys. Res. **78**, 4731–4737 (1973)

Smith, P.H., Bewtra, N.K.: Dependence of the charge exchange lifetimes on mirror latitude, Geophys. Res. Lett. **3**, 689–692 (1976)

Smith, J.P., Thomsen, M.F., Borovsky, J.E., Collier, M.: Solar wind density as a driver for the ring current in mild storms, Geophys Res Lett. **26**, 1797–1800 (1999)

Sojka, J., Schunk, R., Johnson, J., Waite, J., Chappell, C.: Characteristics of Thermal and suprathermal ions associated with the dayside plasma trough as measured by the dynamics explorer retarding ion mass spectrometer, J. Geophys. Res. **88**, 7895–7911 (1983)

Song, X.T., Gendrin, R., Caudal, G.: Refilling process in the plasmasphere and its relation to magnetic activity, J. Atmos. Terrest. Physics **50**, 185–195 (1988)

Song, P., Russell, C.: Model of the formation of the low-latitude boundary layer for strongly northward interplanetary magnetic field, J. Geophys. Res. **97**, 1411–1420 (1992)

Song, P., DeZeeuw, D.L., Gombosi, T.I., Groth, C.P.T., Powell, K.G.: A numerical study of solar wind-magnetosphere interaction for northward interplanetary magnetic field, J. Geophys. Res. **104**, 28361–28378 (1999)

Southwood, D.J., Dungey, J.W., Etherington, R.J.: Bounce resonant interaction between pulsations and trapped particles. Planet. Space Sci. **17**, 349–361 (1969)

Spasojevic, M., Thomsen, M.F., Chi, P.J., Sandel, B.R.: Afternoon subauroral proton precipitation resulting from ring current-plasmasphere interaction. In: Burch, J., Schulz, M., Spence, H.(eds.) Inner magnetosphere interactions: New perspective from Imaging. doi:10.1029/159GM12 (2005), AGU, Washington D.C.

Spence, H.E., Kivelson, M.G., Walker, R.J., McComas, D.J.: Magnetospheric plasma pressures in the midnight meridian: Observations from 2.5 to 35 RE, J. Geophys. Res. **94**, 5264–5272 (1989)

Spence, H.E., Kivelson, M.G.: Contributions of the low-latitude boundary layer to the finite width magnetotail convection model, J. Geophys. Res. **98**, 15487–15496 (1993)

Spiro, R.W., Heelis, R.A., Hanson, W.B.: Rapid subauroral ion drifts observed by Atmospherics Explorer C, Geophys. Res. Lett. **6**, 657–660 (1979)

Spiro, R.W., Wolf, R.A.: Electrodynamics of convection in the inner magnetosphere, in magnetospheric currents, Geophys. Monogr. Ser., **28**, Potemra, T.A. (ed) p. 248, AGU, Washington, D. C. (1984)

Spiro, R.W., Wolf, R.A., Fejer, B.G.: Penetration of high-atitude-electric-field effects to low latitudes during SUNDIAL 1984, Ann. Geophys. **6**, 39–49 (1988)

Stüdemann, W., et al.: The May 2–3, 1986 magnetic storm: First energetic ion composition observations with the MICS instrument on Viking, Geophys. Res. Lett. **14**, 455–458 (1987)

Subbotin, D., Shprits, Y., Ni, B.: Three-dimensional VERB radiation belt simulations including mixed diffusion, J. Geophys. Res. (2010), doi:10.1029/2009JA015070.

Sugiura, M.: Hourly values of equatorial Dst for IGY, pp. 945–948, in Annals of the International Geophysical Year, **35**, Pergamon Press, Oxford (1964)

Sugiura, M., Ledley, B., Skillman, T., Heppner, J.: Magnetospheric-field distortions observed by Ogo 3 and 5, J. Geophys. Res. **76**, 7552–7565 (1971)

Summers, D., Thorne, R.M., Xiao, F.: Relativistic theory of wave-particle resonant diffusion with application to electron acceleration in the magnetosphere. J. Geophys. Res. **103**, 20487–20500 (1998)

Summers, D., Ma, C.: Rapid acceleration of electrons in the magnetosphere by fast-mode MHD waves. J. Geophys. Res. **105**, 15887–15895 (2000)

Summers, D., Thorne, R.M., Xiao, F.: Gyroresonant acceleration of electrons in the magnetosphere by superluminous electromagnetic waves. J. Geophys. Res. **106**, 10853–10868 (2001)

Summers, D., Thorne, R.M.: Relativistic electron pitch-angle scattering by electromagnetic ion cyclotron waves during geomagnetic storms. J. Geophys. Res. **108** (2003). doi:10.1029/2002JA009489

Summers, D.: Quasi-linear diffusion coefficients for field-aligned electromagnetic waves with applications to the magnetosphere, J. Geophys. Res. **110** (2005). doi:10.1029/2005JA011159

Summers, D., Ni, B., Meredith, N. P.: Timescales for radiation belt electron acceleration and loss due to resonant wave-particle interactions: 1. Theory, J. Geophys. Res. **112** (2007), doi:10.1029/2006JA011801.

Søraas, F., Oksavik, K., Aarsnes, K., Evans, D.S., Greer, M.S.: Storm time equatorial belt-an "image" of RC behavior, Geophys. Res. Lett. (2003). doi:10.1029/2002GL015636

Sørbø, M., Søraas, F., Aarsnes, K., Oksavik, K., Evans, D.S.: Latitude distribution of vertically precipitating energetic neutral atoms observed at low altitudes, Geophys. Res. Lett. **33** (2006). doi:10.1029/2005GL025240

Takahashi, K., Ukhorskiy, A.Y.: Solar wind control of Pc5 pulsation power at geosynchronous orbit. J. Geophys. Res. (2007). doi:10.1029/2007JA012483

Takahashi, K., Ohtani, S., Denton, R.E., Hughes, W.J., Anderson, R.R.: Ion composition in the plasma trough and plasma plume derived from a combined release and radiation effects satellite magnetoseismic study, J. Geophys. Res. (2008). doi:10.1029/2008JA013248

Takasaki, S., Kawano, H., Tanaka, Y., Yoshikawa, A., Seto, M., Iizima, M., Obana, Y., Sato, N., Yumoto, K.: A significant mass density increase during a large magnetic storm in October 2003 obtained by ground-based ULF observations at L ~ 1.4, Earth Planet. Space **58**, 617–622 (2006)

Tan, L.C., Fung, S.F., Shao, X.: Observation of magnetospheric relativistic electrons accelerated by Pc–5 ULF waves. Geophys. Res. Lett. (2004). doi:10.1029/2004GL019459

Taylor Jr., H.A.: The light ion trough, Planet. Space Sci. **20**, 1593–1599 (1972)

Terada, N., Iyemori, T., Nose, M., Nagai, T., Matsumoto, H., Goka, T.: Storm–time magnetic field variations observed by the ETS-VI satellite, Earth Planet. Space **50**, 853–864 (1998)

Terasawa, T., et al.: Solar wind control of density and temperature in the near-Earth plasma sheet: WIND/GEOTAIL collaboration, Geophys. Res. Lett. **24**, 935–938 (1997)

Thomsen, M., Borovsky, J., McComas, D., Collier, M.: Variability of the ring current source population, Geophys. Res. Lett. **25**, 3481–3484 (1998)

Thomsen, M.F., Borovsky, J.E., Skoug, R.M., Smith, C.W.: Delivery of cold, dense plasma sheet material into the near-Earth region. J. Geophys. Res. (2003). doi:10.1029/2002JA009544

Thorne, R.M., Kennel, C.F.: Relativistic electron precipitation during magnetic storm main phase. J. Geophys. Res. **76**, 4446–4453 (1971)

Thorne, R.M.: Energetic radiation belt electron precipitation: A natural depletion mechanism for stratospheric ozone. Science **195**, 287–289 (1977)

Thorne, R.M., Horne, R.B.: Energy transfer between energetic ring current H^+ and O^+ by electromagnetic ion cyclotron waves, J. Geophys. Res. **99**, 17275–17282 (1994)

Thorne, R.M., Horne, R.B.: Modulation of electromagnetic ion cyclotron instability due to interaction with ring current O^+ during magnetic storms, J. Geophys. Res. **102**, 14155–14163 (1997)

Thorne, R.M. O'Brien, T.P., Shprits, Y.Y., Summers, D., Horne, R.B.: Timescale for MeV electron microburst loss during geomagnetic storms, J. Geophys. Res. (2005). doi:10.1029/2004JA010882

Tinsley, B.A.: Neutral atom precipitation - A review, J. Atmos. Terr. Phys., **43**, 617–632, (1981)

Tsurutani, B.T., Gonzalez, W.D., Gonzalez, A.L.C., Guarnieri, F.L., Gopalswamy, N., Grande, M., Kamide, Y., Kasahara, Y., Lu, G., Mann, I., McPherron, R., Sorass, F., and Vasyliunas, V.: Corotating solar wind streams and recurrent geomagnetic activity: A review. J. Geophys. Res. (2006). doi:10.1029/2005JA011273

Tu, J., Song, P., Reinisch, B.W., Green, J.L., Huang, X.: Empirical specification of field–aligned plasma density profiles for plasmasphere refilling, J. Geophys. Res. **111** (2006). doi:10.1029/2005JA011582

Turner, N.E., Baker, D.N., Pulkkinen, T.I., Roeder, J.L. Fennell, J.F. Jordanova, V.K.: Energy content in the storm time ring current, J. Geophys. Res. **106**, 19149–19156 (2001)

Tverskaya, L.V., Pavlov, N.N., Blake, J.B., Selesnick, R.S., Fennell, J.F.: Predicting the L-position of the storm-injected relativistic electron belt. Adv. Space Res. **31**, 1039–1044 (2003).

Ukhorskiy, A.Y., Anderson, B.J., Takahashi, K., Tsyganenko, N.A.: Impact of ULF oscillations in solar wind dynamic pressure on the outer radiation belt electrons. Geophys. Res. Lett. (2006). doi:10.1029/2005GL024380

Unwin, R.W., Cummack, C.H.: Drift spikes: The ionospheric signature of large poleward directed electric fields at subauroral latitudes. Mem. Nat. Inst. Polar Res. **16**, 72 (Special Issue "IMS in Antarctica") (1980)

Usanova, M.E., Mann, I.R., Rae, I.J., Kale, Z.C., Angelopoulos, V., Bonnell, J.W., Classmeier, K.-H., Auster, H.U., Singer, H.J.: Multipoint observations of magnetospheric compression-related EMIC Pc1 waves by THEMIS and CARISMA. Geophys. Res. Lett. (2008). doi:10.1029/2008GL034458

Vallance Jones, A.: Aurora, D. Reidel, Norwell, Mass. (1974)

Vallat et al.: First current density measurements in the ring current region using simultaneous multi-spacecraft Cluster-FGM data, Ann. Geophys. **23**, 1849–1865 (2005)

Van Allen, J A., Frank, L.A.: Radiation around the earth to a radial distance of 107400 km. Nature **183**, 430–434 (1959)

Varotsou, A., Boscher, D., Bourdarie, S., Horne, R.B., Glauert, S.A., Meredith, N.P.: Simulation of the outer radiation belt electrons near geosynchronous orbit including both radial diffusion and resonant interaction with whistler-mode chorus waves. Geophys. Res. Lett. (2005). doi:10.1029/2005GL023282

Varotsou, A., Boscher, D., Bourdarie, S., Horne, R.B., Meredith, N.P., Glauert, S.A., Friedel , R.H.: Three-dimensional test simulations of the outer radiation belt electron dynamics including electron-chorus resonant interactions, J. Geophys. Res. (2008). doi:10.1029/2007JA012862

Vassiliadis, D., Klimas, A.J., Weigel, R.S., Baker, D.N., Rigler, E.J., Kanekal, S.G., Nagai, T., Fung, S.F., Friedel, R.W.H., Cayton, T.E.: Structure of Earth's outer radiation belt inferred from long-term electron flux dynamics. Geophys. Res. Lett. (2003). doi:10.1029/2003GL017328

Vassiliadis, D., Fung, S.F., Klimas, A.J.: Solar, interplanetary, and magnetospheric parameters for the radiation belt energetic electron flux. J. Geophys. Res. (2005). doi:10.1029/2004JA010443

Vasyliunas, V.M.: Mathematical models of magnetospheric convection and its couplingt o the ionosphere, to be published in particles and fields in the magnetosphere, McCormac, B.M. (ed), D. Reidel, New York (1970)

Voiculescu, M., Roth, M.: Eastward sub-auroral ion drifts or ASAID, Annales Geophysicae **26**, 1955–1963 (2008)

Walker, R.J., Erickson, K.N., Swanson, R.L., Winckler, J.R.: Substorm-associated particle boundary motion at synchronous orbit, J. Geophys. Res. **81**, 5541–5550 (1976)

Wang, C., Newman, T.S., Gallagher, D.L.: Plasmapause equatorial shape determination via the Minimum L Algorithm: Description and evaluation, J. Geophys. Res. (2007). doi:10.1029/2006JA012202

Wang, H., Ridley, A.J., Lühr, H., Liemohn, M.W., Ma, S.Y.: Statistical study of the subauroral polarization stream: Its dependence on the cross-polar cap potential and subauroral conductance, J. Geophys. Res. (2008). doi:10.1029/2008JA013529

West, H.,Jr., Buck, R., Walton, J.: Electron Pitch Angle Distributions throughout the Magnetosphere as Observed on Ogo 5. J. Geophys. Res. **78**, 1064–1081 (1973)

Weimer, D.R.: An improved model of ionospheric electric potentials including substorm perturbations and application to the Geospace Environment Modeling November 24, 1996, event, J. Geophys. Res. **106**, 407–416 (2001)

Weimer, D.R.: Improved ionospheric electrodynamic models and application to calculating Joule heating rates, J. Geophys. Res. (2005). doi:10.1029/2004JA010884

Williams, D.J., Arens, J.F., Lanzerotti, L.J.: Observations of trapped electrons at low and high altitudes, J. Geophys. Res. **73**, 5673–5696 (1968)

Williams, D.J.: Ring current composition and sources: An update, Planet. Space Sci. **29**, 1195–1203 (1981)

Wolf, R.A.: Effects of ionospheric conductivity on convective flow of plasma in the magnetosphere, J. Geophys. Res. **75**, 4677–4698 (1970)

Wolf, R.A., Harel, M. Spiro, R.W., Voigt, G.-H., Reiff, P.H., Chen, C.-K.: Computer simulation of inner magnetospheric dynamics for the magnetic storm of July 29, 1977, J. Geophys. Res. **87**, 5949–5962 (1982)

Wygant, J.R., Torbert, R.B., Mozer, F.S.: Comparison of S3-3 polar cap potential with the interplanetary magnetic field and models of magnetospheric reconnection, J. Geophys. Res. **88**, 5727–5735 (1983)

Xiao, F., Thorne, R.M., Summers, D.: Higher-order gyroresonant acceleration of electrons by superluminous (AKR) wave modes, Planet. Space Sci. **55**, 1257-1271 (2007)

Xiao, F., Su, Z., Zheng, H., Wang, S.: Three-dimensional simulations of outer radiation belt electron dynamics including cross-diffusion terms, J. Geophys. Res. (2010). doi:10.1029/2009JA014541

Xiao, F., Su, Z., Chen, L, Zheng, H., Wang, S.: A parametric study on outer radiation belt electron evolution by superluminous R-X mode waves, J. Geophys. Res. (2010). doi:10.1029/2010JA015374

Yahnin, A.G., Yahnina, T.A., Frey, H.U.: Subauroral proton spots visualize the Pc1 source, J. Geophys. Res. (2007). doi:10.1029/2007JA012501

Yahnina, T.A., Frey, H.U., Bösinger, T., Yahnin, A.G.: Evidence for subauroral proton flashes on the dayside as the result of the ion cyclotron interaction, J. Geophys. Res. (2008). doi:10.1029/2008JA013099

Yamauchi, M., Lundin, R., Mursula, K., Marklund, G., Potemra, T.A.: Dayside Pc5 pulsation detected by Viking ion data at L=4, Geophys. Res. Lett. **23**, 2517–2520 (1996)

Yamauchi, M., Ebihara, Y., Dandouras, I., Rème, H.: Dual source populations of substorm-associated ring current ions, Ann. Geophys. **27**, 1431–1438 (2009)

Yao Y., Seki, K., Miyoshi, Y., McFadden, J.P., Lund, E.J., Carlson, C.W.: Statistical properties of the multiple ion band structures observed by the FAST satellite, J. Geophys. Res. (2008). doi:10.1029/2008JA013178

Yau, A.W., Beckwith, P.H., Peterson, W.K., Shelley, E.G.: Long-term (solar cycle) and seasonal variations of upflowing ionospheric ion events at DE 1 Altitudes, J. Geophys. Res. **90**, 6395–6407 (1985a)

Yau, A.W., Shelley, E.G., Peterson, W.K., Lenchyshyn, L.: Energetic auroral and polar ion outflow at DE 1 altitudes: Magnitude, composition, magnetic activity dependence, and long-term variations, J. Geophys. Res. **90**, 8417–8432 (1985b)

Yizengaw, E., Wei, H., Moldwin, M.B., Galvan, D., Mandrake, L., Mannucci, A., Pi, X.: The correlation between mid-latitude trough and the plasmapause, Geophys. Res. Lett. (2005) doi:10.1029/2005GL022954

Yizengaw, E., Moldwin, M.B., Galvan, D., Iijima, B.A., Komjathy, A., Mannucci, A.J.: Global plasmaspheric TEC and its relative contribution to GPS TEC, J. Atm. Solar-Terr. Phys. **70**, 1541–1548 (2008)

Yoshikawa, I., Murakami, G., Ogawa, G., Yoshioka, K., Obana, Y., Taguchi, M., Yamazaki, A., Kameda, S., Nakamura, M., Kikuchi, M., Kagitani, M., Okano, S., Miyake, W: Plasmaspheric EUV images seen from lunar orbit: Initial results of the extreme ultraviolet telescope on board the Kaguya spacecraft, J. Geophys. Res. (2010). doi:10.1029/2009JA014978

Young, D.T., Balsiger, H., Geiss, J.: Correlations of magnetospheric ion composition with geomagnetic and solar activity, J. Geophys. Res. **87**, 9077–9096 (1982)

Zaharia, S., Jordanova, V.K., Thomsen, M.F., Reeves, G.D.:Self-consistent modeling of magnetic fields and plasmas in the inner magnetosphere: Application to a geomagnetic storm, J. Geophys. Res. (2006). doi:10.1029/2006JA011619

Zhang, Y., Paxton, L.J., Kozyra, J.U., Kil, H., Brandt, P.C.: Nightside thermospheric FUV emissions due to energetic neutral atom precipitation during magnetic superstorms, J. Geophys. Res. (2006). doi:10.1029/2005JA011152

Zhang, Y., Paxton, L.J., Zheng, Y.: Interplanetary shock induced ring current auroras, J. Geophys. Res. (2008). doi:10.1029/2007JA012554

Zhang, J.-C., Wolf, R.A., Spiro, R.W., Erickson, G.M., Sazykin, S., Toffoletto, F.R., Yang, J.: Rice convection model simulation of the substorm-associated injection of an observed plasma bubble into the inner magnetosphere: 2. Simulation results, J. Geophys. Res. (2009). doi:10.1029/2009JA014131

Zong, Q.-G., Wilken, B.: Bursty energetic oxygen events in the dayside magnetosheath: Geotail observations, Geophys. Res. Lett. **26**, 3349–3352 (1999)

Østgaard, N., Mende, S.B., Frey, H.U., Gladstone, G.R., Lauche, H.: Neutral hydrogen density profiles derived from geocoronal imaging, J. Geophys. Res. (2003). doi:10.1029/2002JA009749

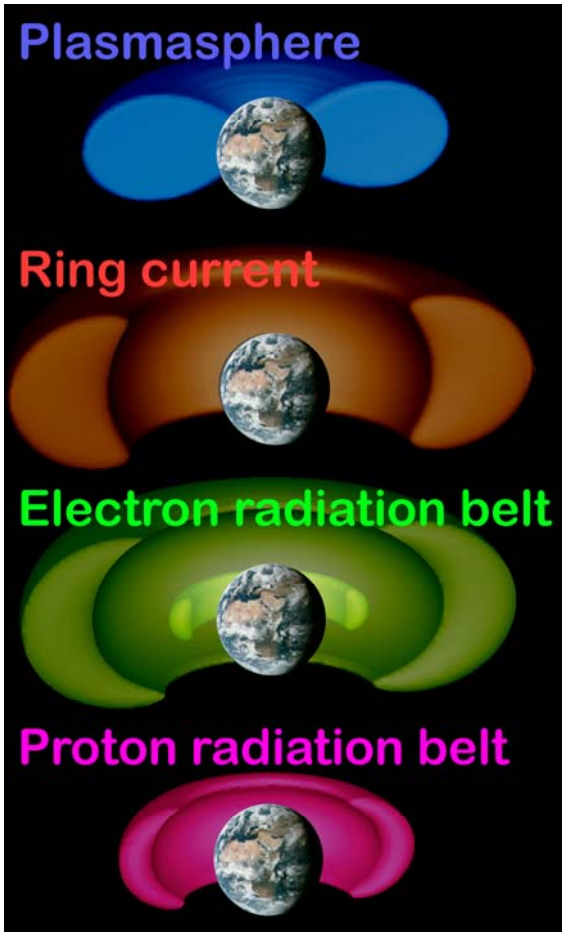

Figure 1: Energy structure of charged particles trapped in the inner magnetosphere.

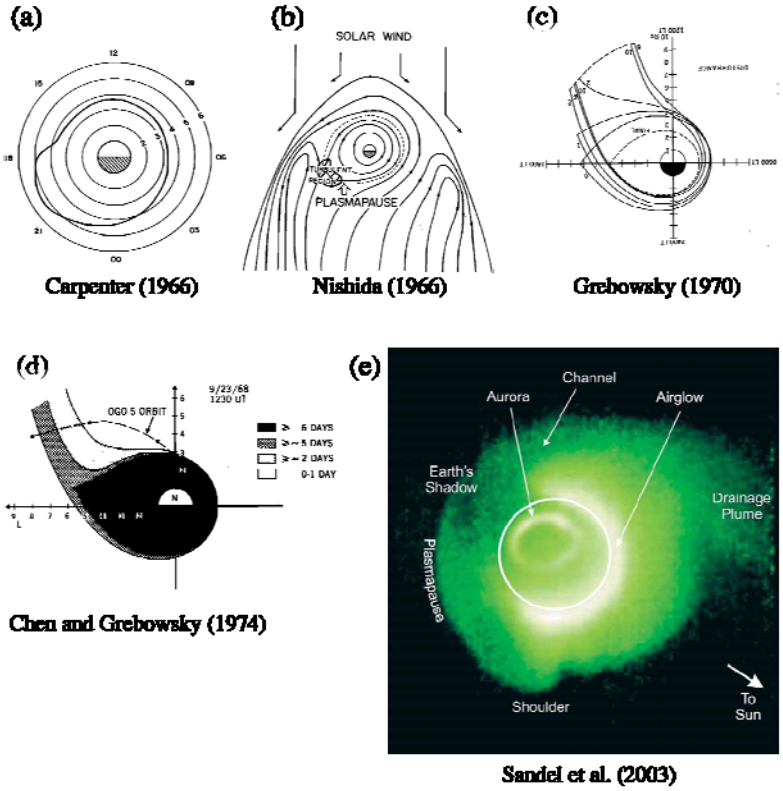

Figure 2. Shape of the plasmasphere.

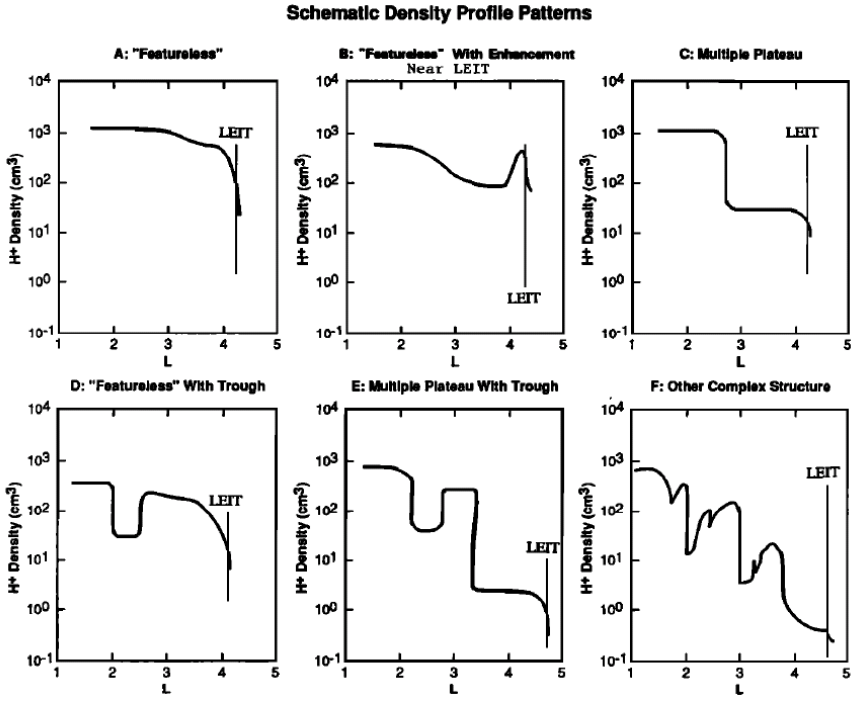

Figure 3. Six schematic plasmaspheric density profiles (Singh and Horwitz 1992).

(a) (b)

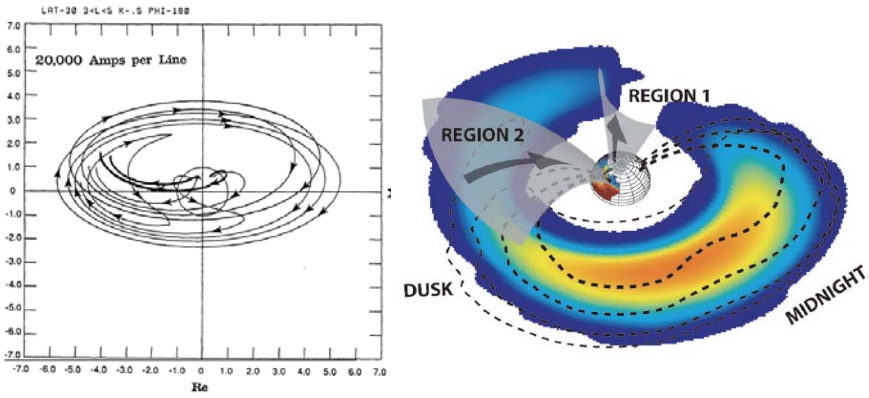

Roelof (1989) Brandt et al. (2008)

Figure4. (a) Global electric current lines deduced from model ring current pressure distribution (Roelof 1989), and (b) ring current plasma pressure deduced from energetic neutral atom observation and possible field-aligned current generated by the plasma pressure (Brandt et al. 2008).

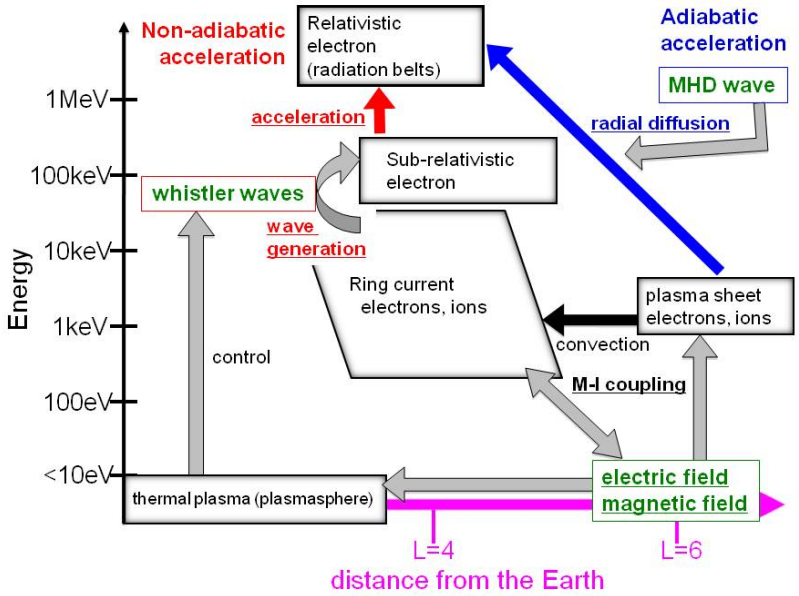

Figure 5. Possible formation processes for the electron radiation belt.

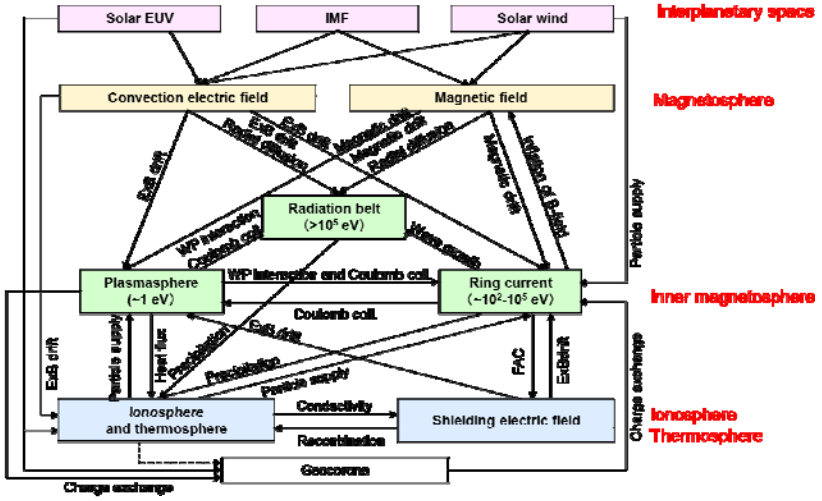

Figure 6. Possible cross energy and cross region couplings in the inner magnetosphere.